*Studies on Nitration of Furan Derivatives. Part I. On the Nitration of Furan-carboxylic Acid**

By Tadashi SASAKI**

(Received February 6, 1954)

Many types of α-nitrofuran derivatives have been synthesized by Saikachi and the present author to find any chemotherapeutically interesting compound.[1] In every case, the nitration of furan derivatives appears to be the most important. The object of the present studies is to find out the relationship between the structure of furan derivatives and the possibility of their nitration. In this paper the nitration of furan-carboxylic acid is reported.

As to the preparation of nitrofuran-carboxylic acid, there have been several methods,[2] but only a few of them are thought to be applicable for practical use. Hill and his collaborators[3,4] succeeded in carrying out the preparation of nitrofuran-carboxylic acid, in which furan-carboxylic acid was at first sulfonated with fuming sulfuric acid, then nitrated with fuming nitric acid. Their results showed that the product of sulfonation was stable against an acidic reagent and when it was treated with fuming nitric acid, it was converted to nitrofuran-carboxylic acid and nitrofuran-sulfonic acid by nitrosubstitution after decarboxylation or desulfonation as follows:

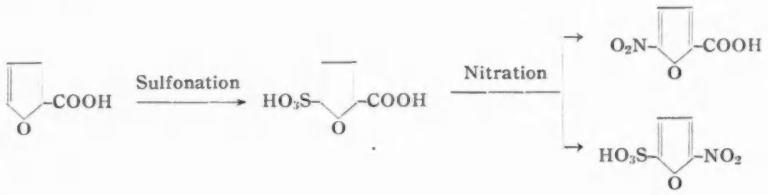

As, unfortunately, their reports lacked details on the experiments, the present study was carried out. In Part I, the nitration of furan-carboxylic acid was carried out in accordance with the procedure of Hill and White[4] and the relation of the yield of the product to the temperature and the time of reaction was studied. In Part II, the yield of the nitration of sulfofuran-carboxylic acid, obtained by the sulfonation of furan-carboxylic acid, in accordance with the procedure of Hill ane Palmer[3], was investigated. In Part III, the nitration of sulfofuran-carboxylic acid by the mixture of fuming nitric acid and acetic anhydride was studied.

Experimental

I. Nitration of Furan-carboxylic Acid

30 g. of furan-carboxylic acid was sulfonated with 90 g. of fuming sulfonic acid (d=1.951), with stirring below 20°C according to the known method[5]. After allowing it to stand at room temperature for one day, the resulting black viscous mixture was nitrated with 75 g. of fuming nitric acid (d=1.46), by dropping it to the solution at 0°, and then warming it gradually to the definite temperature as shown in Table I, and kept for three hours. The further treatment was the same as the procedure of Hill and White[4]. When the reaction mixture was above 40°, considerable bubbling started and the viscosity of the mixture diminished, the color turning to a light yellow. Above 50° the evolution of nitrogen oxide was observed. As shown in Table I, the lower the temperature of the reaction, the larger the yield of nitrofuran-carboxylic acid. The increasing yield of dinitrofuran with the rising of the temperature of the reaction is probably due to the conversion of nitrofuran-carboxylic acid into dinitrofuran and the conversion is presumably promoted by a catalytic action of the present sulfuric acid. Furthermore, in this reaction the production of nitrofuran-sulfonic acid can hardly be seen. This fact clearly shows that nitrofuran-sulfonic acid is more easily convertible to dinitrofuran than nitrofuran-carboxylic acid is. The effect

* This paper was presented before the Annual Meeting of the Chemical Society of Japan in April, 1949.

** Institute of Scientific Research for Practical Life, Medical Faculty of Kyoto University; Yoshida-konoe-cho, Sakyo-ku, Kyoto, Japan.

1) T. Takahashi, H. Saikachi and T. Sasaki, *J. Pharm. Soc. Japan*, **68**, 42 (1948); **69**, 284 (1949).

2) Four methods are given in Beilstein's Org. Chem., **18**, 287 (Hauptband).

3) H. B. Hill and Palmer, *Am. Chem. J.*, **10**, 380 (1888).

4) H. B. Hill and R. White, Ibid., **27**, 196 (1905).

5) H. Schwanert, *Ann.*, **116**, 269 (1860); H. Hodgson and H. R. Davies, *J. Chem. Soc.*, 806 (1939).

with the time of the reaction at 7° after the addition of fuming nitric acid on the yield is given in Table II. The products in the above experiments were identified by their m.p. which were in good accordance with the description of Hill and White[4].

TABLE I

No.	Reaction Temp.	N.F.C.*	Yield	D.F.*	Yield	N.F.S.*	Yield
1	0 °C	13.5 g.	32%**	1.2 g.	3%	Trace	
2	10	12.0	30	1.5	3.5	—	
3	20	7.0	17	2.0	5	—	
4	30	4.0	10	3.5	8	—	
5	40	4.0	10	3.0	7	—	
6	50	1.0	2.5	4.0	10	—	
7	60	—		3.0	7	—	

* N.F.C.: nitrofuran-carboxylic acid, m.p. 184°.
N.F.S.: nitrofuran-sulfonic acid potassium salt.
D.F.: dinitrofuran, m.p. 101°.

** The maximum yield ever reported.

TABLE II

No.	Reaction Time	N.F.C	Yield	D.F.	Yield	N.F.S.	Yield
8	1 hour*	8.5 g.	20%	0.5 g.	1.2%	Trace	
9	1 day*	11.5	28	1.0	2.5	—	
10	3 days**	10.0	24	1.8	4.0	—	
11	7 days**	9.0	22	2.5	6.0	—	

* After nitric acid was added to a strirred solution at 7°, stirring was continued for one hour at 7°.

** After stirring of the mixture was continued for one hour at 7°, the mixture was left to stand at room temperature of 20° for 1, 3 and 7 days, respectively.

II. Indirect Nitration of Furan-carboxylic Acid*

Nitration was carried on the sulfofuran-carboxylic acid which was obtained from furan-calboxylic acid, after sulfonation similar to that in part I. Sulfofuran-carboxylic acid was obtained in the form of the barium salt by Hill and Palmer[3] and no physical constants of the free acid have been reported. The present author obtained free sulfofuran-carboxylic acid from its salt as follows: the calcium salt which was obtained by the same procedure as the barium salt, was treated with the calculated amount of sulfuric acid and the resulting calcium sulfate was filtered off. After the filtrate was condensed on a boiling water bath till its color changed to black, it was left to stand in a desiccator of conc. sulfuric acid for several days to yield a colorless amorphous solid of sulfofuran-carboxylic acid, which was used for nitration. The yield of the acid was 85% of the theoretical amount, calculated from the starting furan-carboxylic acid.

20 g. of sulfofuran-carboxylic acid was portionwise added to a stirred 60 g. of fuming nitric acid (d=1.46), at several reaction temperatures and the mixture was stirred for a while or left to stand at room temperature as shown in Table III. The following procedure and identification of the products were the same as those described by Hill and Palmer[3]. The results are shown in Table III, which indicates that at lower temperature the yield of nitrofuran-sulfonic acid is comparable to that of nitrofuran-carboxylic acid and the production of dinitrofuran can hardly be seen, but with the rising of the temperature, both yields, of nitrofuran-sulfonic acid and -carboxylic acid, decreased.

III. Nitration of Sulfofuran-carboxylic Acid

11 g. of sulfofuran-carboxylic acid was portionwise added at −5° to the nitrating mixture which was previously prepared by mixing 28 g of fuming nitric acid (d=1.46), with 60 g. of acetic anhydride at −10°. After the addition of sulfofuran-carboxylic acid, stirring was continued for three hours and then the reaction mixture was poured on ice and neutralized with potassium carbonate. Following the procedure of Hill and Palmer[3], there were obtained nitrofuran-carboxylic acid as a main product and dinitrofuran as a by-product and the production of nitrofuran-sulfonic acid could not be seen. The results given in Table IV show that desulfonation takes place more easily to some extent than decarboxylation.

* Indirect nitration means that nitrofuran-carboxylic acid was obtained by the nitration of isolated sulfofuran-carboxylic acid, prepared by sulfonation of furan-carboxylic acid.

TABLE III

No.	Reaction Condition	N.F.C.	Yield	D.F.	N.F.S.	Yield
12	Addition at 10°, stirring at 10° for 5 hrs.	3.5 g.	22%	—	5.0 g.	20%
13	Addition at 10°, stirring at 30° for 5 hrs.	5.0	31	Trace	5.5	22
14	Addition at 10°, stirring at 45° for 5 hrs.	4.0	25	Trace	5.0	20
15	Addition at 10°, standing at 20°* for 3 days	5.0	31	—	4.5	18.5
16	Addition at 23°, stirring at 23° for 6 hrs.	4.0	25	—	4.5	18.5
17	Addition at 23°, standing at 20°* for 3 days	4.0	25	—	5.0	20
18	Addition at 60°, stirring at 60° for 6 hrs	2.0	13	1.0 g. (6%)	1.0	4
19	Addition at −3°, stirring at −3° for 2 hrs	3.5	22	—	4.5	18.5

* Room temperature of 20°.

TABLE IV

No.	Reaction Temp.	N.F.C.	Yield	D.F.	Yield	N.F.S.
20	− 5°C	2.5 g.	16%	0.3 g.	2%	—
21*	− 5	2.8	17	0.5	3	—
22	−10	2.5	16	0.15	1	—

* One drop of conc. sulfuric acid was added to the reaction mixture.

Summary

From the preparative point of view, the nitration of furan-carboxylic acid after sulfonation was studied with the following results:

(1) In order to obtain nitrofuran-carboxylic acid, the nitration of furan-carboxylic acid after sulfonation was carried out without separating the sulfonation product at several temperatures and the yield at 0° was about 32%, the highest ever known.

(2) In order to obtain nitrofuran-sulfonic acid, indirect nitration of sulfofurancarboxylic acid should be carried out at a low temperature, such as below 10°; the yield of which amounts to 20–22%. However, in this case, nitrofuran-carboxylic acid is produced simultaneously as a by-product.

(3) When the nitration of sulfofuran-carboxylic acid was carried out by using acetic anhydride and fuming nitric acid, nitrofurancarboxylic acid and dinitrofuran were obtained, but not nitrofuran-sulfonic acid. This showed that desulfo-nitrosubstitution took place more easily than decarboxy-nitrosubstitution.

The author wishes to express his gratitude to Professor H. Saikachi of Kyushu University for his kind advice and encouragement in the course of the study.

Institute of Scientific Research for Practical Life, Medical Faculty of Kyoto University, Kyoto

Studies on Nitration of Furan Derivatives. Part II. On the Nitration of Furfurylidene-type Compounds***

By Tadashi SASAKI

(Received February 6, 1954)

The earliest reported nitro-substituted furan compounds were obtained by the nitration of furan-carboxylic acid[1] or by that of other stable furan compounds such as the products obtained by condensation of furfural with compounds possessing reactive methylene group[2, 3, 4]. In Part I of these studies the former reaction was studied and in the present study the nitration of some furfurylidene compounds belonging to the latter reaction were studied by using two kinds of nitrating reagents, fuming nitric acid (d=1.46) and the mixture of acetic anhydride and fuming nitric acid (d=1.46). Furfurylidene compounds to be nitrated, having a general formula 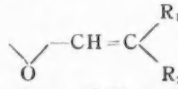 (where R_1 and R_2 are both electrophilic radicals as shown in the experimental part) were prepared by the condensation of furfural with the corresponding reactive methylene compounds.

Experimental

Nitration was carried out on 13 kinds of furfurylidene compounds described below (shown in Table II) by the following two methods of nitration. In method 1, nitration was carried out at −5∼−10° by using the starting material, acetic anhydride and fuming nitric acid in a ratio of 1:5.6:5.6 in mol. unit. In method 2, the starting material was added portionwise at −5° to a stirred fuming nitric acid which was thrice the amount of the starting material. In both cases, stirring was continued for one hour after the addition. When the nitration product was suspended in the reaction mixture, it was filtered. But when the nitration product was dissolved in the reaction mixture, the reaction mixture was poured on cracked ice, and the resulting oil was treated with the solvent suitable to separate the nitration product in a pure state.

(1) Nitration of Ethyl Furylacrylate.—Ethyl furylacrylate was prepared by Claisen condensation[5].

Method 1: Gilman[6] reported already on this nitration by using the starting material, nitric acid and acetic anhydride in mol. ratio of 1:3.2:5.5, yielding 51%. But the present author's experiment with the same mol. ratio resulted in only 29.5%. Furthermore, the yield of the reaction with 1:5.6:5.6 mol. ratio was 49.5%. The m.p. of the product was in good accordance with that described by Gilman, m.p. 123°[4]. In the second method decomposition occurred and the nitrated product was not obtained.

(2) Nitration of Furfurylideneacetone.—Furfurylideneacetone was prepared by the method of Organic Syntheses[5].

Method 1: When the nitration temperature was −5∼−10°, no crystalline product could be isolated from the red oil which was obtained by pouring the clear red reaction mixture on cracked ice. But when nitration was carried out at −25°, a very small amount of a yellow crystalline product, m.p. 120–135°, was obtained by the addition of a very small amount of alcohol to the red oil which was obtained by pouring the reaction mixture on cracked ice. Its semicarbazone, decomposition point 224°, was identified with that prepared by another method[7].

In the second method decomposition occurred.

(3) Nitration of bis-Furfurylideneacetone.—Bis-furfurylideneacetone was prepared by the method of Organic Syntheses[5].

Method 1: 4.3 g. of bis-furfurylideneacetone, m.p. 52–4°, was dissolved in 10 cc. of acetic anhydride and this solution was nitrated at −5° by the mixture of fuming nitric acid (20g.) and acetic anhydride (30 cc.). In a while, precipitation occurred in the stirred reaction mixture. After stirring was continued for two hours, the reaction mixture was filtered off to give a crude product which was recrystallized twice from acetic acid to a yellow needle crystal, m.p. 198–200° (decomp.) with 5% yield.

Found: N, 8.98, Calcd. for $C_{13}H_8O_7N_2$: N, 9.21%.

In the second method decomposition occurred.

(4) Nitration of Furylacrolein.—Furylacrolein was prepared by König's method[8].

Method 1: When the nitration temperature was −5∼−10°, the nitrated product could not be isolated. The nitration was carried out below −15° and the resulting red solution was poured on cracked ice. The red oil, separated, was dissolved in ethylacetate and the solution was left to stand in an ice box for several days to give a small amount

* Part I, this Bulletin, **27**, 345 (1954).

** A portion of this paper was presented before the Annual Meeting of the Chemical Society of Japan in April, 1949.

1) H. B. Hill and Palmer, *Am. Chem. J.*, **10**, 380 (1888); H. B. Hill and R. White, Ibid., **27**, 196 (1905).
2) B. Priebs, *Ber.*, **18**, 1362 (1885).
3) R. Heuck, Ibid., **28**, 2256 (1895).
4) H. Gilman, *J. Am. Chem. Soc.*, **52**, 2550 (1930).
5) L. Claisen, *Ber.*, **24**, 143 (1891).
6) Org. Syn., Col. Vol. I, 301.
7) This will be reported in Part IV of this study.
8) W. König, *Ber.*, **58**, 2559 (1925).

of a red needle-like crystal, m.p. 112–4°, which was recrystallized from methanol to result in a brilliant red crystal, m.p. 114–5°; the yield was as low as 0.4%. This compound was identical with the specimen prepared by another method which is a more suitable preparation for this compound[9].

In the second method decomposition occurred.

(5) Nitration of Furylacrylic Acid.—Furylacrylic acid was prepared by the method of Organic Syntheses[10].

Method 1: Nitration of furylacrylic acid, F.A.A., was carried out in detail as a standard for nitration of other furfurylidene compounds. Gilman's procedure, slightly modified, was used[4]. The results by changing the ratio of F.A.A. and the nitration mixture are given in Table I, which shows that the maximum yield was obtained when F.A.A., nitric acid and acetic anhydride were in mol. ratio of 1:5.6:5.6. The yield in this mol. ratio was 48.5% at the nitration temperature of −7° and 55% at that of −15°, which seems to indicate that the yield is higher when the nitration temperature is lower. Both yields were higher than that of Gilman whose yield was 40%[4]. In this case, however, the addition of a small amount of conc. sulfuric acid made the yield less and the color of the reaction mixture more reddish. Excess of the nitration mixture decreased the yield and especially the excess of nitric acid resulted in the oxidative destruction occurring during the filtration of the nitration product. On the contrary, the yield became greater when F.A.A. was added directly to the nitrating mixture than when it was added in the form of a solution in acetic anhydride according to the procedure of Gilman[4].

In the second method decomposition occurred.

(6) Nitration of Nitrovinylfuran. Nitrovinylfuran was prepared by Thiele's method[11].

Method 1: The nitration product appeared in the form of a suspension in a red colored nitration mixture. The precipitate was filtered and washed with cold water to give a crude product, m.p. 134–9°, which was identical with that prepared by method 2.

Method 2: Priebs[2] reported on this nitration, in which the yield was not described. A dark red solution, obtained by nitration, was poured on cracked ice and the resulting brown precipitate was filtered and washed with water to give a crude product, m.p. 132–5°, which was identified by mixed melting point with the specimen of Priebs, m.p. 143°, after recrystallization from alcohol.

(7) Nitration of Ethyl Furfuralmalonate.—Ethyl furfuralmalonate was prepared by Knoevenagel's condensation[12].

Method 1: A yellow solution which was obtained by nitration, was poured on cracked ice and the resulting yellow oil gradually solidified. It was filtered to result in a crude product, m.p. 75–83°, which was recrystallized from ethanol and identified with the specimen prepared by method 2.

Method 2: Heuck[3] reported on this nitration qualitatively. The dark blue solution which resulted from the nitration was poured on cracked ice and the resulting oil gradually solidified to give a crude product, m.p. 84–89°, which was identified after recrystallization from ethanol with the specimen prepared by Heuck, m.p. 106–8°[3].

(8) Nitration of Ethyl 3-(2-furyl)-2-Acetylacrylate.—Ethyl 3-(2-furyl)-2-acetylacrylate was prepared by Claisen condensation[13].

Method 1: The reddish blue reaction mixture was poured on cracked ice and the resulting red oil was washed several times with cold water by decantation and mixed with a small amount of ethanol. A crystalline product was separated from the mixture and it was purified by recrystallization from ethanol to give a light yellow, corn-like crystal, m.p. 127–9°.

Found: N, 5.62, Calcd. for $C_{11}H_{11}O_5N$: N, 5.57.

Method 2: The reaction mixture changed to dark red. By the same procedure as method 1, a crude product was obtained. This was recrystallized from ethanol and identified by mixed melting point with the specimen prepared by method 1.

(9) Nitration of Ethyl 3-(2-furyl)-2-Cyanoacrylate.—Ethyl 3-(2-furyl)-2-cyanoacrylate was prepared by Beckert's method[14].

Method 1: The nitrated product appeared in the form of a suspension in the reaction mixture after being dissolved once completely. The precipitate was filtered to give a crude product, decomposition point 145–50°, which was identified with the specimen prepared by method 2.

Method 2: Heuck[3] reported concerning this nitration, but did not describe the yield. The nitrated product was obtained in the form of a suspension in the reaction mixture. By pouring it on cracked ice a crude product, m.p. 130–45°, was obtained which was recrystallized from ethanol to give the same m.p. 153° as described by Heuck[3]. In this case, the addition of one drop of conc. sulfuric acid to the reaction mixture was useful to prevent the mixing of a small amount of the unreacted material.

(10) Nitration of Diacetylvinylfuran.—Diacetylvinylfuran was prepared as follows: 5 g. of freshly distilled furfural, b.p.$_{19}$ 62°, and 5 g. of acetylacetone, b.p. 136–137°, were dissolved in 15 cc. of ethanol. To this solution was added 3 cc. of piperidine in pyridine solution (1%) and the resulting mixture was heated in a water bath of 70° for four hours. The solvent was removed under reduced pressure and the residual oil was extracted with ether. The ether layer was washed twice with 15 cc. of water and dried with anhydrous sodium sulfate. After removing ether, the residual dark red oil was distilled under reduced pressure. The greater part distilled at 138–140°/3 mm. Hg., amounting to 6 g., and the yield was 65%.

Found: C, 67.26; H, 5.45, Calcd. for $C_{10}H_{10}O_8$: C, 67.41; H, 5.61%.

Method 1: When the starting material was

9) H. Saikachi et al; *Japan J. Pharm. & Chem.*, **22**, 258 (1950); **23**, 188, 270 (1951).
10) Org. Syn. Col. Vol II, 956.
11) J. Thiele and H. Landers, *Ann.*, **269**, 303 (1909).
12) E. Knoevenagel, *Ber.*, **31**, 2595 (1895).
13) H. Claisen and F. E. Mathews, *Ann.*, **218**, 175 (1883).
14) C. Beckert, *J. prakt. Chem.*, (2), **50**, 17 (1894).

added in the form of a solution in a small amount of acetic anhydride, a clear yellow solution was obtained. After pouring the reaction mixture on cracked ice, the resulting oil was cooled by ice water to give a yellow crystal with a low melting point, 28°.

Found: N, 6.50, Calcd. for $C_{10}H_9O_5N$: N, 6.28%.

Method 2: The nitration product was obtained instantly after the addition of the starting material to stirred fuming nitric acid. After pouring the reaction mixture on cracked ice, the same procedure as that used in the above method 1 was applied for isolating the nitrated product to give a product of m.p. 28°, which was identified with the specimen of method 1.

(11) Nitration of Furfuralmalonitrile.—Furfuralmalonitrile was prepared by Heuck's method[15].

Method 1: A small amount of the nitrated product precipitated from the yellow clear solution. The reaction mixture was poured on cracked ice and the precitate was filtered to give a crude product of m.p. 173° (decomp.), which was identified with the specimen of method 2 after recrystallization from ethanol by a mixed melting point.

Method 2: Heuck[3] reported on this nitration, but did not describe the yield. A clear solution was obtained in the course of the nitration. Following the same procedure as method 1, a crude product of m.p. 173–5° was obtained, which was recrystallized from ethanol to result in raising its melting point to 179°, which was in good accordance with the description of Heuck[3].

(12) Nitration of 2-Cyano-3-(2-furyl) acrylic Acid.—2-Cyano-3-(2-furyl)acrylic acid was prepared by Heuck's method[15].

Method 1: The color of the reaction mixture changed to blue and the nitrated product precipitated gradually. After pouring the reaction mixture on cracked ice, a dark red precipitate was filtered and washed with water to give a crude product of m.p. 241–5° (decomp.), which was recrystallized from ethanol and was identical with the specimen of method 2.

Method 2: The same procedure as method 1 was applied on the dark red reaction mixture. A crude product of m.p. 246–9° (decomp.) was recrystallized from ethanol to give a compound of m.p. 250° (decomp.), the same as that of Heuck[3].

(13) Nitration of Furfuralmalonic Acid.—Furfuralmalonic acid was prepared by Knoevenagel's condensation[17]. Method 1 and 2 were applied to this compound. The evolution of carbon dioxide was observed and the nitrated product could not be isolated. This nitrated product was prepared by another method[10].

The results of the above experiments are summarized in Table II.

TABLE I

NITRATION OF FURYLACRYLIC ACID (F.A.A.)

F.A.A.	Nitration Mixture		Temp. of Nitration	Yield	(decomp. of the Product
	HNO_3	Ac_2O			
mol.	mol.	mol.	°C	%	°C
0.25	0.25	1.40	−7	10.77	228°
"	0.50	1.40	"	23.73	223°
"	0.65	1.40	"	28.02	"
"	1.00	1.40	"	32.32	"
"	1.15	1.40	"	38.88	"
"	1.40	1.40	"	43.09	"
"	1.55	1.40	"	38.88	"
0.25*	0.75	0.75	"	43.60	"
"	1.40	1.40	"	48.50	"
"	1.75	1.75	"	43.00	"
"	1.40	1.40	−15	55.00**	"
"	1.40	1.40	−15	49.00***	"

* Furylacrylic acid was added directly into the nitration mixture. In other experiments without asterisk the same acid was added in the form of a solution in acetic anhydride.

** The maximum yield ever known.

*** One drop of conc. sulfuric acid was added to the reaction mixture.

TABLE II

NITRATION OF FURFURYLIDENE COMPOUNDS

Ex. No.	Compound to be nitrated	Method 1		Method 2	
		Yield %	m.p. of the product °C	Yield %	m.p. of the product °C
(1)	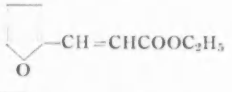	49.5	123°	*	

15) R. Heuck, *Ber.*, **28**, 2253 (1895).
16) R. Heuck, Ibid., **27**, 2625 (1894).
17) E. Knoevenagel, *Ber.*, **31**, 2612 (1898).

(2)	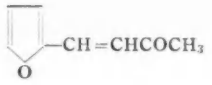	0.1	224 (dec.)**	*	
(3)		5.0	200 (dec.)	*	
(4)	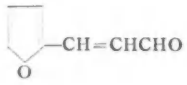	0.4	114 (dec.)	*	
(5)	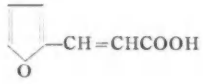	48.5	223 (dec.)	*	
(6)	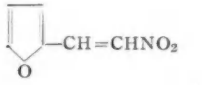	23.0	134–9	35.8	128–32
(7)	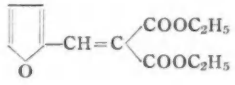	96.5	75–83	92.5	84–89
(8)	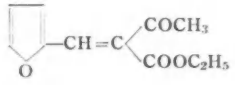	10.3	127–9	11.8	128–9
(9)	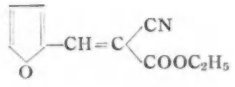	26.8	145–50 (dec.)	61.0	130–45 (dec.)
(10)	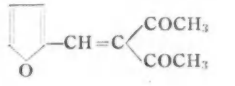	60.0	28	20.0	28
(11)	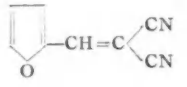	30.0	173	52.5	173–74
(12)	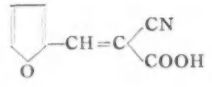	35.3	241–5 (dec.)	54.9	246–49 (dec.)
(13)	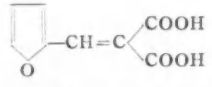	*		*	

* Decomposition occurred and no crystalline product was obtained.

** The m.p. (dec.) is that of its semicarbazone of the produced nitro-furfurylideneacetone.

Summary

The nitration, by using both fuming nitric acid mixed with acetic anhydride and fuming nitric acid alone, was carried out on 13 kinds of furfurylidene compounds,

C_4H_3O–CH=CR_1R_2.

(1) These furfurylidene-type compounds in which R_1 and R_2 are electro-groups are stable against both acidic reagents and can be nitrated without formation of the nitration intermediate.

(2) In the case of a group being –CHO or –$COCH_3$, the nitration temperature must be

kept low enough to avoid decomposition.

The author wishes to acknowledge the help of Professor H. Saikachi for his constructive advice on this work. Gratitude is also extended to Mr. K. Suzuki, Instructor of Kyoto Pharmaceutical College, for assistance given the author in the preparations. Elementary analysis was carried out by Miss H. Iwata and Mr. K. Imaeda, Pharmaceutical Department, Medical Faculty of Kyoto University.

Institute of Scientific Research for Practical Life, Medical Faculty of Kyoto University, Kyoto

On the Distribution and Variation of Nutrient Salts in the Adjacent Water to the Aleutian Islands in the North Pacific

By Rinnosuke FUKAI

(Received February 27, 1954)

Introduction

Oceanographical observations in the salmon fishing ground have been carried out in the region adjacent to the Aleutian Islands on board R. V. "Tenyo-maru", covering over 80 days from May to July in 1952. The author has been engaged in these observations and had an opportunity of analysing a number of water samples on board the vessel. On the basis of the data obtained in the field as well as in the laboratory, the distribution and variation of nutrient salts in the waters of this region have been considered in the present paper.

Although the sea region under consideration has been regarded as one of the most important fishing grounds of the world together with the vicinity of Newfoundland and the North Sea, systematic investigations concerning chemical problems in this region have scarcely been reported except those carried out by Ratomanov (1936)[1] and Barnes and Thompson (1938)[2]. Even in the comprehensive investigation conducted by Barnes and Thompson, the regions mainly concerned were restricted to the eastern side of long. 180° while little information on the Eastern Hemisphere has been available up to now.

Some problems related to the consumption of nutrient salts by marine organisms will also be discussed here.

The Sea Region under Consideration

The region under study is located within the square enclosed by the longitudes of 170°E and 180° and the latitudes of 50°N and 55°N, extending over both sides of the Aleutian Ridge as it is indicated in Fig. 1 with

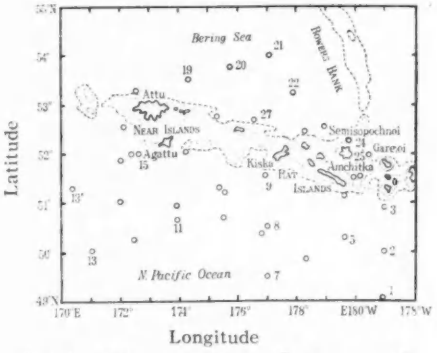

Fig. 1. Oceanographical Stations and Bottom topography near the Western Aleutian Islands. Dotted and broken lines indicate bottom contours of 200 m. and 500 m. depths, respectively.

oceanographical stations and bottom contours. As shown in the figure, the Bering Sea covers an area north of the ridge and the southern area is covered with a portion of the North Pacific. In this region, the Bering Sea forms a very deep basin, while in the east part off the region it becomes much shallower to form the continental shelf of Alaska.

Collection of Samples and Analytical Methods Adopted

Determinations of phosphate-phosphorus, silicate-silicon and dissolved oxygen were made on board ship as soon as possible after collection. Water samples for chlorine and nitrate-nitrogen determinations were brought to the author's laboratory

* Contribution B-No. 137 from the Tokai Regional Fisheries Research Laboratory, Tokyo, Japan.

1) C. E. Ratomanov, "Research of the Sea", Vol. 2, Moscow, 1936 (in Russian with English summary).

2) C. A. Barnes and T. G. Thompson, University of Washington "Publications in Oceanography", Vol. 3, No. 2 (1938).

(Tokyo) and analysed. To the samples for nitrate determination mercuric chloride solution was added in order to avoid the change in concentration due to bacterial growth.

The improved method of Denigès-Atkins[3] was adopted for the determination of phosphate-phosphorus. In this method color development was accomplished by the original procedure, but sea water free from phosphate was used as the media of diluted standards.

Silicate-silicon was estimated by means of Dienert-Wandenbulcke's method in which a buffered potassium chromate solution containing borax was adopted as the color standard. It was standardized against sodium silicate solution both with Beckman's spectrophotometer and by the visual method[4]. Color comparison aboard ship was performed by using improved Hehner tubes with the length of 25 cm.

Stock solutions of standards for phosphate and silicate determinations were prepared in duplicate, one of which served as reference and the other as the working standard, both being checked against each other from time to time. After the completion of the cruise it has been confirmed that the changes in concentration of the reference were negligibly small during the period.

Dissolved oxygen was determined by means of Winkler's iodometric titration[5]; and for chlorine determination the argentometric titration using uranine as the indicator[6] was adopted.

Determination of nitrate-nitrogen was made by colorimetric methods using Harvey's reduced strychnine reagent; and as the artificial color standard the standardized safranine solution was used[7].

Results and Discussion

1. Distribution of Water Temperature and Chlorinity.—As mentioned above, the region under consideration is topographically devided into two areas by the Aleutian Ridge running through the central part of the region. Therefore, it may be convenient to examine the distributions of water temperature, chlorinity and so on separately, by area. Data obtained from several stations within each area in the first decade of June were averaged and considered as representative values for each area.

Fig. 2 shows vertical distributions of water temperature and chlorinity. From the figure it is clear that distributions of water temperature are quite identical in both areas except for slight differences recognized beyond a depth of 200 m. A characteristic feature of

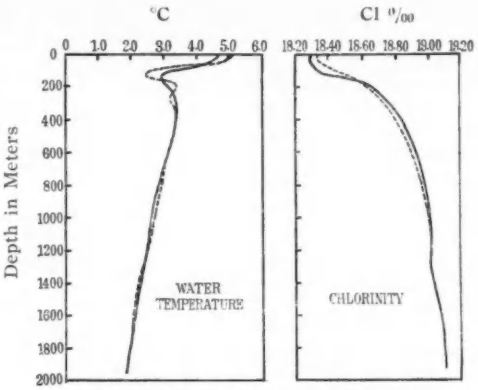

Fig. 2. Vertical distributions of water temperature and chlorinity. Solid lines represent the distributions in the Pacific side of the Aleutian Ridge, and broken lines those in the Bering Sea.

the distribution of water temperature in this region is that the marked temperature minimum and the gentle maximum appear at depths of 100 m. and 400 m., respectively. Below the depth of 400 m. the water temperature falls gradually and the gradients of the fall are much gentler than those in other regions such as tropical waters.

Distributions of chlorinity in these areas also are almost identical and chlorinity increases continuously with depth.

Close agreements in vertical distributions both of water temperature and of chlorinity between these areas suggest that horizontally uniform water masses may exist there. This type of distribution is in striking contrast to those in the Kuroshio or equatorial region.[8]

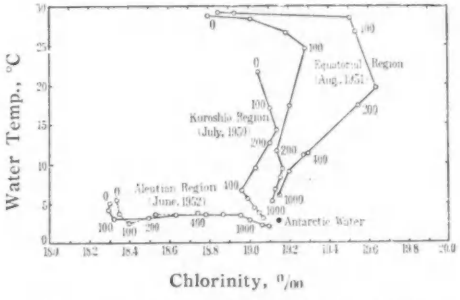

Fig. 3. Temperature-Chlorinity diagram representing water masses in various regions. Numbers in the figure indicate the depths in meters at which temperature and chlorinity for each point were obtained.

3) R. J. Robinson, *J. Mar. Res.*, **7**, 33 (1948).
4) R. Fukai, *J. Oceanogr. Soc., Japan*, in press.
5) W. S. Wooster, "Technical report of the California Cooperative Sardine Program", No. 25, Scripps Inst. of Oceanogr. (1950).
6) Y. Miyake, This Bulletin, **14**, 29 (1939).
7) H. Wattenberg, *Rapp. et Proc.-Verb. des Reunions, Conseil permanent intern. pour l'explosation de la mer*, **103**, 19 (1937).
8) R. Fukai, This Bulletin, **26**, 485 (1953).

In Fig. 3, T–Cl curves which were previously obtained by the author are compared with those from the present data. It should be noticed that although T–Cl curves differ greatly from each other in the upper layers, they tend to converge on a point which represents water temperature and the chlorinity of a water mass having Antarctic origin.

2. Distribution of Dissolved Oxygen.—Vertical distributions of dissolved oxygen in these two areas are shown in Fig. 4 compared

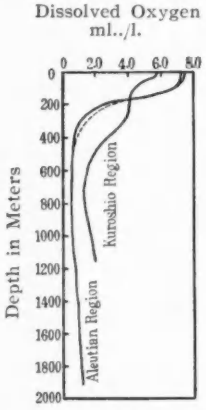

Fig. 4. Vertical distributions of dissolved oxygen. Solid lines: in the Pacific; broken line: in the Bering Sea.

with those in the Kuroshio region. The distributions in the areas are in close agreement with each other as well as those of water temperature and chlorinity. As for characteristic features of the distribution, it may be pointed out that high contents of oxygen are encountered at and near the surface and they suddenly decrease in depths within 100–300m. forming a jumping layer. Oxygen at depths of 400–1000 m. is less than 1 cc. O_2/l., being the minimum value among those oceanic waters of the North Pacific.

As shown in Table I, a remakable fact is

TABLE I
AVERAGE CONTENTS OF DISSOLVED OXYGEN IN THE UPPER LAYERS

Depth m.	O_2 ml./l. obs.	O_2 ml./l. calc.	Saturation percentage
0	7.37	7.23	101.9
10	7.44	7.29	102.1
25	7.46	7.34	101.6
50	7.36	7·37	99.9
75	7.24	7.53	96.1
100*	6.99	7.62	91.7
150	4.94	7.50	65.9

* The layer of minimum water temperature.

that the oxygen contents at the layers of 10 m. and 25 m. are higher than at the surface. This may probably result from photosynthesis by phytoplankton, since this type of distribution without biological support would be destroyed by the strong turbulence prevailing in the region.

The thickness of the euphotic layer may be estimated to be about 50 m. from the fact that the oxygen content at 50 m. layer is just saturated whereas the contents above this layer are supersaturated.

3. Distribution of Phosphate-phosphorus and Nitrate-nitrogen.—Vertical distributions of phosphate and nitrate are given in Fig. 5.

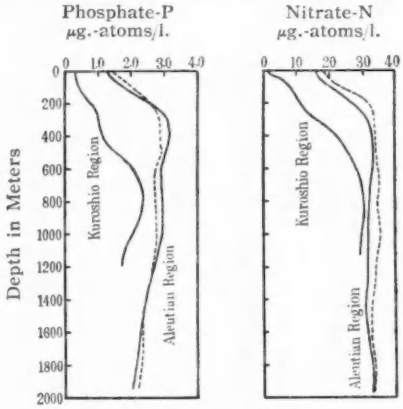

Fig. 5. Vertical distributions of phosphate-phosphorus and nitrate-nitrogen. Solid lines: in the Pacific; broken lines: in the Bering Sea.

The distributions of each of the constituents are almost the same in the two areas. The causes of slight differences recognized between the areas are not clear. Yet it may be remarkable that the phosphate contents at depths within 200–800 m. are lower in the waters of the Bering Sea than in the other area, while the contents of nitrate are higher in the former than in the latter.

Characteristics of the vertical distributions are that the high contents of both constituents are found at and near the surface and that the concentrations increase abruptly in a layer corresponding to the jumping layer of dissolved oxygen. The maximum amount of phosphate appears at a depth within 400–600 m., while the maximum of nitrate is not obvious. Attention is called to the fact that considerable amounts of both constituents (above 1.0 μg.-atoms PO_4-P/l. and 150 μg.-atoms NO_3-N/l.) were present in spite of the fact that abundant crops of phytoplankton existed there. The fact means that the nutrient salts in the upper layers have not been exhausted so that potential ability for organic production could still remain in the layers.

4. Distribution of Silicate-silicon.—Fig. 6 illustrates vertical distribution of silicate in the areas compared with those in the Kuroshio region and in the Northeast Pacific. As

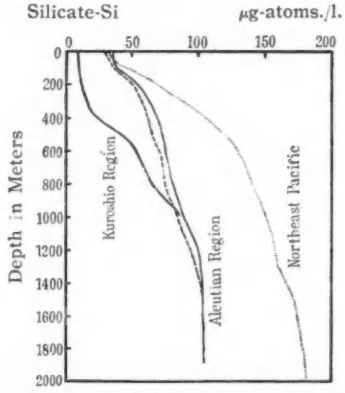

Fig. 6. Vertical distributions of silicate-silicon. Solid lines: in the Pacific; broken line: in the Bering Sea; dotted line: in the Northeast Pacific obtained by Thompson (1938).

in cases of other constituents, considerable amounts of silicate are found at the surface and they further increase in the deeper layers. Referring to some differences in distributions between two areas, the contents are slightly lower on the side of the Bering Sea. It is conspicuous that the distributions differ greatly from those obtained by Thompson.

5. Relationship between Distributions of Nutrient Salts.—As described above, the prevailing features of the nutrient salt distribution are summarized as follows:

(i) Distributions are horizontally uniform except those in limited areas such as the vicinity of islands,

(ii) concentrations are high even in the surface layer,

(iii) and increase further with maximum gradients in depths within 100–300 m.

From the type of distributions, it is expected that parallel correlation may exist between concentrations of these constituents. From Fig. 7 which shows the correlation between phosphate and nitrate, it is concluded that the average atomic ratio of N : P is 12, although points plotted in the figure are somewhat scattered. This value is lower than the normal ratio of 15 proposed by Cooper[9]. As the author has recently pointed out[10], the ratios in the waters below subsurface

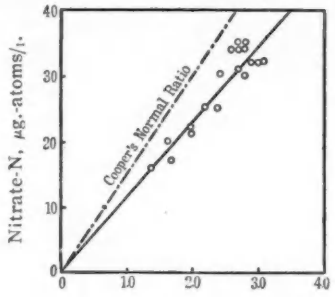

Fig. 7. Relationship between nitrate-nitrogen and phosphate-phosphorus in the adjacent region to the Aleutian Islands.

layers in the Kuroshio region coincide with the normal ratio. So far it has not been conclusive, however, whether the deviation from the normal ratio in the Aleutian region is attributed to local differences or related to the rate of regeneration of these constituents.

In case of the regeneration of these constituents, in general, dissolved oxygen would be consumed. The relationship between phosphate contents and oxygen depletion (the difference between the saturation value and observed value) is shown in Fig. 8. Oxy-

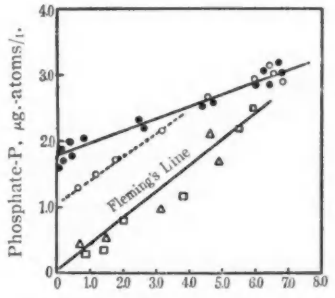

Fig. 8. Relationship between phosphate-phosphorus and oxygen depletion in various regions. Dots designate points for the Aleutian Region in 1st decade of June; circles for those at the end of June. Squares: for the Kuroshio Region; triangles: for the Equatorial Region.

gen depletion may serve as a measure of oxygen consumption.

In the figure, was added a line which was proposed by Fleming[11] on the basis of the proportion between liberated oxygen and as-

9) L. H. N. Cooper, *J. Mar. Biol. Assoc., United Kingdom*, **22**, 177 (1938).

10) R. Fukai, This Bulletin, **25**, 323 (1952).

11) R. H. Fleming, "Proc. the 6th Pacific Science Congress", Vol. 3 (1939).

similated phosphorus, both due to photosynthesis. It can be stated that points plotted for the Kuroshio and Equatorial regions are in close agreement with Fleming's line, while the slope of the line derived from the points for the Aleutian region differs greatly from that of Fleming's line. In addition, the slope had been altered in the course of time and it came to coincide with that of Fleming's line after about a month. This indicates that a constant ratio between phosphate and oxygen depletion has not been maintained during the period and that the decrease in dissolved oxygen has taken place in association with the decrease in phosphate contents in the subsurface layer. Although the mechanism of this decrease in dissolved oxygen may be complicated, it may relate to the decomposition processes in the layer in question. The deficiency of dissolved oxygen in the subsurface layer should be emphasized as a feature in the Aleutian region together with the deviation of N-P ratios from the normal ratio.

6. Quantitative Consideration on the Rate of Organic Production by Phytoplankton.—In the above it has been concluded that the potential ability for organic production still remained in this region at the beginning of June. As the duration of this condition depends upon the rate of organic production, it is desirable to find out the production rate.

Oceanographical observations were repeatedly carried out at sea around 150 nautical miles S. of Attu Island on June 5–6 and 29–30. Table II has been made by averaging a number of data obtained from several stations occupied there. On these materials the following computations have been based.

TABLE II

DATA USED FOR THE ESTIMATION OF THE PRODUCTION RATE

Water layer m.	June 5–6		June 29–30	
	Water temp. °C	PO_4-P μg-at./l.	Water temp. °C	PO_4-P μg.-at./l.
0–25	4.50	1.33	6.08	0.93
25–50	4.29	1.47	5.12	1.19
50–75	4.00	1.60	4.03	1.41

At first, the rise in water temperature may be expressed by

$$\frac{\partial T}{\partial t} = \frac{A_z}{\delta} \cdot \frac{\partial}{\partial z}\left(\frac{\partial T}{\partial z}\right) - V_x \cdot \frac{\partial T}{\partial x}, \qquad (1)$$

where, T is water temperature, A_z, coefficient of eddy diffusivity, δ, specific gravity of sea water, and V_x, current velocity component along x-axis.

In the equation, we may conveniently take x-axis from the west to the east and z-axis from the surface to the bottom. In equation 1, the lateral mixing of water masses was ignored because the horizontal gradients of water temperature were so small; and current velocity components except that along x-axis were of no account.

Let us rewrite equation 1 as

$$A_z = \delta\left(\frac{\partial T}{\partial t} + V_x \cdot \frac{\partial T}{\partial x}\right) \Big/ \frac{\partial^2 T}{\partial z^2}. \qquad (2)$$

Since gradients of temperature distribution, current velocity component and specific gravity of sea water are known, we can obtain the value of A_z from the equation 2. The calculated values of A_z are shown in the first column in Table III.

TABLE III

COMPUTED VALUES FOR NET PRODUCTION RATE

Water layer m.	A_z	R PO_4-P μg.-at./l./sec.	Net production rate mg.C/m²./day
0–25	(10)	-5.1×10^{-7}	56
25–50	10	-1.0×10^{-7}	11

On the other hand, the decrease in phosphate contents during the period may be expressed by

$$\frac{\partial C}{\partial t} = R + \frac{A_z}{\delta} \cdot \frac{\partial}{\partial z}\left(\frac{\partial C}{\partial z}\right), \qquad (3)$$

where C is concentration of phosphate R, biological rate of change (rate of net consumption).

In equation 3, the horizontal eddy diffusion and advection were ignored since the horizontal distribution of phosphate was uniform as previously stated. From Eq. 3, we may obtain

$$R = \frac{\partial C}{\partial t} - \frac{A_z}{\delta} \cdot \frac{\partial^2 C}{\partial z^2}. \qquad (4)$$

Then, on the basis of Eq. 4, the value of R can be calculated by introducing into the equation the values of A_z, which have been obtained from Eq. 2, and gradients in phosphate distribution. The values of R thus obtained for each layer are shown in the second column in Table III.

Since photosynthesis by phytoplankton is usually accompanied by the consumption of phosphate, the rate of carbon assimilation can be computed as in the third column of Table III from the values of R, using the proportion given by Fleming.

Few data have been available for comparing these values, except those which were derived from Reiley's data concerning the annual

variations of plankton carbon on Georges Bank[12] (Table IV). The values for the Aleutian region agree well with the value for the spring burst of phytoplankton given by Riley.

TABLE IV

NET PRODUCTION RATES COMPUTED FROM THE DATA OBTAINED BY RILEY ON GEORGES BANK (1947)

Period	Net production rate mg.C/m³./day
Feb.–Mar.	4
Mar.–Apr.	20
Apr.–May	50

Most recently, Nielsen[13] has pointed out on the basis of the results obtained from the determinations using radiocarbon C^{14} that the production rates hitherto estimated were too high, especially in the tropical regions, criticizing the experiments carried out by Riley[14] in the Sargasso Sea. However, Nielsen himself has admitted that Riley's values are reliable so far as the waters on the coastal bank are concerned.

Thus, if we assume that the organic production continues at the rate obtained above, and that the nutrient supply from the substratum is prevented by the development of stratification, the potential ability for organic production is reckoned to last for about 20 days more. Consequently, the production may actually continue till the end of summer without deficiency in nutrient salts.

7. Estimation of the Production Rate based upon the Diurnal Variations of Dissolved Oxygen.—Anchored observations on the diurnal variations of oxygen throughout 24 hours were carried out at Station 24, situated north of Semisopochnoi Island, in the last decade of May. Results obtained are shown in Fig. 9. Values plotted for dissolved oxygen in the figure represent integral mean concentrations from the surface to a depth of 50 m. Although the water was shifted continuously by tidal current during the period, the temperature and chlorinity of water were kept strictly constant. For this reason, it can be assumed that the changes in dissolved oxygen were caused by biological activity in a water mass.

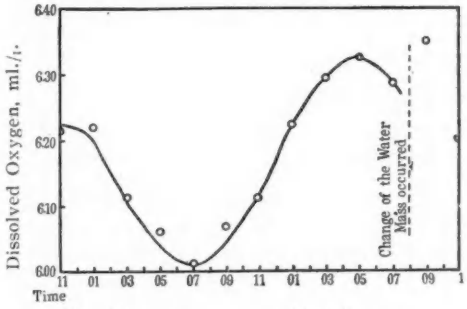

May 21, p.m. May 22, a.m.
(Japanese Standard Time)

Fig. 9. Diurnal variation of dissolved oxygen at St. 24, off Semisopochnoi Island.

According to the figure, the net increase in the oxygen content amounting to 0.3 ml/l. took place in 10 hours from 7:00 P. M. to 5:00 A. M. (Japanese Standard Time). When this amount of oxygen is converted into the amount of assimilated carbon, we may obtain 165 mg.C/m³.

On the other hand, the author's experiment[15] showed that in case of the carbon assimilation by phytoplankton, 30–50% of assimilated carbon was simultaneously consumed through the respiration processes. Consequently, an estimate of 85 mg.C/m³/day for the net production rate may be obtained by subtracting the quantity for respiration from the net quantity for assimilation during 10 hours.

This value is considered to represent the upper limit for the assimilation rate, since it was estimated for the area in the vicinity of an island, and since carbon was also consumed by zooplankton possessing no assimilating activity. With these views in mind, the values based upon the phosphate consumption seem to be reliable.

Summary

The author was engaged in the oceanographical observations carried out in a region adjacent to the Aleutian Islands in 1952 and obtained a number of data, on which the present discussions are based.

As the results, slight differences in distributions of nitrate-nitrogen, phosphate-phosphorus and silicate-silicon were found between the northern and southern areas separated by the Aleutian Ridge, although distributions are almost the same in the two areas.

Characteristic features in distributions of these nutrient salts are that the high concentrations were found even in the surface layer, increasing further with maximum gradients in depths within 100–300 m.

The ratios of N:P in the region under

12) G. A. Riley, *J. Mar. Res.*, **6**, 104 (1947).
13) E. S. Nielsen, *J. Couseil. perm. intern. pour l'exploration de la mer*, **18**, 117 (1952).
14) G. A. Riley, *J. Mar. Res.*, **2**, 145 (1939).
15) R. Fukai and K. Okubo, not yet published.

study are lower than the normal ratio given by Cooper; and deficiencies in dissolved oxygen were recognized in the subsurface layers. These facts seem to be related to the characteristics of the decomposition processes in the Aleutian region.

On the basis of the rate of phosphate consumption in the upper layers, the net production rate has been computed by introducing some simplifying assumptions; and has obtained the value of 56 mg. C/m³/day. This value is considered to be reliable, since it coincides with that derived from Riley's data and with that calculated from the data concerning the diurnal variations of dissolved oxygen.

The author is pleased to acknowledge his indebtedness to Prof. Kenjiro Kimura of Tokyo University and Dr. Masao Migita of the Takoi Regional Laboratory for their valuable advice. Acknowledgement is made to Mr. N. Watanabe, who was the leader of the present cruise, for his encouragement and cooperation during the course of the work. The author desires to express appreciation also for the valuable assistance of Miss F. Shiokawa and Miss S. Kojima in the laboratory and all of the members of R. V. "Tenyô-maru," without whose assistance the present work would hardly have been accomplished.

Tokai Regional Fisheries Research Laboratory, Tokyo

Seasonal Variations of Minor Chemical Constituents in the Waters of the Zunan-Kuroshio Region. II. Silicate Contents of Sea Water and Changes in Quality of the Kuroshio*

By Rinnosuke FUKAI

(Received March 20, 1954)

Introduction

In the previous paper[1], the author has studied the problem concerning variations of nitrate and phosphate contents in the waters of the Kuroshio region. The present paper deals with the seasonal variations of silicate contents of water in connection with the changes in quality of the Kuroshio. Although silicate has been regarded as one of the most essential nutrient salts for marine organisms, especially for diatoms, together with phosphate and nitrate, it differs from the other nutrient salts in respect to circulation, the magnitude of the concentration and the physiological significance for organisms.

The author previously made a chemical study on Omura Bay[2] (Nagasaki prefecture, Japan), reporting that, contrary to general expectation, silicate contents of sea water in the estuary of the Kôri river were lower than in the adjacent areas. In this case, however, the physico-chemical state of silicon-compounds colorimetrically determined has not been made clear.

Later, a number of studies were conducted by various authors as to the state of silicon-compounds colorimetrically estimated[3][4], changes in silicate coloration when sea water was diluted with natural fresh water[5] and the state of silicon-ccompounds in hot springs and land waters[6], yielding valuable results.

Although a decisive conclusion has not been reached up to now, it is probable that the most part of silicon-compounds in the oceanic waters may be in a colorimetrically measurable state[7], seasonal variations of which were mainly considered in this paper, not referring to the state of silicon-compounds.

Materials and the Analytical Method

The following discussions are based upon the data obtained for the samples collected from the oceanographical stations illustrated in Fig. 1 of the previous report during the period from January 1950 to Feburuary 1951. The analyses of the samples were carried out as soon as possible after

* Contribution B-No. 144 from the Tokai Regional Fisheries Research Laboratory, Tokyo.

1) R. Fukai, This Bulletin, **25**, 323 (1952).

2) R. Fukai, M. Osako and H. Hamada, *Oceanogr. and Meteorol., Nagasaki Marine Observatory*, **3**, No. 3 (1949) (in Japanese).

3) F. Aoki, *J. Chem. Soc. Japan*, **71**, 634 (1950); **72**, 15 (1951).

4) T. Okura, *J. Chem. Soc. Japan*, **72**, 927 (1951).

5) A. Saeki, *J. Oceanogr. Soc. Japan*, **5**, 41 (1949); **6**, 39 (1950).

6) I. Iwasaki, T. Katsura & T. Tarutani, This Bulletin, **24**, 227 (1951).

7) T. Chow and R. J. Robinson, *Anal. Chem.*, **25**, 645 (1953).

collections either on board ship or on the land, depending on the sea conditions in each observation cruise.

For the analysis was adopted the Dienert-Wandenbulcke's method in which the yellow color of silicomolybdate was developed by addition of ammonium molybdate solution and sulfuric acid. Although further reduction of silicomolybdate by stannous chloride provides the more sensitive method[8], the ordinary method was followed with regard to conditions on board ship. For the color comparison were used the color standard of buffered potassium chromate solution containing borax and improved Hehner tubes with the length of 25 cm., or Beckman's spectrophotometer at a wave length of 380 mμ. Checking experiments were made as to the changes in concentration of silicate which occurred during the standing period of the samples, proving that no change was recognized unless water samples were kept in contact with the glass walls of containers.[9]

Results and Discussions

In order to examine the seasonal variations of silicate in the region under study, it is necessary to distinguish the variations in the surface layers (0–200 m.) from the fluctuations of vertical distributions. The former may be related to prevalence or decline of coastal water masses; and the latter to vertical mixing of water strata due to mechanical disturbance and vartical diffusion.

1. Variations in the Surface Layer.— Variations of silicate contents in the surface layers (0–100 m. and 100–200 m. layers) with those of chlorinity (in 0–100m. layer) at Stations 3 and 6 are shown in Figs. 1 and 2, respectively. The values plotted in the figures are the integral mean values for each water layer.

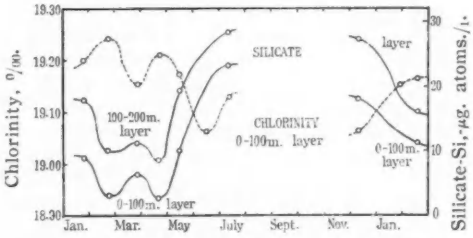

Fig. 1. Seasonal variations of silicate and chlorinity in the surface layers at Station 3. Solid curves: silicate. Broken curves: chlorinity.

From the figure, it is readily noted that chlorinities of the waters in the region decreased in summer, while they increased in winter. It seems to be a remarkable fact that the decrease at Station 6, which is located within the main current of the Kuroshio and is not likely to be affected immediately by land waters, is larger than that at Station 3 located in the mixing region of the Kuroshio with coastal water masses. This may suggest that the decrease in chlorinity of the Kuroshio itself ought to take place before the Kuroshio flows into the region under consideration.

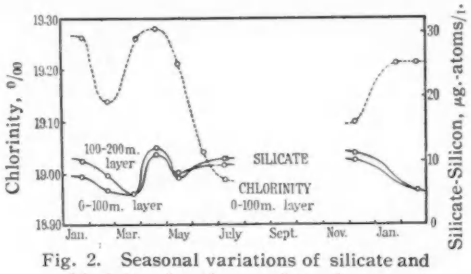

Fig. 2. Seasonal variations of silicate and chlorinity in the surface layers at Station 6. Solid curves: silicate. Brokenc curves: chlorinity.

Silicate contents tend to increase in summer and decrease in winter, being contrary to the variations in chlorinity. This inverse proportionality is remarkable at Station 3. Although the relationship may indicate that silicate contents fluctuate in accordance with the prevalence or decline of coastal water masses, quantitative correlations do not exist.

Now, let us assume that the maximum chlorinity of 19.30‰ represents the normal chlorinity of water in the Zunan-Kuroshio region and that the normal sea water of the region is only mixed up with the fresh water; moreover, let us define the mixing percentage of fresh water, M_f, as follows;

$$M_f = \frac{[Cl]_n - [Cl]_s}{[Cl]_n} \times 100 \qquad (1)$$

where $[Cl]_n$ is the normal chlorinity, namely 19.30‰ in this case, and $[Cl]_s$ is the chlorinity in summer.

The values of mixing percentage calculated from the equation 1 did not exceed 2% as shown in Table I. On the basis of the mixing percentage and silicate contents of sea water in summer, silicate contents of assumed fresh water were computed as shown in the last column of Table I. Among these values, the one for July 1950 is three times higher than the mean value for river waters in Japan. This may indicate that the variations of silicate contents in the surface layers are not controlled only by direct invasion of terrestrial water, even at Station 3, located relatively coastward.

8) A. B. Carlson and C. V. Banks, *Anal. Chem.*, **24**, 472 (1952).

9) R. Fukai, *J. Oceanogr. Soc. Japan*, in press.

TABLE I
ESTIMATED SILICATE CONTENTS OF FRESH WATERS

	ΔCl ‰	Percentage of fresh water mixed	Si in sea water μg.-at./l.	Estimated Si of fresh water mg.-at./l
Station 3				
May 1950	0.13	0.7	9.7	0.5
July ,,	0.17	0.9	27	2.5
Station 6				
May 1950	0.09	0.5	8.2	1.2
July ,,	0.31	1.6	9.3	0.3

As the other origin of *excess silicate* in sea water, the following may be considered:

(1) the silicate-rich substratum,
(2) the decomposition processes of abundant populations of diatoms in summer,
(3) a water mass having high silicate content and low chlorinity.

Among these cases, the former two can hardly be accepted, since the Kuroshio is a stably stratified and origotrophic water mass of the southern origin. Therefore, the last case should be most probable. It cannot be immediately concluded, however, where the origin of a mixing water mass is.

In the variations of silicate and chlorinity, the conditions are quite different between Stations 3 and 6. This suggests that the causes of the variations are not the same at these stations. Whereas it is probable that the variations in the main current of the Kuroshio are being affected by the water of southern origin such as the adjacent water to Formosa or the water of the East China Sea, the effect of the Oyashio might be taken into consideration as the cause of the variation at Station 3, since the Oyashio from the northern areas of the N. W. Pacific prevails along the coastal region of Japan in summer months.

In order to estimate the silicate content of a water mass of northern or southern origin which is likely to mix with the Kuroshio, the mixing percentage of water masses is computed by using the following equation, defining the normal chlorinity of each water mass from the data previously obtained[10,11];

$$M = \frac{[Cl]_n - [Cl]_x}{[Cl]_n - [Cl]_m} \times 100. \qquad (2)$$

The notations in Eq. 2 are the same as in Eq. 1, except that $[Cl]_m$ designates the postulated chlorinity for the mixing water mass.

From the values in Table II, it may be concluded that the actual circumstances are

TABLE II
ESTIMATED SILICATE CONTENTS OF WATER MASSES MIXED WITH THE KUROSHIO
(July 1950)

Water mass	Cl ‰ of water mixed	Mixing percentage	Estimated Si of water mixed μg.-at./l.	Si found in the Kuroshio μg.-at./l.
Northern				
Station 3	18.35	17.9	130	30
Station 6	18.35	32.6	20	30
Southern				
Station 3	17.50	9.4	250	—
Station 6	17.50	17.2	30	—

not explained so far as only the mixing of different sea waters is concerned. Consequently, the mixing with both fresh and sea water must be taken into consideration.

As described above, the variations of silicate contents in the surface layer are complicated. Nevertheless, it is noteworthy that silicate which appears to originate primarily from land waters is related to the changes in quality of the oceanic water mass such as the Kuroshio.

2. Variations below the Subsurface Layer.—The variations of silicate below the subsurface layer cannot be discussed simply. In general, vertical distributions of silicate contents tend to have parallel correlations with those of phosphate above a depth of 1000 m. In the Kuroshio region, phosphate contents reach the maximum at a depth of about 1000 m., while silicate contents increase continuously.

In Fig. 3 is given the relationship between silicate and phosphate contents above the maximum layer of phosphate, together with the data obtained as to the water samples

10) R. Fukai, This Bulletin, in press (1954).
11) Y. Matsudaira and S. Inoue, *J. of Oceanography, Imperial Marine Observatory, Kobe, Japan*, 705 (1939).

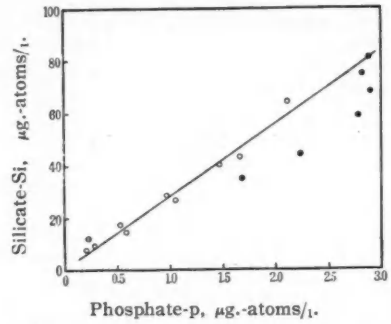

Fig. 3. Relationship between silicate and phosphate. Circles: for the Kuroshio region. Dots: for the Aleutian region.

collected from the Aleutian region. Points in the figure were plotted on the basis of the annual mean values for each of the constituents. A close linear correlation was obtained from these values, although the data for each month were considerably fluctuated. The mean value of Si : P was 28. On the other hand, no linear correlations recognized as to the points for the Aleutian region.

Deviations from the mean ratio of Si : P in the Kuroshio region are especially large in the upper layers. Although relatively close values were obtained as to the waters below subsurface layers, the values tend to fluctuate due to mixing with the waters of deeper layers.

In Fig. 4 are shown the annual mean ver-

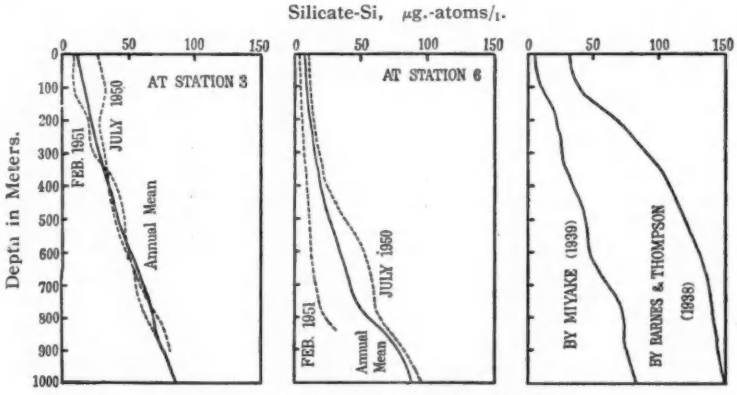

Fig. 4. Vertical distributions of silicate.

tical distributions of silicate and examples of vertical distribution for summer and winter. For a comparison, the vertical distributions obtained by various investigators[12] from the North Pacific were added.

Although the causes for the fluctuation of vertical distributions are not obvious, it should be noted that the whole water column tends to become uniform at Station 6 in winter, suggesting that the mixing with the waters of the substratum due to convection process which may be acting as the controlling factor.

Summary

Seasonal variations of silicate have been considered in the present paper on the basis of the data obtained from the observations carried out from January 1950 to February 1951.

The variations of silicate in the surface layers tend to have an inverse proportionality with those of chlorinity, increasing in summer while decreasing in winter. It is not sufficient to consider that the cause of the variations merely lies in the mixing either with fresh waters from the coast of Japan or with a water mass having low chlorinity and high silicate content. The actual circumstances may probably be caused by the overlapping effect of these two causes.

Although the fluctuation of vertical distributions of silicate below subsurface layer was also complicated, a close linear correlation between annual mean silicate contents and those of phosphate was obtained, to be expressed as the Si : P ratio of 28. However, the vertical distributions fluctuated considerably in the course of time, tending to become uniform in winter.

As the conclusion, it may be estimated that the vertical and lateral mixing of water

12) Y. Miyake, This Bulletin, **14**, 467 (1939); C. A. Barnes & T. G. Thompson, "Univ. of Washington Publ. in Oceanogr.", **3**, No. 2 (1938).

masses is the prevailing factor for the variations of silicate in the region under consideration.

Sincere acknowledgement is made to Prof. Kenjiro Kimura of the Tokyo University for his encouragement and valuable advice during the course of the investigation. The critical reading of the manuscript of Dr. Masao Migita of the Tokai Regional Laboratory is also acknowledged. The author desires to express appreciation for the assistance and untiring zeal of Miss F. Shiokawa throughout the course of the study.

Tokai Regional Fisheries Research Laboratory, Tokyo

Surface Chemistry of High Polymers. V. The Monolayer of Polymethacrylic Acid and its Copolymers with Diethylaminoethyl Vinyl Ether at the Oil/Water Interface

By Hiroshi HOTTA

(Received March 22, 1954)

Previously we studied the monolayer of polymethacrylic acid and its copolymers with diethylaminoethyl vinyl ether at the air/water interface by measuring their surface pressure and potential.[1] Subsequently, we have studied the monolayer of the same samples at the petroleum ether/water interface. The results will be described in the present paper. The effect of the *p*H of substrate on the surface behaviour of polyelectrolyte can be perfectly inferred by comparison between the results at both interfaces. The present investigation provides an useful key to elucidate the nature of the biocolloidal substances.

Experimental

The polymethacrylic acid and its copolymers with diethylaminoethyl vinyl ether (CH_2=CH–O–C_2H_4–N–(C_2H_5)$_2$) (DAV) used in the present study were the same samples as those used in the preceding investigation,[1] and had the composition shown in Table I. Their films were spread from the aqueous solution containing 20% pyridine at the petroleum ether/water interface, using a micrometer syringe according to Alexander and Teorell's method.[2] The *p*H of substrate was adjusted with hydrochloric acid or sodium hydroxide, and measured with "TOYO" *p*H test paper. The occasional test of this value checked by the Beckman glass electrode *p*H meter agreed satisfactorily with each other. The interfacial pressure was measured by ring method,[3] and the interfacial potential by vibrating electrode method using the same apparatus as that described in the previous paper.[4] Detailed descriptions of the spreading technique and of the measurement of interfacial pressure were given in the previous paper.[5] The application of the vibrating electrode method to the measurement of interfacial potential at the oil/water interface has been already tried by Davies.[6, 7] Although the vibrating electrode was immersed in the petroleum ether phase, we took care sufficiently of the amplitude of vibration and the distance of the electrode from the interface not to disturb the film.

TABLE I

THE COMPOSITION OF COPOLYMERS OF METHACRYLIC ACID (MA) WITH DIETHYLAMINOETHYL VINYL ETHER (DAV).

Sample	Mole percentage of DAV in copolymer	Mean molecular weight per vinyl unit
K	31	112
L	20	97
M	0	86

Results

The interfacial pressure (π)-area (A) curves and interfacial potential-area curves at the petroleum ether/aqueous phase at various *p*H interfaces are shown in Figs. 1, 2 and 3, and Figs. 6 and 7, respectively. In these figures, the area was calculated as the mean

1) T. Isemura, H. Hotta and S. Otsuka, This Bulletin, **27**, 93 (1954).
2) A. E. Alexander and T. Teorell, *Trans. Faraday Soc.*, **35**, 727 (1939).
3) A. E. Alexander, "Surface Chemistry" (Supplement of Research) (1949) p. 123.
4) T. Isemura, H. Hotta and T. Miwa, This Bulletin, **26**, 380 (1953).
5) H. Hotta, ibid. **26**, 386 (1953).
6) J. T. Davies, *Nature*, **167**, 193 (1951).
7) J. T. Davies, *Z. Elektrochem.*, **55**, 559 (1951),

area per vinyl unit with the mean molecular weight in Table I. The interfacial moment-area curves, shown by dotted lines in Figs. 6 and 7, were calculated by the usual method as mentioned in the previous paper.[4] Since the measurements of interfacial pressure and potential were carried out separately at room temperature for the reasons of apparatus, the temperature for the two curves was not the same, namely, 17-22°C. for interfacial pressure and 8-11°C. for interfacial potential.

The results for all samples were sufficiently reproducible up to *p*H about 4. On the other hand, the reproduciblity was good for sample K, fairly good for sample L, but somewhat uncertain for sample M in the *p*H range, in which carboxyl groups might be ionized. Therefore, the area in figures is the apparent mean area calculated mathematically in this *p*H range. Uncertainty increases somewhat in the narrower area range. The interfacial potential-area curve for sample M is given only in the case of *p*H 1.6 as a representative in Fig. 7.

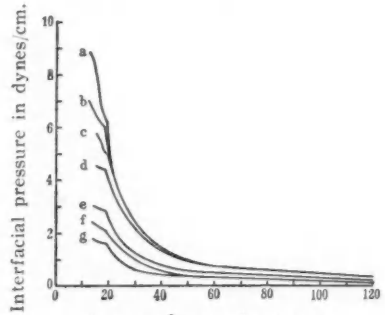

Fig. 1. The interfacial pressure-area curves of sample K at the various *p*H of substrate: curve a, *p*H 1.2; curve b, *p*H 2.8; curve c, *p*H 3.2; curve d, *p*H 3.5; curve e, *p*H 4.0; curve f, *p*H 4.8; and curve g, *p*H 5.7.

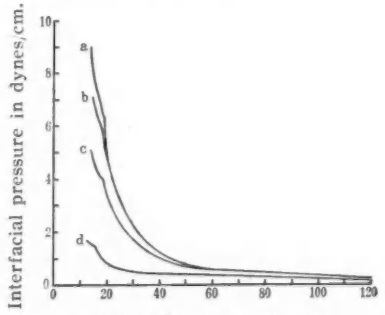

Fig. 2. The interfacial pressure-area curves of sample L at the various *p*H of substrate: curve a, *p*H 1.6; curve b, *p*H 2.6; curve c, *p*H 3.5; and curve d, *p*H 5.8.

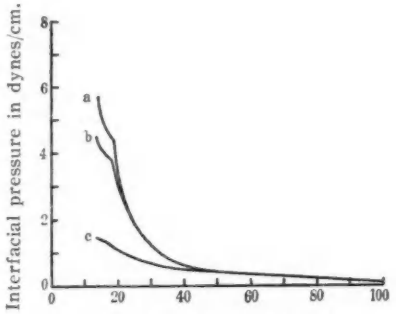

Fig. 3. The interfacial pressure-area curves of sample M at the various *p*H of substrate; curve a, *p*H 1.6; curve b, *p*H 3.0; and curve c, *p*H 3.5.

Discussion

It was concluded from the measurement of surface potential in the preceding paper[1] that, at the air/water interface, the amine groups of the present polyelectrolytes can be ionized by about 20 mol. per cent[8] at the maximum, and that the behaviour of their film can be perfectly understood by Katchalsky's interpretation[9] for the relationship between the state of a molecule and the degree of ionization (or *p*H). In view of the present results, our conclusion was still confirmed.

The film of the present polyelectrolytes is of expanded type as in the case of all other synthetic linear polymers at the oil/water interface[5, 10] as shown in Figs. 1, 2 and 3. The value of $(\pi A)_{A=\infty}$ and the collapse pressure (the interfacial pressure at a kink point) from these figures are plotted against the *p*H of substrate in Figs. 4 and 5, respectively. On comparing these figures with the curve of surface moment against the *p*H of substrate (Fig. 7 in the preceding paper[1]), we noticed that all the curves in these figures are constant up to a certain (and almost same) *p*H, and bend sharply from this *p*H. This tendency might be interpreted as in the case of the air/water interface.[1] That is, up to this critical *p*H the acid groups may be perfectly undissociated and

8) The total ionizable group, namely, the sum of MA and DAV is taken as the unity of the degree of ionization as in the preceding paper.

9) A. Katchalsky, *J. Polymer Sci.*, **7**, 393 (1951).

10) H. Hotta, *Mem. Inst. Sci. & Ind. Research Osaka Univ.*, **11**, 179 (1954).

the amine groups perfectly dissociated; from this *p*H, the total degree of ionization is rapidly affected by the appreciable ionization of the acid group; and at *p*H more than about 6 the film becomes soluble, due to the higher degree of ionization of the acid group. Since the effect of the liberation from lateral cohesion due to the oil phase joins the effect of ionization, the dissociation of the acid group is promoted more and more. Therefore, this effect becomes more considerable at the oil/water interface than at the air/water interface if the *p*H of substrate is the same. It should be more considerable in the case of polyelectrolyte having the higher content of the acid group. The difference of *p*H at a bending point between the three figures can be understood in the light of the effect of the oil phase as mentioned above.

From these reasons, the value of $(\pi A)_{A=\infty}$ for sample M up to a bending point (*p*H 3.5) in Fig. 4 might correspond to that in the undissociated state. Therefore, the length of a statistical kinetic unit in atom unit in the main chain at the oil/water interface, n_{atom}, which is derived from $\left(\frac{kT}{\pi A}\right)_{A=\infty}$, for polymethacrylic acid in the undissociated state is 53 (see Table II). In the range of

TABLE II

THE LENGTH OF STATISTICAL KINETIC UNIT IN ATOM UNIT IN THE MAIN CHAIN (n_{atom})

Sample	n_{atom}
K and L at *p*H 5 (surface isoelectric point)	47
M in undissociated state	53

*p*H more than 3.5 the value of $(\pi A)_{A=\infty}$ increases gradually due to ionization. On the other hand, the values for samples K and L are great at the low *p*H range due to the dissociation of the amine group, but decrease sharply when approaching to *p*H 5, and become 17×10^{-16} erg/vinyl unit for both samples at *p*H 5, which seems to be a surface isoelectric point at the air/water interface.[11] Therefore, the value of n_{atom} for them at this *p*H is 47 (see Table II). The value of $(\pi A)_{A=\infty}$ at the high *p*H range is uncertain, due to the high solubility by the dissociation. The detailed meaning for n_{atom} has been already given in the previous papers.[5,10] On comparing the present values in Table II with the previous ones,[10,11] the value of n_{atom} for the previous non-electrolytic linear polymers (polymethyl methacrylate and amilan) is identical to that for samples K and L, and somewhat smaller than that for polymethacrylic acid. The latter fact may be due to the strong cohesion between undissociated acid groups.[1,11] Of course, all the values are compared in the non-electric state.

The values of $(\pi A)_{A=\infty}$ for samples K and L in Fig. 4 are entirely different at least up to *p*H 3.5, while their collapse pressures in Fig. 5 are completely identical in spite of their

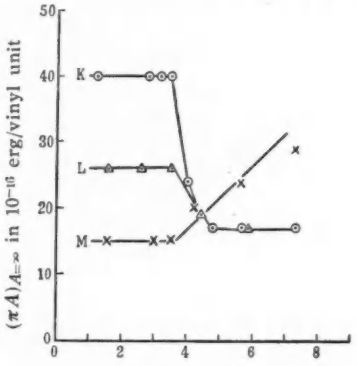

Fig. 4. The $(\pi A)_{A=\infty}$ at the various *p*H of substrate: ⊙, sample K; △, sample L; and ×, sample M.

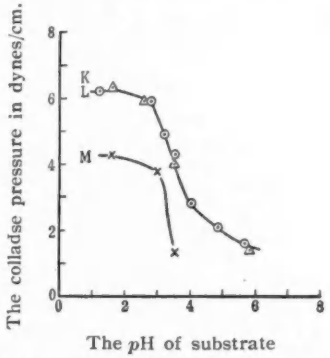

Fig. 5. The collapse pressure at the various *p*H of substrate: ⊙, sample K; △, sample L; and ×, sample M.

different composition as shown in Table I. It is concluded from these facts that the amine groups of these copolymers are perfectly dissociated at the larger area at least up to *p*H 3.5 without the mutual restriction of dissociation due to electrostatic interaction. This may be caused by the liberation from lateral cohesion due to the oil phase. However, the difference between them is no more appeared at the narrow area such as a collapse point similar to at the air/water

11) H. Hotta, This Bulletin, **27**, 80 (1954).

interface, since their dissociation is considerably restricted due to mutual electrostatic interaction, as in the case of condensed film at the air/water interface, and the side chains are immersed into the aqueous phase as discussed in the preceding paper.[1] The present conclusions are also derived from the measurement of interfacial potential as mentioned just below.

The interfacial moments in Figs. 6 and 7 are constant at the area larger than about 50 Å² per vinyl unit, and converge at the narrower area so as to become about 100 mD at 10 Å². When the interfacial moment at the constant range is plotted against the *p*H of substrate in Fig. 8, it has the same

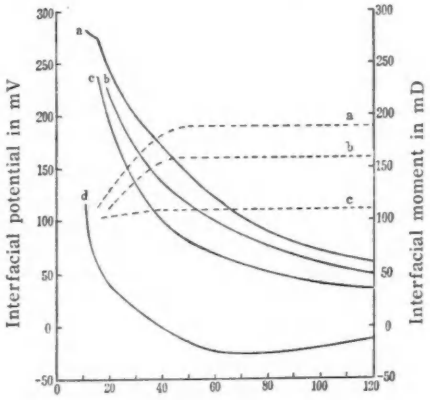

Fig. 6. The interfacial potential (or interfacial moment)-area curves of sample K at the various *p*H of substrate. The interfacial moment-area curve is shown by a dotted line. Curve a, *p*H 1.4 and 3.5; curve b, *p*H 4.2; curve c, *p*H 4.7; and curve d, *p*H 5.6.

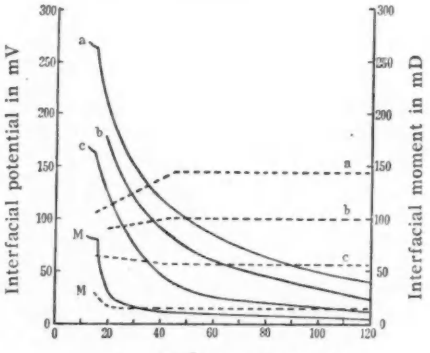

Fig. 7. The interfacial potential (or interfacial moment)-area curves of samples L and M at the various *p*H of substrate. The interfacial moment-area curve is shown by a dotted line. Sample L: curve a, *p*H 1.4 and 3.5; curve b, *p*H 4.2; and curve c, *p*H 4.7. Sample M; curve M, *p*H 1.6.

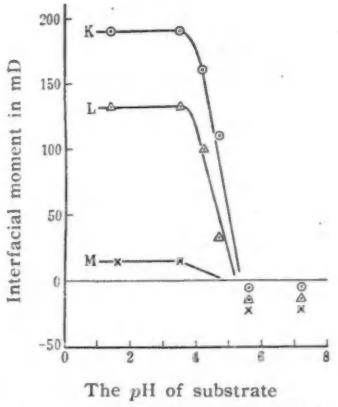

Fig. 8. The interfacial moment at the large area plotted against the *p*H of substrate. ⊙, sample K; △, sample L; and ×, sample M.

tendency as in Figs. 4, 5 and Fig. 7 in the preceding paper,[1] which can be interpreted as mentioned above. The points in the negative side of this figure mean only the inversion of sign qualitatively. The interfacial moments for samples K and L up to *p*H 3.5 in Fig. 8 differ considerably from each other, in contrast to their surface moments which are almost identical at the air/water interface. Assuming the perfect dissociation of the amine group and the perfect undissociation of the acid group, the interfacial moment of the dissociated amine group which is evaluated from their interfacial moment at this *p*H range and their composition in Table I, is 600 mD for both samples. In this evaluation the interfacial moment of the undissociated acid group is assumed to be 15 mD) from the curve of sample M. This value (600 mD) is completely identical with to that found at the air/water interface.[1] It is analogous to the result reported by Davies[6,7] that the surface potential of $C_{18}H_{37}N(CH_3)^+_3$ on 10^{-2} N-NaCl is identical at the air/water and oil/water interfaces. The interfacial moment extrapolated to 10 Å² (100 mD) is almost identical with that at 10 Å² at the air/water interface.[1] These facts correspond exactly to the results of interfacial pressure measurements mentioned above.

The interfacial moment of polymethacrylic

acid at the larger area in the undissociated state (15 mD) is far smaller than that in the same state at the air/water interface (90 mD)[1] This difference is due to the difference of the type of film at the two interfaces. With the increase of the content of methacrylic acid and the decrease of the total degree of ionization, the bending point of interfacial moment-area curves shifts to a smaller area and approaches to 30 Å^2 found at the air-water interface.

Glazer and Dogan[12] recently investigated the state of ionization of insoluble monolayers by the measurement of maximum surface potential at the air/aqueous phase at various *p*H interface. Although they found that the value of *pK* from their surface technique agrees fairly well with that from the measurement in the bulk solution in the case of protein, but not in the case of the low molecules as stearic acid and octadecylamine, they could not explain the latter disagreement satisfactorily. On the other hand, these facts may be understood in the light of our present investigation. The method of maximum surface potential is applicable to protein, which has a rigid structure even at the larger area as well as at a collapse point.[10] But it is unsuitable to low molecules, which have a loosely packed structure between them at the larger area, for the *pK* from bulk solution corresponds to that at an expanded film. To obtain *pK* by the surface technique for such low molecules, the surface moment in a constant range at the larger area should be investigated. Both methods are consistent only in the case, where the surface moment is constant up to a collapse point such as in the case of polymethyl methacrylate and polymethacrylic acid at the undissociated state at the air/water interface.[11] This is the case of protein.

12) J. Glazer and M. Z. Dogan, *Trans. Faraday Soc.*, **49**, 448 (1953).

Summary

As the result of the comparison of interfacial pressure and potential of polymethacrylic acid and its copolymers with diethylaminoethyl vinyl ether at the various *p*H of substrate between the air/water and oil/water interfaces, it is concluded that their films are of the expanded type without the mutual restriction of dissociation at the larger area at the oil/water interface, and, on the other hand, they are of condensed type with such a restriction even at the larger area at the air/water interface. The difference at the two interfaces disappears at a collapse point, where these films are of condensed type.

In conclusion, the author expresses his hearty thanks to Professor T. Isemura for his kind guidance throughout the present work, and to Mr. S. Otsuka in the Institute who kindly supplied many samples to him.

The Institute of Scientific and Industrial Research, Osaka University, Sakai, Osaka

---

The Effects of Substituents on the Hydrolysis of Substituted Cyanamides in Sulfuric acid Solution

By Teruaki MUKAIYAMA, Shin OHISHI[1] and Hiroshi TAKAMURA[1]

(Received April 21, 1954)

Introduction

Mono- and di-substituted cyanamides are hydrolysed in a sulfuric acid solution to give the corresponding ureas. Several works have already been given on the hydrolysis of cyanamide in aqueous acid solutions. In these earlier communications,[2,3,4], it was shown that the reaction is of the first order with respect to the concentration of cyanamide, and the rate increases steadily with increase in acid concentration. The reaction was also shown as an example of hydrogen-ion catalysis which was accepted by Hammett and Paul as an illustration of specific hydrogen ion catalysis.[5]

1) Laboratory of Organic Chemistry, Tokyo Institute of Technology.
2) H. C. Hetherington and J. M. Braham, *J. Am. Chem. Soc.* **45**, 824 (1923).
3) G. Grube and Motz, *Z. phys. Chem.*, **118**, 145 (1925).
4) G. Grube and G. Schmid, ibid., **119**, 19 (1926).
5) L. P. Hammett and M. A. Paul, *J. Am. Chem. Soc.*, **56**, 830 (1934).

Sullivan and Kilpatrick[6] studied the rate of hydrolysis of cyanamide in solutions of nitric, hydrochloric, hydrobromic and trichloroacetic acids, and they explained the results by assuming a two-stage protolysis, the rate-determining step being the reaction between the hydrated cation of cyanamide, $H_2N-C(=NH)-O^+H_2$ and any base present.

Kilpatrick[7] also presented the following paths for the hydrolysis of cyanamide in acid solution,

$$H_2N-C\equiv N \rightleftharpoons H-N=C=N-H \quad (1)$$

$$H-N=C=N-H + A \rightleftharpoons B^- + H_2N-C^+=N-H \quad (2)$$
(I)

$$H_2N-C^+=N-H + HOH \rightleftharpoons H_2N-C(=NH)-O^+H_2 \quad (3)$$
(II)

$$H_2N-C(=NH)-O^+H_2 + B^- \rightleftharpoons A + H_2N-C(=NH)-OH \quad (4)$$

$$H_2N-C(=NH)-OH \rightleftharpoons H_2N-C(=O)-NH_2 \quad (5)$$
(III)

where A is an acid and B is its conjugate base. Step (4) was shown as the rate-determining step.

In the present work, the rate constants of the hydrolysis of mono- and di-substituted cyanamides in 20% sulfuric acid solution were measured. Based on the energies of activation and the entropies of activation obtained, the effect of substituents on the reaction was discussed.

Experimental Part

The hydrolysis of cyanamide to urea is accompanied by a contraction in volume which we made use of to follow the reactions dilatometrically. The experiments were performed in a dilatometer like that described by Broensted, Kilpatrick and Kilpatrick.[8] The dilatometer was a bulb of 10 cc. capacity, from the top of which extended a capillary tube 0.3 mm. in diameter and 15 cm. long. The readings were taken by using a cathetometer.

In order to avoid the formation of air bubbles during the reaction, prior to each run, the solvent was degassed under reduced pressure. The temperature control of the reaction thermostat was accurate to $\pm 0.05°$ within the temperature range 5~85°C.

As an aqueous sulfuric acid is not suitable for kinetic studies owing to the low solubility of cyanamides, dioxane was used as a diluent. Sulfuric acid concentration was 20% by weight in dioxane-water (3:1) solution. In these experiments the initial cyanamide concentration was 0.1 mol.

Mono-substituted Cyanamides.—Ethyl, *n*-butyl, isopropyl, *t*-butyl, allyl and phenyl cyanamides were used. They were synthesized by adding gradually a solution of an amine (1 mol.) in anhydrous ether to cyanogen bromide[9] (1.5 mol.) in anhydrous ether. The temperature of the reaction mixture was kept below 0°C. (except in the case of phenylcyanamide which was prepared at room temperature). After the reaction was completed, the precipitate (amine hydrobromide) was filtered and then ether and unreacted cyanogen bromide were distilled under reduced pressure. The residual cyanamide was then carefully distilled in vacuo. Methylcyanamide and heptylcyanamide synthesized by the above method could not be distilled.

The attempted distillation resulted in the formation of the corresponding melamines in the claisen distilling flask. They were therefore used without further purification. The boiling points and melting point for the amines and the cyanamides are shown in Table III.

TABLE III

Amine	b.p.(C°.)	reference	Cyanamide	b.p.(C°.)	m.p.(C°.)
ethyl-	16.6		ethyl-	94~95/4 mm.	
n-butyl-	77		*n*-butyl-	117/14 mm.	
n-heptyl-	152	(10)	*n*-heptyl-		
isopropyl-	62	(11)	isopropyl-	108/10 mm.	
t-butyl-	44	(12)	*t*-butyl-	109~110/11 mm.	
allyl-	55	(13)	allyl-	92/3 mm.	
phenyl-			phenyl-		42

6) M. J. Sullivan and M. L. Kilpatrick, *J. Am. Chem. Soc.*, **67**, 1815 (1945).
7) M. L. Kilpatrick, *J. Am. Chem. Soc.*, **69**, 40 (1947).
8) J. N. Broensted, M. Kilpatrick and M. Kilpatrick, *J. Am. Chem. Soc.*, **51**, 428 (1929).
9) Organic Syntheses, **11**, 30.
10) Organic Syntheses, **11**, 58.
11) R. Paul, Bull. soc. chem., (5), **4**, 1121 (1937).
12) Organic Syntheses, **29**, 18.
13) Organic Syntheses, **2**, 732.

Di-substituted Cyanamides.—Di-ethyl, di-*n*-butyl, di-isopropyl, di-allyl and di-benzylcyanamides were used. Diethylcyanamide was synthesized from diethylamine and cyanogen bromide. Di-*n*-butylcyanamide,[14] di-allylcyanamide[14] di-isopropylcyanamide[15] were synthesized from the corresponding bromide or chloride by the action of sodium cyanamide. The boiling points and melting point for these cyanamides are shown in Table IV.

TABLE IV

Cyanamide	b.p.(C°.)	m.p.(C°.)
di-ethyl-	78/16 mm.	
di-n-butyl-	120–121/16 mm.	
di-isopropyl-	93–94/25 mm.	
di-allyl-	107–108/18 mm.	
di-benzyl-		53.5

Dioxane used as the diluent was purified by distillation from sodium metal. The reation products, ureas, were identified by their melting points. Diallylurea, which is not recorded in the literature, melted at 64°C, after recrystallization from petroleum ether (Found: N, 19.6. Calcd. for $C_7H_{12}N_2O$: N, 20.0%)

Results and Disscussion

Under the condition of the experiments, as the concentration of (H^+) and (H_2O) can be considered to be constant during the reaction, the reaction velocity can be expressed as follows:

$$v = k \times \left(\begin{matrix} R \\ R \end{matrix} \!\!>\!\! N-C\equiv N \right) \times K$$

where

$$K = \begin{matrix} R \\ R \end{matrix} \!\!>\!\! N-\underset{\underset{O-SO_3H}{|}}{C}=NH \Big/ \left(\begin{matrix} R \\ R \end{matrix} \!\!>\!\! N-C\equiv N \right)(H_2SO_4)$$

On plotting against time t the logarithm of the contraction in volume, ΔY, which had taken place in a constant period of time beginning at time t, we have obtained a straight line. This indicates a first order reaction rate with respect to cyanamide. The rate constant is given[16] by the gradient of such a plot, as shown in Fig. I. The results are shown in Table I.

The rate data were further analyzed by means of the Arrehenius equation

$$\ln k = \ln A - E/RT,$$

and by the absolute rate equation

$$\ln(k/T) = \ln(R\kappa/Nh) + \Delta S^*/R - \Delta H^*/RT$$

The transmission coefficient, κ, was set equal to unity. The calculated kinetic functions are collected in Table II.

14) Organic Syntheses., **1**, 197.
15) W. Traube and A. Engelhardt, *Ber.*, **44**, 3151 (1911).
16) E. A. Guggenheim, *Phil. Mag.*, **2**, 538 (1926).

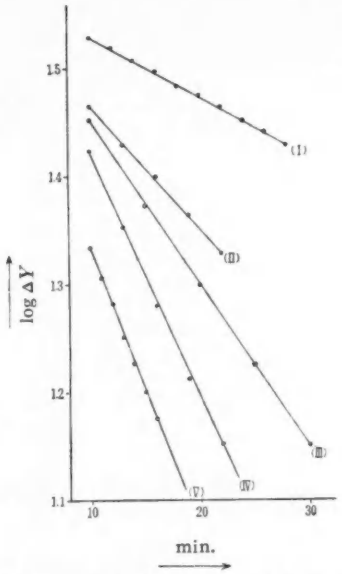

Fig. 1. Hydrolysis of di-ethylcyanamide in 20% sulfuric acid solution: the plot of log ΔY against t.
(I) 26.14° (II) 33.56° (III) 38.50°
(IV) 44.19° (V) 48.15°

TABLE I

THE RATE CONSTANTS OF THE HYDROLYSIS OF SUBSTITUTED CYANAMIDES IN 20% SULFURIC ACID SOLUTION

Cyanamide	t (C°.)	$k \times 10^{-5}$ (sec.$^{-1}$)
methyl-	2.55	5.10
	3.62	6.0
	4.50	6.57
	5.57	7.02
	6.50	7.90
	7.65	8.63
ethyl-	5.55	3.46
	8.25	4.56
	9.21	5.06
	11.25	6.02
	12.15	6.48
	13.10	6.82
n-butyl-	10.0	5.56
	11.13	6.29
	12.15	6.78
	13.20	7.40
	14.18	8.05
	16.78	9.54
n-heptyl-	5.92	5.00
isopropyl	16.52	5.12
	17.32	5.37
	18.06	6.06
	19.08	6.30
	20.10	6.78
	21.20	8.06
	22.50	9.26

t-butyl-	34.10	1.47
	35.07	1.81
	37.47	2.09
	39.0	2.55
	40.83	2.92
allyl-	12.98	6.70
	14.10	7.83
	15.05	8.24
	16.00	9.22
	17.85	11.90
	18.91	14.10
	19.83	14.60
phenyl-	42.75	2.54
cyanamide-	27.07	2.75
diethyl-	26.14	0.394
	33.56	0.613
	38.50	1.06
	41.05	1.25
	44.19	1.72
	48.15	2.06
di-*n*-butyl-	32.45	0.505
	42.55	1.10
	45.92	1.43
	48.60	1.53
	52.10	2.64
	55.20	3.20
di-allyl-	31.10	0.407
	35.16	0.576
	40.03	0.885
	42.88	1.28
	46.80	1.62
	52.50	2.99
di-benzyl-	60.90	0.274
	65.05	0.335
	66.81	0.357
	69.12	0.485
	70.56	0.502
	74.09	0.730
di-isopropyl-	60.90	0.464
	66.04	0.715
	70.74	0.760
	76.22	1.55
	79.81	1.89
	85.04	3.20

TABLE II

THE ACTIVATION ENERGY AND THE ENTROPY OF ACTIVATION FOR THE HYDROLYSIS OF CYANAMIDES IN SULFURIC ACID SOLUTION

Cyanamide	Activation Energy (kcal. mol.$^{-1}$)	Entropy of Activation (cal. mol.$^{-1}$ deg.$^{-1}$)
methyl-	14.8	−26.4
ethyl-	14.4	−29.2
n-butyl-	13.1	−33.6
isopropyl-	17.1	−21.6
t-butyl-	16.6	−28.6
allyl-	19.0	−13.1
di-ethyl-	15.7	−31.4
di-*n*-butyl-	15.9	−30.4
di-allyl-	18.9	−21.6
di-benzyl-	19.5	−21.8
di-isopropyl-	20.2	−23.4

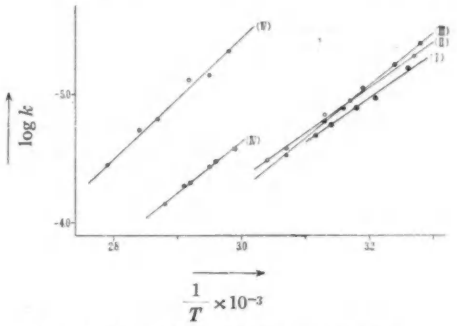

Fig. 2. Hydrolysis of di-substituted cyanamides in 20% sulfuric acid solution: the plot of log k against $1/T$.
(I) di-ethylcyanamide. (II) di-n-butylcyanamide. (III) di-allylcyanamide. (IV) di-benzylcyanamide. (V) di-isoprophylcyanamide.

Cyanamide is hydrolysed to give urea in sulfuric acid solution and the rate of reaction increases as the acid concentration increases. In 10% sulfuric adid solution, the reaction proceeds very slowly.

The effects of substituents on the hydrolysis of the cyanamides in 20% sulfuric acid solution reported in this paper may be summarized as follows:

According to the values of the energies of activation observed for the reaction, the substituents are classified in three groups, (1) normal alkyl groups (13.1–15.9 Kcal.), (2) branched alkyl groups (16.6–20.2 Kcal.) and (3) unsaturated groups (19.0–20.5 Kcal.). The first group contains methyl, ethyl, di-ethyl, *n*-butyl and di-*n*-butylcyanamides, the second isopropyl di-isopropyl and *t*-butyl cyanamides and the third allyl, di-allyl and di-benzyl cyanamides.

As shown in Table I, the rate of reaction for the following eight cyanamides increases in the series:

di-isopropyl- < di-ethyl- < phenyl- < *t*-butyl- < cyanamide < isopropyl- < ethyl- < heptyl-.

The results described above allow the following conclusions to be drawn.

(a) The cyanamide with branched alkyl group requires more energy of activation than the cyanamides with *n*-alkyl group.

(b) The energy required for the hydrolysis of the cyanamides with unsaturated group is nearly equal to those of the cyanamides with branched alkyl group.

(c) In comparing the mono-substituted cyanamide and the di-substituted cyanamide, the latter requires several kilocalories more than the former.

(d) Mono-alkyl cyanamides and mono-isopropyl cyanamide are hydrolysed more easily than the unsubstituted cyanamide.

(e) Phenylcyanamide is hydrolysed more slowly than that which is unsubstituted.

According to the mechanism of hydrolysis of cyanamide in nitric acid solution proposed by Kilpatrick,[7] as mentioned before, the rate-determining step is step (4), which means that (II), the hydrated cation, splits off a molecule of water much more frequently than it yields a proton to an approaching base. In view of experimental results obtained (a)~(e) in this work, however, step (4) is not suitable as the rate-determining step.

On the basis of the electronic effects, supposing that step (4) is the rate-determining step, cyanamides with unsaturated groups would be hydrolysed more readily than the cyanamides with *n*-alkyl groups, because the former cyanamides might be considered to yield a proton to the base more easily than the latter, on account of the negativities of substituents, which make the hydrated cation more acidic. Also, if step (4) limits the reaction, the rates for the hydrolysis of ethylcyanamide, cyanamide and phenylcyanamide should fall into the series,

phenylcyanamide > cyanamide
> ethylcyanamide.

However, the experiments show the reversed order. The result shows that the cyanamides with electron-releasing groups are hydrolysed more easily than the cyanamide with electron-attracting group, like phenylcyanamide.

These experimental results do not support a mechanism which identifies the rate-determining step with the process of attacking by a water molecule of cyanamide cation.

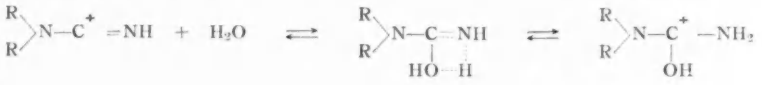

The results (a)~(e) can be rationalized by considering the following paths for the hydrolysis of cyanamide in 20% sulfuric acid solution.

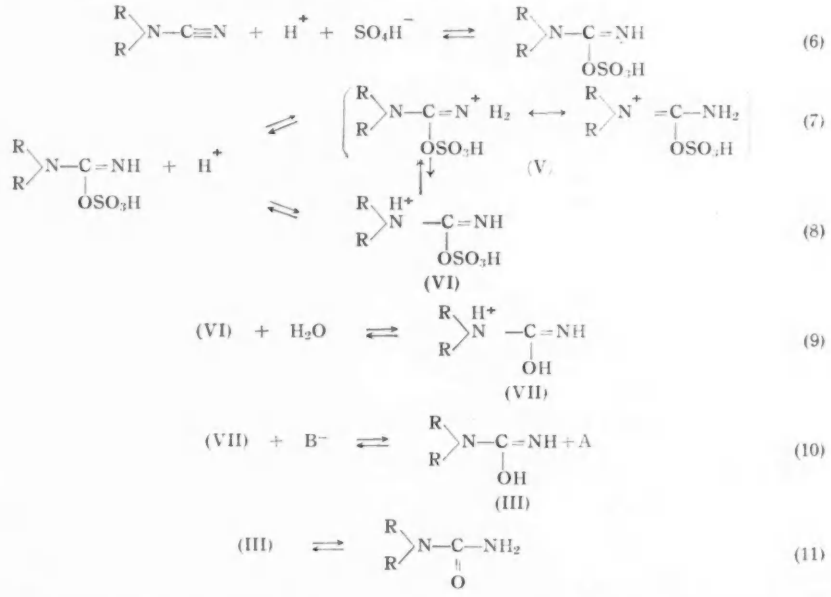

Under the condition of the experiment, cyanamide-sulfate may be formed in the first place, and by the further protonation, formation of disulfate (VI) and (V) may be expected. The less stable tautomer (VI) is hydrolysed very easily to give an isourea cation, which yields a proton to a base to give urea. On the other hand, the stable tautomer

(V) is more difficult to hydrolyse than (VI) and the isourea is formed via process (8) alone.

It is deemed probable that one nitrogen in a mono-substituted cyanamide has a similiar property to a secondary amine and in a di-subtituted cyanamide to a tertiary amine. As explained by the idea of B-strain introduced by C. H. Brown, the tertiary amines are anomalously weak bases even toward protonic acid. The ability of alkyl amine to add a proton at the nitrogen atom by coordination increases along the series:

$$R_3N < H_3N < RNH_2 < R_2NH.$$

This suggests that a second protonation of cyanamide to form disulfate (VI) is more favorable in cyanamides with *n*-alkyl group and mono-substituted ones than in cyanamides with branched alkyl group and di-subtituted ones, respectively.

As shown in Table V, the basic strength of amines are expressed by their pK_b scale.

TABLE V

ethylamine	ammonia	aniline
3.27	4.75	9.4

The order of the rates for mono-substituted cyanamides (ethylcyanamide, cyanamide and phenylcyanamide) have the same order as to the strength of amines.

Therefore, the second protonation of cyanamide, step (8), can be considered as the rate-determining step.

Summary

The energies and the entropies of activation have been determined for the hydrolysis of mono- and di-substituted cyanamides in 20% sulfuric acid solution.

The effect of substituents are distinctly shown in these kinetic data and the substituents are classified in three groups, (1) normal alkyl group substituted, (2) branched alkyl group substituted and (3) unsaturated group substituted cyanamides. The difference in energy of activation required for the hydrolysis of cyanamides may be explained by assuming the intermediate cyanamide-disulfate, the rate-determining step being the second protonation of cyanamide to give cyanamide-disulfate.

Acknowledgment

The authors wish to express their sincere thanks to Professor T. Hoshino for his many helpful suggestions throughout the course of this work, and to Mr. S. Koyanagi for his help in the early stages of this research.

Department of Physics and Chemistry
Gakushuin Univeasity
Mejiro, Tokyo

Sterols and Other Unsaponifiable Substances in the Lipids of Shell Fishes, Crustacea and Echinoderms. XV. Occurrence of Δ7:8-Cholestenol as a Sterol Component of Star Fish, Asterias amurensis Lütken

By Yoshiyuki TOYAMA and Toru TAKAGI

(Received April 26, 1954)

It was shown in the 5th report[1] of this series that the unsaponifiable substances of the lipid of star fish,* *Asterias amurensis* Lütken, caught around Himagajima Island in Aichi Prefecture contained batyl alcohol as a non-steroid component and hitodesterol** as a sterol component. The present paper describes the results of our studies on the sterol components separated from the star fish of the same species, caught around the southern coast of Hokkaido. The acetate of crude sterol mixture was subjected to fractional crystallization, by which an acetate fraction having a constant melting point of 119—120° and other higher melting fractions were easily separated. The acetate of m.p. 119—120° had a saponification value and an iodine value which agreed closely with the calculated values for cholestenyl acetate. The melting points of the acetate, free sterol and benzoate were found to be close to those reported by previous authors for the corresponding derivatives of Δ 7:8-cholestenol (γ-cholestenol). The identity of this star fish sterol with

1) M. Matsumoto, M. Yajima and Y. Toyama, *J. Chem. Soc. Japan*, **64**, 1203 (1943).

* The name of the species *Asterias amurensis* Lütken, was formerly designated as *Asterias rollestoni* Bell.

** Later investigation in our laboratory showed that this sterol has the formula $C_{28}H_{46}O$ or $C_{29}H_{48}O$, having a close resemblance to stellasterol, chondrillasterol and spinasterol, possibly identical with one of them. Cf. The 13th report of this series, Y. Toyama and T. Takagi, This Bulletin, **27**, 39 (1954).

Δ 7 : 8-cholestenol was demonstrated further by conversion of the steryl acetate to Δ 8 : 14-isomer (α-cholestenyl acetate) and Δ 7 : 8, 9-11-cholestadienyl acetate. The higher melting acetate fractions separated from the acetate fraction of m.p. 119—120° yielded, after further recrystallizations a fraction of m.p. 148—153°. Though this fraction was not a single steryl acetate, the easy conversion to its isomer and the saponification and iodine values of the latter appeared to indicate that the fraction of m.p. 148~153° contains predominantly the acetate of Δ 7 : 8-sterol of C_{28} or C_{29} series.

Comparing the above results with those obtained in the previous study, there exists a remarkable difference. While batyl alcohol was easily separated in the previous study, it was not so in the present study. This may be attributable to a far smaller content, if any, of batyl alcohol in the unsaponifiable substances of the present lipid sample. While di-unsaturated hitodesterol was found in the previous study, the sterol mixture of the present lipid sample, as a whole, consisted mainly of mono-unsaturated sterols which contained convincibly Δ 7 : 8-cholestenol. Analogous instances when striking differences exist within an individual lot of aquatic invertebrate of the same species in its unsaponifiable component have already been noted in the case of chiton[2] and corbicula[3]. These facts may possibly be mentioned as a characteristic feature of the unsaponifiable substances of the lipids of some aquatic invertebrates.

Experimental

Some sun-dried star fish, *Asterias amurensis* Lütken, used for these experiments were received from M. Yamada of the Faculty of Fisheries, Hokkaido University. The fish were caught around the southern coast of Hokkaido. The sun-dried material (952 g.) was cut into small pieces. Extraction with ether yielded 84 g. of a dark reddish orange viscous lipid. On treating the lipid with one liter of acetone, an acetone-insoluble oil (73 g.) with the following constants was obtained: d_4^{25} 0.9266, n_D^{25} 1.4733, acid value 71.2, saponification value 162.5, iodine value (Wijs method) 141.5, unsaponifiable matter 15.93%.

Unsaponifiable matter. — The unsaponifiable matter obtained from the acetone-soluble oil by the usual method was a reddish orange solid. The sterol content in the unsaponifiable matter was found to be 52.9% by the digitonide method. The unsaponifiable matter (8.5 g) was recrystallized from 80 cc. of ethanol, yielding a crude sterol (4.2 g.) of m.p. 115–117°. Acetylation of the crude sterol gave a crude steryl acetate of m.p. 115–118° and iodine value* 63.8. Four grams of this acetate was repeatedly recrystallized as shown in Table I.

TABLE I

No. of recrystallization	Solvent	Acetate, crystallized out		Acetate, recovered from mother liquor	
		Yield (g.)	m.p. (°C.)	m.p. (°C.)	Iodine V.
1	Acetone	2.5	125–129	115–116	60.1
2	,,	1.6	127–131	115–116	—
3	,,	0.7	127–137	121–122	66.1
4	Ethanol-ether	0.3	133–145	125–127	66.4
5	Acetone	0.25	140–147	125–132	—
6	,,	0.18	142–147	128–138	—
7	,,	0.12	148–153	135–138	—

Acetate of m.p. 119–120°.—The acetates recovered from the mother liquors of recrystallizations, Nos. 1, 2 and 3, in Table I were united and fractionally crystallized from acetone. After removing a small amount of high melting fraction, a fraction (1.4 g.) of m.p. 119–120° was separated. The melting point was unaltered by further recrystallization from acetone and ethanol-ether, and the fraction recovered from the mother liquors of further recrystallizations showed the same melting point. The fraction of m.p. 119–120° showed $[\alpha]_D^{20} = +5.1°$**, saponification value 131.7 and iodine value 60.5 (calculated for $C_{29}H_{48}O_2$: saponification value 130.8 and iodine value 59.2). Free sterol obtained by saponification of this fraction showed, after recrystallization from ethanol, m.p. 122–123° and $[\alpha]_D^{15} = +4.0$. Benzoate prepared from the free sterol showed, after recrystallization from acetone, m.p. 154–155° and $[\alpha]_D^{15} = +6.8°$.

Δ 8 : 14-Cholestenyl acetate.—The acetate fraction (0.12 g.) of m.p. 119–120° was dissolved in

2) Y. Toyama and T. Tanaka, This Bulletin, **26**, 497 (1953).

3) Y. Toyama and T. Tanaka, This Bulletin, **27** 264 (1954).

* Unless stated otherwise, the iodine values recorded in this paper were determined by the perbenzoic acid method. The pyridine sulfate dibromide method gave an enormously high iodine value of 185.4 for this steryl acetate.

** All rotation were measured with the samples dissolved in chloroform.

15 cc. of glacial acetic acid, and the solution was agitated for 3 hours in an atmosphere of hydrogen in the presence of palladium black. Hydrogen was not absorbed, but isomerization occurred, giving a product of m.p. 76–78° and $[\alpha]_D^4 = +10.8°$. Free strerol from this product showed m.p. 118–120°.

Δ7:8, 9:11-Cholestadienyl acetate.—A solution of 1 g. of the acetate fraction of m.p. 119–120° in 15 cc. of chloroform was mixed with a solution of 2 g. of mercuric acetate in 30 cc. of glacial acetic acid, and the mixture was allowed to stand for 18 hours with frequent stirring.[4] The product, after purification by fractional crystallization from methanol and acetone, showed m.p. 113–115° and $[\alpha]_D^{15} = +32.1°$. It exhibited an ultraviolet absorption curve as shown in Fig. 1

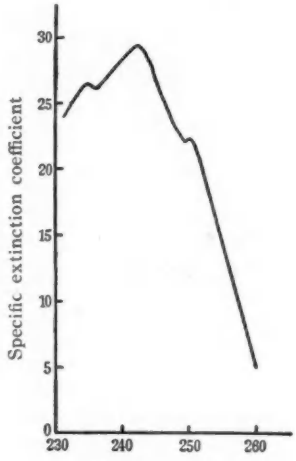

Fig. 1

with the characteristic absorption maxima of 7:8, 9:11-conjugated sterol; log ε_{235} 4.05, log ε_{243} 4.10 and log ε_{250} 3.98 (Fieser[5] give 4.10, 4.15 and 3.96 for the corresponding values).

Higher melting acetate fraction.—The acetate fraction of m.p. 148–153° in Table I had iodine value 67.5. Free sterol from this fraction had m.p. 146–149° and $[\alpha]_D^{15} = +4.3°$. On treating this acetate fraction in a way similar to that described for the acetate fraction of m.p. 119–120°, it underwent isomerization with little hydrogen absorption. The isomerization product, after recrystallization from methanol, showed m.p. 111–113°, saponification value 125.1 (calculated: $C_{30}H_{50}O_2$ 126.7, $C_{31}H_{52}O_2$ 122.8) and iodine value 60.1 (calculated: $C_{30}H_{50}O_2$ 57.3, $C_{31}H_{52}O_2$ 55.6).

Summary

Sterol mixture of star fish, *Asterias amurensis* Lütken, caught around the southern coast of Hokkaido has been found to consist largely of mono-unsaturated sterols. By fractional crystallization of steryl acetate mixture, an acetate fraction of m.p. 119—120° and a higher melting fraction were separated. The fraction of m.p. 119—120° was identified with the acetate of Δ7:8-cholestenol. The higher melting fraction was not a single steryl acetate, but it appeared to contain predominantly the acetate of Δ7:8-sterol of C_{28} or C_{29} series.

The expence of this study was defrayed in part by a grant from the Hattori Hokokai to whom the authors' thanks are due.

Department of Applied Chemistry,
Faculty of Engineering,
Nagoya University, Nagoya

4) Cf. W. Bergmann and P. G. Stevens, *J. Org. Chem.*, **13**, 10 (1948); W. V. Ruyle et al., *J. Am. Chem. Soc.*, **75**, 2604 (1953).

5) L. F. Fieser, *J. Am. Chem. Soc.*, **73**, 5007 (1951).

Theory of Substitution in Conjugated Molecules[1]

By Kenichi FUKUI, Teijiro YONEZAWA and Chikayoshi NAGATA

(Received May 17, 1954)

I. Introduction

What we call the *frontier electron theory*, which has been put forward to explain the reactivity of conjugated molecules, was first introduced in discussing the orientation in electrophilic substitutions in non-substituted aromatic hydrocarbons.[2] Afterwards, this method has been applied not only to electrophilic, but also to radical and nucleophilic substitutions as well as additions in substituted aromatic, heteroaromatic and other conjugated molecules, showing its utility, through a satis-

1) This paper was presented at 7th annual meeting of the Chemical Society of Japan, April 1, 1954.

2) K. Fukui, T. Yonezawa and H. Shingu, *J. Chem. Phys.*, **20**, 722 (1952); K. Fukui, T. Yonezawa and C. Nagata, ibid., **21**, 174 (1953).

factory agreement of theory with experiment, for predicting the reactivity of the π-electron system.[3]

The frontier electron method is based on the assumption that the reaction should occur at the position of the largest density of the electrons in the frontier orbitals, which are defined according to the type of reaction, namely, the highest occupied orbital in the electrophilic reaction, the lowest vacant orbital in the nucleophilic reaction, and both the above in the radical reaction.

Among the existing theories of the chemical reactivity, the frontier electron method is characterized by the fact that it has not been derived deductively from any physical principle established, but has been found from an intuitive but chemical idea relating to the transition state in the process of substitution. By means of comparing the density distribution of the frontier electrons with the experimental positions of attack in the molecule, it has been recognized, rather as a solid fact than as a theory with a strong physical foundation, that frontier electrons must play some important role in the chemical activation.

In this connection, if a theory of substitution in conjugated molecules could be established in such a form as the frontier electron method which is deduced naturally from the mechanism assumed in the theory, it may be said that this theory would give a physical ground on the frontier electron method, and moreover, the mechanism assumed there would provide us with an important key for obtaining the knowledge of the transition state.

Under these circumstances, the present paper treats a theory of substitution in conjugated molecules, which, therefore, involves not a few assumptions. The validity of them can hardly be demonstrated directly, but can be inferred indirectly on the basis of the availability of the frontier electron method derived from them. This is ture because the agreement of the theory with the experiment proved in the preceding papers[2),3)] is sufficiently satisfactory to convince us that the inference mentioned above is probably reasonable.

II. σ-Part of the Energy of the System

As to the theoretical treatment of a substitution in conjugated molecules, there exists no current theory in which the mechanism of formation and dissociation of σ-bonds is taken into consideration explicitly. Consider a substitution in which the substituent atom X, attached to the rth carbon atom in the substrate π-electron system AX is replaced by a certain atom in a reagent B. The substitution is understood to proceed in such a way that the two σ-electrons shift gradually from AX σ-bond to AB σ-bond. A reaction parameter ρ is introduced, which acts as a measure of proceeding of the reaction and is defined by the following equations:

$$\delta_{AB}=\rho b, \tag{1}$$

$$\delta_{AX}=(1-\rho)a. \tag{2}$$

Here δ_{AB} and δ_{AX} are equal to $\int\chi_A H\chi_B d\tau$ and $\int\chi_A H\chi_X d\tau$, respectively, where χ_A, χ_X are the σ-atomic orbital (real) of the rth atom in A, and of the atom X in AX σ-bond, χ_B is the atomic orbital (real) of B which will form a σ-bond in the reaction, H is the effective Hamiltonian operator for a σ-electron, and a and b are the values of δ_{AX} and δ_{AB} in the isolated molecules AX and AB, respectively. The assumption of (1) and (2) may correspond to the mechanism called "bimolecular" by organic chemists. Then, the initial state is represented by putting ρ equal to zero and the final state by putting ρ equal to unity in the equation.

One electron energy can be obtained by solving the secular equation

$$\Delta\sigma(\varepsilon,\rho)=\begin{vmatrix} \alpha_B-\varepsilon & 0 & \delta_{AB} \\ 0 & \alpha_X-\varepsilon & \delta_{AX} \\ \delta_{AB} & \delta_{AX} & \alpha_A-\varepsilon \end{vmatrix}=0 \tag{3}$$

for any value of ρ, where α_A, α_X and α_B are $\int\chi_A H\chi_A d\tau$, $\int\chi_X H\chi_X d\tau$ and $\int\chi_B H\chi_B d\tau$, respectively.

For simplicity, the changes of α_A, α_B and α_X due to the change of ρ are ignored, because they are expected to have less serious influence upon the essence of the theory than the changes of δ_{AB} and δ_{AX}.‡ The following results are obtained by some algebraic manipulations of Equation (3):

(1) Among three roots $\varepsilon_1(\rho)$, $\varepsilon_2(\rho)$ and $\varepsilon_3(\rho)$ of Equation (3) ($\varepsilon_1<\varepsilon_2<\varepsilon_3$), $\varepsilon_1(\rho)$ has a maximum value when ρ varies from zero to unity if either one of the following two conditions, i and ii, is satisfied.

i $\alpha_B>\alpha_X$ and $(\alpha_B-\alpha_X)(\alpha_A-\alpha_X)<b^2$, (4)

ii $\alpha_B<\alpha_X$ and $(\alpha_X-\alpha_B)(\alpha_A-\alpha_B)<a^2$. (5)

(2) As long as the condition (4) or (5) is satisfied, $\varepsilon_1(0)$ is equal to the lower σ-level of AX σ-bond in the isolated AX molecule and $\varepsilon_1(1)$ is the lower σ-level of AB σ-bond in the isolated AB molecule. In this case two σ-electrons in AX σ-bond enter into AB σ-bond across a point of the maximum energy along a continuous curve $\varepsilon_1(\rho)$. Thus (4) or (5) may be regarded as the condition which must be satisfied when the substitution

3) K. Fukui, T. Yonezawa, C. Nagata and H. Shingu, *J. Chem. Phys.*, **22**, 1433 (1954); K, Fukui, T. Yonezawa, C. Nagata and H. Shingu, Summary of the Symposium on Atoms and Molecules, *Japan Phys. Soc.*, p. 27 (1953).

‡ But this is a point which may need further investigation. Especially, it should be noted that the assumption of constancy of both α_A etc. and δ_{AB} etc. sometimes leads us to an unreasonable result (compare e.g. the calculation of H_3 molecule by Van Vleck and Sherman (*Rev. Mod. Phys.*, **7**, 167 (1935)), which is, however, not the present case, where the mode of change of δ's is assumed by the equation (1) and (2).

proceeds adiabatically. In the present paper only the case when this condition is satisfied is treated.

(3) The maximum value of $\varepsilon_1(\rho)$, $\varepsilon_1{}^*$, is given by

$$\varepsilon_1{}^* = \frac{1}{2}[\alpha_A + \alpha_{BX} - \{(\alpha_A - \alpha_{BX})^2 + c^2\}^{1/2}], \qquad (6)$$

and ρ^*, the value of ρ at the maximum point, is also given by

$$\rho^* = \frac{1}{2(a^2+b^2)}[[2a^2 + (\alpha_B - \alpha_X)[\alpha_A - \alpha_{BX} + \{(\alpha_A - \alpha_{BX})^2 + c^2\}^{1/2}]]], \qquad (7)$$

where $\alpha_{BX} = (a^2\alpha_B + b^2\alpha_X)/(a^2+b^2)$, and $c^2 = 4a^2b^2/(a^2+b^2)$. Conditions (4) and (5) correspond to the condition that ρ^* is in the range from zero to unity.

(4) The higher level $\varepsilon_2(\rho)$, which varies continuously from α_B to α_X when ρ changes from zero to unity, has neither maximum nor minimum at $0<\rho<1$, when the condition (4) or (5) is satisfied.

(5) When the eigenfunctions belonging to the eigenvalues $\varepsilon_i(\rho)$ (i=1, 2, 3) are written as

$$\psi_\sigma{}^{(i)} = c_A{}^{(i)}\chi_A + c_X{}^{(i)}\chi_X + c_B{}^{(i)}\chi_B,$$

the following relations always hold between the coefficients in the wave functions.

$$c_X{}^{(1)} \cdot c_B{}^{(1)} > 0$$
$$c_X{}^{(2)} \cdot c_B{}^{(2)} < 0$$
$$c_X{}^{(3)} \cdot c_B{}^{(3)} > 0$$

All of these characteristics derived mathematically from Equation (3) have an important meaning in constructing the theory of substitution.

The energy $\Delta\varepsilon_\sigma$, which is twice as much as the difference between $\varepsilon_1{}^*$ given by Equation (6) and $\varepsilon_1(0)$ and hence may be considered as the σ-part of the activation energy in the substitution, is given by

$$\Delta\varepsilon_\sigma = \frac{a^2(\alpha_B - \alpha_X)}{a^2+b^2} + \sqrt{(\alpha_A - \alpha_X)^2 + 4a^2} - \sqrt{\left(\alpha_A - \frac{a^2\alpha_B + b^2\alpha_X}{a^2+b^2}\right)^2 + \frac{4a^2b^2}{a^2+b^2}}. \qquad (8)$$

The fact that $c_X{}^{(2)}$ and $c_B{}^{(2)}$ have opposite signs is important in connection witn the statement in the next section.

III. Hyper Conjugation in the Transition State

In Section II, it is stated that the coefficients $c_X{}^{(2)}$ and $c_B{}^{(2)}$ in the eigenfunction belonging to $\varepsilon_2(\rho)$ always have opposite signs. Here it is desired to examine generally the quantitative relation between $|c_X{}^{(2)}|^2$ and $|c_B{}^{(2)}|^2$ when ρ is equal to ρ^*, but this is too complicated to be carried out analytically. For this reason the case when B is equal to X is at first considered. We could distinguish B from X e.g. by means of labelling them isotopically. In this case eigenfunctions and ρ^* are easily written explicitly as

$$\begin{aligned}
\psi_\sigma{}^{(1)*} &= 2^{-1/2}A^{-1/2}\{(A - \alpha_A + \alpha_B)^{1/2}\chi_A + 2^{-1/2}(A + \alpha_A - \alpha_B)^{1/2}(\chi_B + c_X)\} \\
\psi_\sigma{}^{(2)*} &= 2^{-1/2}(\chi_B - \chi_X) \\
\psi_\rho{}^{(3)*} &= 2^{-1/2}A^{-1/2}\{(A + \alpha_A - \alpha_B)^{1/2}\chi_A - 2^{-1/2}(A - \alpha_A + \alpha_B)^{1/2}(\chi_B + \chi_X)\} \\
\rho^* &= 1/2
\end{aligned} \qquad (9)$$

where $\psi_\sigma{}^*$ corresponds to ψ_σ when ρ is equal to ρ^*, and $A = \{(\alpha_A - \alpha_B)^2 + 2a^2\}^{1/2}$. The orbital $\psi_\sigma{}^{(2)*}$ in Equation (9) is antisymmetric with respect to the plane which is perpendicular to the line connecting B to X across its middle point.

As the reagent B is believed to approach to the rth atom in A from the direction perpendicular to the plane in which all the carbon atoms of AX lie, this plane is considered to cross the line BX at its middle point when ρ is equal to ρ^*. Thus the orbital $\psi_\sigma{}^{(2)*}$ is parallel to the π-orbitals in A and is antisymmetric to the above-stated plane. This fact is, therefore, sufficient to make us believe the possibility of a hyperconjugation between the π-orbitals in A and the orbital $\psi_\sigma{}^{(2)*}$.* It is not so unreasonable to consider that the hyperconjugation may take place more or less even when B is not equal to X. It is our opinion similar to Mulliken et al. that this hyperconjugation, taking part in the electronic interaction of the system near the transition state, causes a delocalization of π-electrons from A to the reaction center or vice versa and plays an important role in decreasing the activation energy.

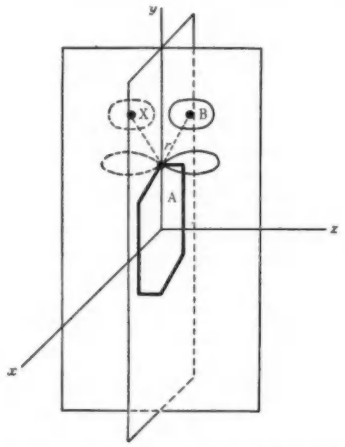

Fig. 1. Schematic diagram of hyperconjugation in the transition state.

IV. π-Part of the Energy of the System

As can be seen in Equation (9) the orbitals $\psi_\sigma{}^{(1)*}$ and $\psi_\sigma{}^{(3)}$ in which coefficient of χ_B is equal to that of χ_X, are free from conjugation with A. In calculating the π-part of the energy, therefore, these orbitals are left out of consideration, even when B is not equal to X, according to the relation mentioned in (5).

The state, in which the total energy of the whole system is maximum, is not always equal to the state $\rho=\rho^*$, except when B is equal to X. Thus, in a strict sence, it is not correct to regard the state $\rho=\rho^*$ as the transition state. But, in order to avoid complicating the problem and missing more

* This consideration was first introduced by Mulliken et al. (L. W. Pickett, N. Muller, and R. S. Mulliken, *J. Chem. Phys.*, **21**, 1400 (1953).) to explain the stabilization of $C_6H_7^+$ ion. Their work modifies the excessively large value of localization energy reported by Wheland (*J. Am. Chem. Soc.* **64**, 900 (1940)).

important conclusions, it might be allowable here to proceed with the discussion taking the state $\rho=\rho^{*}$ as the transition state. The eigenvalue ε_2 belonging to $\psi_\sigma{}^{(2)*}\equiv\psi_h$ is denoted by α_h, and the orbital ψ_h is referred to as a *pseudo-π-orbital*.

The empirical classification of substitution reached by organic chemists, i.e. electrophilic, radical and nucleoppilic is naturally introduced into the theory in the following manner. Namely, acoording as the the reagent B is electrophilic, radical or nucleophilic, the orbital ψ_h is considered to be occupied by 0, 1 or 2 electrons, respectively.

Now the π-energy in the transition state can be calculated by means of ordinary LCAO method. The secular equation for the transition state is written as

$$\Delta_\pi=\begin{vmatrix} \alpha_h-\varepsilon & \tau & 0 & \\ \tau & \alpha_r-\varepsilon & \beta_{r,r+1} & \\ 0 & \beta_{r,r+1} & \alpha_{r+1}-\varepsilon & \\ \vdots & \multicolumn{2}{c}{\left(\begin{array}{c}\text{Secular equation}\\ \text{for AX}\end{array}\right)} & \end{vmatrix}=0, \qquad (10)$$

where each α_s and β_{st} is the Coulomb integral of the sth atom and the resonance integral between the sth and the tth atomic orbitals in the isolated AX molecule, and τ is the resonance integral of the quasi-bond between the pseudo-π-orbital and the rth atom in A. The values of these integrals in Equation (10), which concerns the transition state, differ from those in the isolated molecule, but these differences, which are believed to have no any serious influence on the present theory, are here ignored.

In fact, the change in the Coulomb integral α_r caused electrostatically by the approaching reagent in a heterolytic substitution has no longer any essential significance,* so long as a considerable amount of delocalization of electrons, which will be stated below, takes place.

It is rather easy to extend the present theory to the case when a conjugation occurs between AX and B which possesses π-electrons, but this extension is not included in the present paper[4]

Making use of the perturbation theory by regarding τ as small, the π-activation energy for a non-degenerate system** is obtained as

$$\Delta E_\pi=\sum_{j=1}^{N}\frac{(\nu_j-\nu)C_r(j)^2}{\varepsilon_j-\alpha_h}\tau^2+\nu(\alpha_h-\alpha_B), \qquad (11)$$

where N is the total number of π-orbitals in the isolated AX molecule, ν_j and $C_r(j)$ are the number of electrons (0, 1, or 2) and the coefficient of the rth atomic π-orbital in the jth molecular orbital, respectively, the energy of which is ε_j, and ν is 0, 1 or 2 according as the reagent B is electrophilic, radical and nucleophilic, respectively.

The extent of mutual delocalization of electrons between the pseudo-π-orbital and the initial π-electrons system AX, is represented by

$$\Delta q_h=\sum_{j=1}^{N}\frac{(\nu_j-\nu)C_r(j)^2}{(\varepsilon_j-\alpha_h)^2}\tau^2, \qquad (12)$$

where Δq_h is the difference between the total electron density at BX-part in the transition state and the value ν.

The value of α_h is generally understood to be small for an electrophilic reaction and large for a nucleophilic reaction, but this is not necessarily so in the case when the electron delocalization represented by (12) exists. It can easily be shown that Δq_h is always positive for an electrophilic reaction and is negative for a nucleophilic reaction. The delocalization which occurs in an electrophilic substitution from AX to pseudo-π-orbital makes the value of α_h increase and the delocalization from the pseudo-π-orbital to AX in a nucleophilic substitution makes it decrease, and in both the cases the delocalization will cease after the values of integrals in the whole system become self-consistent. Moreover, in heterolytic reactions, the positive or the negative charge in the activated complex distributes over the whole system and never localizes at the orbital ψ_h. In a homolytic reaction, of course, the value of α_h is very close to that of Coulomb integral of the rth atom in the isolated AX molecule. In these circumstances an assumption is made that α_h is always equal to α, the value of Coulomb integral of a carbon atom in benzene. This assumption may have room for improvement in case of modification of the theory in such a way that the self-consistency is satisfied, but it seems rather more concise and useful in the present stage to grasp the essential feature of the mechanism of substitution.

Putting α_h equal to α, the first term in the right side in Equation (11) is always negative, and so it is seen that the hyperconjugation in the transition state decreases the activation energy in a substitution.

V. Relation to the Frontier Electron Theory

Since the σ-part of the activation energy, (8), is a constant if the reagent B and the substituent X are fixed, the relative rate of substitution of a definite type in conjugated molecules by a definite reagent can be measured by the amount of the coefficient of τ^2 in Equation (11). This quantity referred to tentatively as *super-delocalizability* and denoted by S_r, that is

$$S_r=\sum_{j=1}^{N}\frac{(\nu_j-\nu)C_r(j)^2}{\varepsilon_j-\alpha}\beta, \qquad (13)$$

in which the resonance integral of a C-C bond in benzene, β, is multiplied to make it dimensionless. When ε_j is expressed in the form $\alpha+\lambda_j\beta$,

$$S_r=\sum_{j=1}^{N}\frac{(\nu_j-\nu)C_r(j)^2}{\lambda_j} \qquad (13)'$$

* But the change of β_{XR} must be taken into account when the atom X possesses π-electrons or a π-orbital which can conjugate with the π-electrons in A, because a considerable change in the bond AX may occur in the transition state.

4) C. A. Coulson and H. C. Longuet-Higgins, *Proc. Roy. Soc.*, A **195**, 188 (1948); M. J. S. Dewar, *J. Am. Chem. Soc.*, **74**, 3341 (1952); T. Yonezawa, K. Hayashi, C. Nagata and K. Fukui, *Summary of the Symposium on π-electrons*, Jap. Chem. Soc., p. 26 (1952).

** For a degenerate system a similar equation can easily be derived.

‡ When AX is an odd molecule an equation of type of (15) should be used instead of (11).

Then S_r is positive for almost all of the usual compounds, and the greater the value, the more reactive is the rth position of the compound.

When AX is an even molecule and its occupied levels are denoted by 1, 2,....., m and the unoccupied levels by m+1, m+2,....., N, S_r is written in three cases as:

(i) For an electrophilic reaction

$$S_r^{(E)} = 2\sum_{j=1}^{m} \frac{C_r(j)^2}{\lambda_j},$$

(ii) for a radical reaction

$$S_r^{(R)} = \sum_{j=1}^{m} \frac{C_r(j)^2}{\lambda_j} + \sum_{j=m+1}^{N} \frac{C_r(j)^2}{(-\lambda_j)},$$

(iii) for a nucleophilic reaction

$$S_r^{(N)} = 2\sum_{j=m+1}^{N} \frac{C_r(j)^2}{(-\lambda_j)}. \qquad (14)$$

Since, in many compounds especially in large molecules, λ_m and λ_{m+1} are considerably small compared with the other λ's, the magnitude of S_r is determined predominantly by the term whose j is m+1 or m. $S_r^{(E)}$ is large when $2\,C_r^{(m)2}$, i.e. the electron density at the rth atom in the highest occupied orbital, is large, and $S_r^{(N)}$ is large when $2C_r^{(m+1)2}$, i.e. the electron density at the rth atom in the lowest vacant orbital, is large. In a radical substitution $S_r^{(R)}$ is large when $C_r^{(m)2}+C_r^{(m+1)2}$ is large, so far as λ_m is approximately equal to $(-\lambda_{m+1})$.

When AX is a neutral odd molecule, in which the mth orbital is partly occupied and its energy is approximately equal to α, the perturbation theory for a degenerate system is available. The π-activation energies are obtained as:

(i) For an electrophilic reaction.

$$\Delta E_\pi = |C_r^{(m)}|\gamma + S_r^{(E)}\frac{\gamma_2}{\beta},$$

$$S_r^{(E)} = 2\sum_{j=1}^{m-1} \frac{C_r(j)^2}{\lambda_j} \backsim 2\,\frac{C_r^{(m-1)2}}{\lambda_{m-1}}$$

(ii) For a radical reaction

$$\Delta E_\pi = 2|C_r^{(m)}|\gamma + S_r^{(R)}\frac{\gamma^2}{\beta} + (\alpha-\alpha_B) \backsim 2|C_r^{(m)}|\gamma, \qquad +(\alpha-\alpha_B)$$

$$S_r^{(R)} = \sum_{j=1}^{m-1} \frac{C_r(j)^2}{\lambda_j} + \sum_{j=m+1}^{N} \frac{C_r(j)^2}{(-\lambda_j)},$$

and in this case the first order perturbation term is dominant,

(iii) For a nucleophilic reaction

$$\Delta E_\pi = |C_r^{(m)}|\gamma + S_r^{(N)}\frac{\gamma^2}{\beta} + 2(\alpha-\alpha_B),$$

$$S_r^{(N)} = 2\sum_{j=m+1}^{N} \frac{C_r^{(m+1)2}}{(-\lambda_j)} \backsim 2\,\frac{C_r^{(m+1)2}}{(-\lambda_{m+1})}, \qquad (15)$$

The orbital which determines dominantly the value of S_r in each type of reaction is the same as the *frontier orbitals* which have previously been pointed out by the present authors as playing an important role in the course of reaction. Thus the frontier electron theory is deduced naturally.

If ΔE_π is calculated in the case of naphthalene, as an example, by solving Equation (10) directly without using the perturbation theory, it can be shown that $|\Delta E_\pi|$ of α-position is always larger than that of β-position for any value of γ, and the circumstances are entirely the same concerning 1 and 2 positions in butadiene. The conclusion obtained in the present paper, therefore, never depends on the assumption that the value of γ in (10) is so small that the perturbation method may be used for solving Equation (10).

IV. Summary

A theory concerning the mechanism of substitution in conjugated molecules is stated. The energy of the whole system is divided into σ- and π-parts. When certain relations hold between some integrals of σ-electrons, the σ-part of the energy of the system has a maximum in the process of the reaction, by which the transition state is defined. In the transition state a hyperconjugation may take place between the initial π-electron system and the pseudo-π-orbital in the vicinity of the reaction center. By means of the perturbation method, the π-part of the energy of the system involving the pseudo-π-orbital is obtained. The perturbation energy is always negative and by the magnitude of its absolute value, the reactivity of conjugated molecules can be discussed in a definite type of reaction with a definite reagent. From an approximate expression of this perturbation energy, the frontier electron theory is derived, which has previously been proposed by the present authors, whose coincidence with chemical experiences has already been ascertained. The mechanism stated above, therefore may supply us with a key to grasp a feature of the transition state and at the same time may present us with a physical meaning of the frontier electron theory.

The authors wish to express their heartfelt gratitudes to Professor R.S. Mulliken and to Professor C. A. Coulson for their suggestive discussions on the present problem at the International Conference of Theoretical Physics in Japan, September 1953.

Financial support for this work has been received in part from GAFSR, (1953-59168), Education Ministry, Japanese Government.

Faculty of Engineering,
Kyoto University

Alkylalkoxypolysiloxanes. I. Ethylethoxypolysiloxanes

By Rokuro ŌKAWARA

(Received May 20, 1954)

A series of ethylethoxypolysiloxanes as indicated by formula I and a somewhat similar series[1] were prepared by hydrolyzing the corresponding alkyltriethoxysilane, but the products were not accurately characterized.

$$C_2H_5O\left(\begin{array}{c}C_2H_5\\|\\SiO\\|\\OC_2H_5\end{array}\right)_n C_2H_5 \qquad \text{I}$$

The methylethoxypolysiloxanes[2], having the similar structure as the series I, have also been prepared by the partial hydrolysis of methyltriethoxysilane.

This paper will describe a series of lower members (n=1~4) of ethylethoxypolysiloxanes (series I) which were prepared by a thermal reaction between ethylethoxychlorosilanes and ethyltriethoxysilane at the refluxing temperature.

The thermal reaction between ethyldiethoxychlorosilane and ethyltriethoxysilane was found in the quantitative study of partial ethanolysis of ethyltrichlorosilane to determine the ratio of reaction rate of this competitive consecutive reaction[3]. For the purpose of characterizing these polymerized products, pure ethyldiethoxychlorosilanes and ethyltriethoxysilane were mixed in various mol ratios and refluxed. Changings of the weight, the chlorine content and the boiling point of the mixture were pursued through the reaction. When the chlorine content of the mixture was reduced practically to zero, the mixture was fractionated. A series of linear polymers (series I) was obtained. The first plateau was unreacted ethyltriethoxysilane and subsequent plateaus were the succeeding members of this series. By redistilling these polymers, the presence of a small amount of cyclo-compounds, probably cyclotrimer and cyclotetramer, were found between the succeeding plateaus of linear polymers, but owing to the small amount these cyclo-compounds could not be characterized. Analysis and physical properties of the linear polymers are given in Table II. Properties of the ethyltriethoxysilane are also included for the purpose of comparison.

This thermal reaction was not limited in the case of ethylethoxypolysiloxanes, but the case of ethyl isopropoxy-, ethylmethoxy-, and methylmethoxy-polysiloxanes will soon be reported.

Experimental

Starting Materials.—The ethylethoxychlorosilanes and ethyltriethoxysilane used in this experiment were prepared by the partial ethanolysis of ethyltrichlorosilane[3]. The partial ethanolysis products were fractionated twice through a stedman column of about 20 theoretical plates. Ethylethoxydichlorosilane, ethyldiethoxychlorosilane and ethyltriethoxysilane thus obtained have the following properties.

Ethylethoxydichlorosilane: b.p. 66°C/100 mm Hg, n_D^{20} 1.4100, d_4^{20} 1.0876. Anal. Calcd. for $C_2H_5Si(OC_2H_5)Cl_2$: Cl, 41.0. Found: Cl, 40.4%.

Ethyldiethoxychlorosilane: b.p. 85°C/85 mm Hg, n_D^{20} 1.4007, d_4^{20} 0.9793. Anal. Calcd. for $C_2H_5Si(OC_2H_5)_2Cl$: Cl, 19.4. Found; Cl, 19.1%.

Ethyltriethoxysilane: b.p. 61°C/14 mmHg, n_D^{20} 1.3911, d_4^{20} 0.8963. Anal. Calcd. for $C_2H_5Si(OC_2H_5)_3$: Si, 14.57. Found: Si, 14.50%.

A. Thermal Reaction of Ethyltriethoxysilane and Ethylethoxychlorosilanes: Preparation of the Compounds of the Series I.—Ethylethoxychlorosilane and ethyltriethoxysilane were mixed as shown in Table I. By refluxing, the weight of the mixture and the chlorine content were gradually decreased. After the chlorine content of the mixture practically disappeared, the mixture was further refluxed and tested with Beilstein test to assure that no trace of chlorine compound was found in it. The time needed to produce chlorine free mixture and the highest refluxing temperature attained are cited in Table I.

The products were fractionated through a semimicro stedman column of about 30 theoretical plates under reduced pressure. Unreacted ethyltriethoxysilane was distilled out between 66°–76° C/22–30 mmHg. The disiloxane and trisiloxane fractions were the succeeding plateaus which were obtained at 64°–66° C/0.8 mmHg and 101°–6° C/0.8 mmHg. The amounts in percentage of these plateaus including the intermediate fractions cut on the distillation curve are also shown in Table I.

B. Redistillation of the Polysiloxanes. Isolation and Characterization of Linear Poly-

1) K. Andrianov, *J. Gen. Chem.* (*U.S.S.R.*), **8**, 1255 (1938); **16**, 939 (1946).
2) H. J. Fletcher and M. J. Hunter, *J. Am. Chem. Soc.*, **71**, 2922 (1946).
3) R. Okawara, S. Numa and T. Watase, *J. Chem. Soc. Japan, Ind. Sec.* **57**, 118 (1954) (in Japanese).

TABLE I

RESULTS OF THE THERMAL REACTION

Exp. No.	Starting Material: Compound	(g)	(mol.)	Reaction: Time (hr)	Temp. (°C)	Product: (g)	(% theory)	Polysiloxane Fraction: Monomer (%)	Dimer (%)	Trimer (%)	Residue (%)
1	$C_2H_5Si(OC_2H_5)_2Cl$	11	0.06	45	189	17	90	17	31	22	30
	$C_2H_5Si(OC_2H_5)_3$	11.6	0.06								
2	$C_2H_5Si(OC_2H_5)Cl_2$	8.6	0.05	45	192	20	82	13	10	16	61
	$C_2H_5Si(OC_2H_5)_3$	19.2	0.1								
3	$C_2H_5Si(OC_2H_5)_2Cl$	18.5	0.1	47	212	19.5	91	13	27	27	33
	$C_2H_5Si(OC_2H_5)_3$	9.6	0.05								
4	$C_2H_5Si(OC_2H_5)Cl_2$	9	0.05	62	192	26	88	19	19	29	33
	$C_2H_5Si(OC_2H_5)_3$	24	0.12								

TABLE II

ETHYLETHOXYPOLYSILOXANES

Polymer size	Name	Formula	Boiling Point °C/mm	Density d_4^{20}	Refractive Index n_D^{20}	Molar Refraction Found (Calcd.)*	Molecular Weight Found** (Calcd.)	%Si Found (Calcd.)	%C Found (Calcd.)	%H Found (Calcd.)
Monomer	Triethoxyethylsilane	$C_2H_5O(SiO(OC_2H_5)_2)_1C_2H_5$	61/14	0.8963	1.3911	50.98 (51.08)	—	14.50 (14.57)	—	—
Dimer	Tetraethoxy-1, 3-diethyldisiloxane	— $(SiO(OC_2H_5)_2)_2$ —	65/0.8	0.9473	1.4006	79.53 (79.74)	315 (310)	18.12 (18.06)	46.26 (46.49)	9.44 (9.68)
Trimer	Pentaethoxy-1, 3, 5-triethyltrisiloxane	— $(SiO(OC_2H_5)_2)_3$ —	101/0.8	0.9750	1.4074	108.4 (108.4)	435 (429)	19.70 (19.64)	44.83 (44.82)	9.39 (9.34)
Tetramer	Hexaethoxy-1, 3, 5, 7-tetraethyltetrasiloxane	— $(SiO(OC_2H_5)_2)_4$ —	122/0.8	0.9960	1.4148	137.2 (137.0)	556 (546)	20.63 (20.64)	44.20 (43.92)	8.93 (9.17)

* Calculated from bond refractivities by Warrick, *J. Am. Chem. Soc.*, **68** 2455 (1946)

** Cryoscopic measurements in benzene

mers of Series I.—As the amounts of disiloxane and trisiloxane fraction were small in each experiment, all the polysiloxane fractions except monosilane fraction were gathered (55g.) and again fractionated rigorously through the same column. The distillation curve and the refractive index of the small portions are shown in Fig. I.

The plateaus A, B and C in Fig. I were found to be dimer (tetraethoxy-1, 3-diethyldisiloxane), linear trimer (pentaethoxy-1,3,5-triethyltrisiloxane) and linear tetramer (hexaethoxy-1, 3, 5, 7-tetraethyltetrasiloxane) respectively. Properties of these compounds are given in Table II.

From the knick point of the distillation curve between A and B, and the high refractive index at this portion, the presence of a compound was supposed at this point, but owing to the small amount this compound could not be isolated. Appearance of cyclotrimer (triethoxy-1, 3, 5-triethylcyclotrisiloxane) may be probable at this point, for in the analogous case of ethylisopropoxypolysiloxanes prepared by the same method, the cyclotrimer, which was isolated and characterized, was found

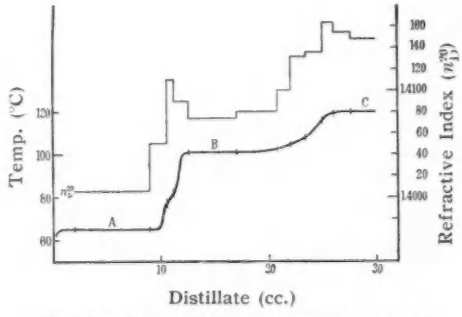

Fig. I. Redistillation curve of ethylethoxypolysiloxanes and the refractive index of the distillates.

A: Dimer
B: Linear trimer
C: Linear tetramer

to be distilled out between the plateaus of dimer and linear trimer. The high refractive index which was found between B and C may also seem to be caused by the presence of cyclo-compound, probably cyclotetramer.

C. Analysis of Silicon.—Silicon was determined by decomposing the sample with concentrated sulfuric acid.

Summary

(1) Ethylethoxypolysiloxanes have been prepared by a thermal reaction of ethylethoxychlorosilanes and ethyltriethoxysilane.

(2) Linear ethylethoxypolysiloxanes containing from 2 to 4 silicon atoms have been prepared and characterized.

(3) Certainly, a small amount of ethylethoxycyclopolysiloxanes were formed by the thermal reaction but they could not be isolated.

Department of Applied Chemistry
Faculty of Engineering
Osaka University
Osaka

On the Synthesis of 8-Hydroxyquinoline

By Akira INOUE, Michio SUGIURA and Yojiro TSUZUKI

(Received May 25, 1954)

Introduction

The object of this investigation is to prepare 8-hydroxyquinoline for the purpose of utilizing quinoline, a constituent of the coal tar bases contained in considerable quantity (ca. 18%). On the synthesis of this substance from quinoline, however, no systematic investigations have been made, in spite of the fact that 8-hydroxyquinoline has been reported to be useful as an organic reagent for the microanalysis of metal irons, as a stabilizer of P.V.A.[1], and a fungicide in the form of its copper salt[2], etc.

The present research was undertaken to find out the best condition of the sulfonation of quinoline, that of the alkali fusion of sulfoquinoline, and that of the preparation of copper 8-hydroxyquinolate in order to obtain 8-hydroxyquinoline as well as its copper salt with good yield.

Sulfonation of Quinoline

The process of sulfonation was adopted as the first stage of the synthesis, because the 8-position of quinoline is, from the view-point of active complex, most active in cationic substitution, is as its highest in electron density (see Fig. 1), and finally because the sulfonic group is expected to enter preferentially into the 8-position considering the previous experimental result.[4]

Purification of Material—Crude quinoline was subjected to fractional distillation with a column

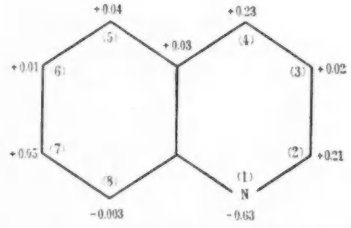

Fig. 1. Electron density of quinoline (C. A. Coulson)

of 2 cmϕ×50 cm under reduce pressure. The boiling point of thus purified quinoline was 113–114°C/17 mm. The content was 65% of the crude material. Isoquinoline distilled at 117–118C°/17 mm; the content was 27%.

Procedure—50 g. of quinoline was dropped gradually in to 150 g. of 50% oleum (fuming sulfuric acid) contained in a 300 cc. flask, equipped with an air-tight stirrer, a dropping funnel, and a reflux condenser. The temperature was kept below 50°C while adding; then the whole was gradually heated to a given temperature, and kept constant there for some hours, as shown in Table I and II. On pouring the reaction product onto ice, 8-sulfoquinoline separated in the form of white precipitate or crystals (m.p. 312°C), while 5-sulfoquinoline (m.p. 59°C), the main by-product, was dissolved into water.

Results—The influence of the temperature on the yield of 8-sulfoquinoline is shown in Table I. The maximum yield (80.3%) was obtained at 140°C. When the reaction is carried out above this temperature, the product is colored brown, the purification becomes difficult and hence the yield is reduced-

1) F. W. Cox, U.S.P. 2,396,555, March 12 (1946).
2) P. G. Benignus, *Ind. Eng. Chem.* **40**, 1426 (1948).

TABLE I
INFLUENCE OF REACTION TEMPERATURE ON THE YIELD OF 8-SULFOQUINOLINE
(The reaction time: 2 hrs.)

Temp. (°C)	Yield (%)	Temp. (°C)	Yield (%)
100	40.7	130	61.7
110	49.4	135	70.4
120	63.9	140	80.3

The influence of the reaction time on the yield of 8-sulfoxuinoline was investigated at 120° and 140°C. The results are shown in Table II.

TABLE II
INFLUENCE OF REACTION TIME ON THE YIELD OF 8-SULFOQUINOLINE

	Yield	
Time (hr.)	120°C	140°C
1	41.7	54.9
2	63.9	80.3
3	53.1	42.4
4	46.9	32.1

G. M. McCasland[2] obtained a lower yield (54%) in the sulfonation of quinoline with 30% oleum at 90°C and 40 hrs. The unfavorable result is probably due to the long heating by which 7- and 5-sulfoquinoline and disulfoquinolines,[4] all soluble in water, are formed. It may be attributed to the formation of these reaction products that the yield decreases, when the reaction is continued further than 2 hrs., as observed in our case (Table II).

Alkali Fusion of 8-Sulfoquinoline

To a quantity of molten (260°C) sodium hydroxide in a graphite crucible is gradually added 20.9 g. (1/10 mol) of 8-sulfoquinoline, and the whole is kept at 300-310°C for 10 to 15 min. Table III shows how the yield of 8-hydroxyquinoline varies with the quantity of sodium hydroxide, which is expressed by a unit of the theoretical quantity, 3 moles of NaOH being theoretically required for one mole of 8-sulfoquinoline.

$$C_9H_6NSO_3H + 3NaOH = C_9H_6NSO_3Na + Na_2SO_3 + 2H_2O.$$

The yield of 8-hydroxyquinoline is expressed by the quantity obtained by distilling with steam for 1.5 hrs.* after alkali fusion.

TABLE III
INFLUENCE OF THE QUANTITY OF SODIUM HYDROXIDE ON THE YIELD OF 8-HYDROXQUINOLINE

NaOH	Yield (%)	NaOH	Yield
1	0	3	38.6
1.5	38.6	3.5	29.0
2	40.7	4	22.1

3) *J. org. Chem.*, **11**, 277 (1946).
4) Claus, Stelzner *J. prakt. Chem.*, [2], **53**, 390 (1896).
* It takes more than one hour, for the black product formed by neutralization with NaOH to turn entirely to a tarry precipitate.

8-Hydroxyquinoline and its Copper Salt

In order to isolate 8-hydroxyquinoline from the product of alkali fusion the following procedure was adopted:

acid decomposition→neutralizaton→steam distillation→8-hydroxyquinoline.

However, complete isolation is not realized by such a simple method, since 8-hydroxyquinoline is slightly soluble in water, and readily soluble both in acid and concentrated alkali, namely, 8-hydroxyquinoline remains in the residue as well as in the filtrate of steam distillation. The following modifications were, therefore, to be made: the product of alkali fusion was decomposed by dilute sulfuric acid, the liquid was carefully neutralized with both concentrated sodium hydroxide and sodium carbonate to a *p*H 7.2, the isoelectric point[5] of 8-hydroxyquinoline, where the solubility in water is the minimum.

These processes were carried out always below 35°C in order to prevent the evaporation of 8-hydroxyquinoline with steam and also to prevent the formation of a cake from the black body formed by the neutralization. The steam distillation is continued for 1.5 hrs. (the quantity of water ca. 1.7 l.), the distillate is cooled, and 8-hydroxyquinoline filtered. The filtrate from 8-hydroxyquinoline, (I), is combined with the filtrate (II), mentioned below. The residue of steam distillation is, after cooling, acidified with dilute sulfuric acid to a *p*H 2.8, so as to precipitate the ferrous 8-hydroxyquinolinate completely, where 8-hydroxyquinoline itself is soluble. The filtrate of ferrous 8-hydroxyquinolinate, (II), is combined with the filtrate (I), and a calculated quantity of crystalline copper sulfate is added, in the state of warm solution, to this combined filtrate, in order to prepare the copper salt of 8-hydroxyquinoline. The crystalline powder of the copper salt, thus formed is filtered at *p*H 2.7–3.2 by treating the mixture with concentrated sodium hydroxide solution at which *p*H the solubility of the copper salt is least and the precipitate of cupric hydroxide dissolved[6]. The copper salt is washed with warm water, and dried at 100°C in an air-bath. The copper salt is prepared from 8-hydroxyquinoline in the following: an aqueous solution containing a little more than the calculated quantity (0.86 times the weight of 8-hydroxyquinoline) of $CuSO_4 \cdot 5H_2O$ is warmed at 80° to 100° and 8-hydroxyquinoline is gradually added to this warm solution, the precipitate is filtered, while still not, at *p*H 2.7–3.2, and dried at 100°C. The yield of the copper salt is nearly 100%.

In Table IV is shown the yield of 8-hydroxyquinoline including copper salt from 8-sulfoquinoline. Even in respect of the yield the present method is superior to the most

5) I. M. Kolthoff, *Chem. Weekblad*, **24**, 606 (1927).
6) H. Gotô, *Sci. Rept. Tôhoku Imp. Univ.*, 1 ser., **26**, 391 (1937).

recent method (67%) of Skraup synthesis[7] from *o*-aminophenol as well as from *o*-nitrophenol.

TABLE IV

NaOH (theoret. quantity=1)	Yield max. (%)	Yield mean (%)	Experimental condition at the max. yield temp. (°C)	Experimental condition at the max. yield time (min.)
2	61.4	50.3	300–325	5
2.5	77.9	59.3	300–310	10
3	84.1	62.6	300–313	10

8-Hydroxyquinoline obtained from the steam distillate was always pure colorless needles, m.p. 73–74°C. Found: C, 74.64; H, 4.93; N, 9.77. Calc. for C_9H_7NO (145.15): C, 74.48; H, 4.83; N, 9.65%. The copper 8-hydroxyquinolinate obtained from the filtrate was a yellowish green crystalline powder, changed to a brown power on heating and carbonized completely at 245°C. Found: CuO, 21.67; calc. for $C_{18}H_{12}N_2O_2Cu \cdot 1/2\ H_2O$[8] (360.84): 22.05%.

7) W. R. Ashford, *U.S.P.*, 2,591,553, July 24 (1951).
8) Y. Nakatsuka. This Bulletin, **11**, 47 (1936).

Summary

1) 8-Sulfoquinoline has been obtained with a yield of 80.3% by sulfonating quinoline with 50% oleum at 140°C for 2 hrs.

2) 8-Hydroxyquinoline has been synthesized by fusing 1 mole of 8-sulfoquinoline with 9 moles of NaOH at 300–315°C for 10 to 15 minutes, decomposing the with dilute sulfuric acid, neutralizing with sodium hydroxide and soda to a *p*H 7.2, and by distilling with steam for 1.5 hrs. The remaining 8-hydroxyquinoline in the residue and in the filtrate was collected in the form of its copper salt. The highest yield of 8-hydroxyquinoline including its copper salt was 84.14%.

3) Copper 8-hydroxyquinolinate has been obtained with a yield of nearly 100% by heating 8-hydroxyquinoline with 0.86 times its weight of crystalline copper sulfate together with a large quantity of water at 80° to 100°C.

The authors are deeply indebted to Mr. K. Arakawa of the Nippon Steel Co., Kawasaki, for his suggestions and help.

Tokyo College of Science
Shinjuku-ku, Tokyo

Rheology of Surface Films. III. A New Type of Surface Rheometer using Electromagnetic Driving Technique[1]

By Kiyoshi INOKUCHI

(Received May 23, 1954)

Introduction

In the course of our effort to establish the standard set of surface rheometry, which involves the rheological measurements of films at liquid surface, the author has previously presented a surface rheometer of wire ring type[2] which enables the film creep to be measured under constant shear stress by using a phototube relay system. This apparatus, although it showed considerable merit in facilitating quantitative analysis of the creep data, was somewhat unsatisfactory in practice, since the construction was comparatively complicated and the operation was not so easy. In addition, it was not readily accessible to the measurements other than the creep test, that is, the stress relaxation test or the dynamic measurement. In order to eliminate these objections and permit wide application to various sorts of measurement, the author again originated a new type of apparatus, using electromagnetic driving technique. The advantage of this equipment lies not only in its ease of operation and simplicity of construction, but also in its accessibility to both static and dynamic measurements. Moreover, the remote control of the instrument, being readily capable using a pair of wires, greatly reduced the experimental care to provide vibration-free operation. The present paper describes the construction of this surface rheometer for static measurement while the description for dynamic measurement will be made in the near future.

1) Presented at the Symposium on High Polymer Chemistry of the Chemical Society of Japan, Oct., 1953, Tokyo.
2) K. Inokuchi, This Bulletin, **27**, 203 (1954).

Construction of Apparatus

The general view of this apparatus is shown in Fig. 1. Principal construction bears resemblance

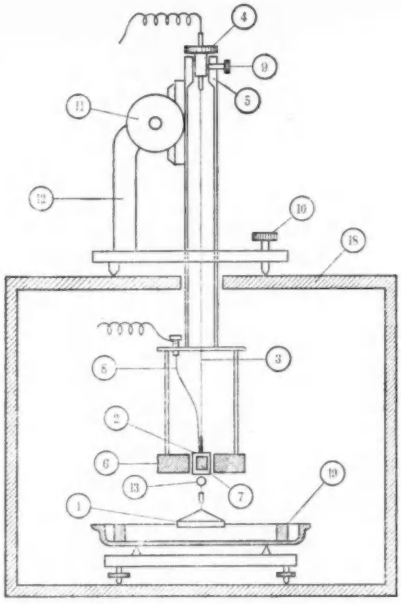

Fig. 1. Elevation view of the instrument.

to the d'Arsonval galvanometer. The actual suspension consists of a ring (1), a moving coil (2), a suspension wire (3), a support rod (4), and a guide (5). The moving coil is just situated between the poles of the permanent magnet (6). The ring is fixed to the moving coil through a small chuck. A light rectangular moving coil is suspended so that its sides lie in the air gaps between the two poles of a permanent magnet and a soft-iron cylinder (7) inside the poles. The suspension wire is an extremely thin strip of copper, which also serves as one of the leads to the coil, the other lead being a loosely hanging thin wire (8) leading upwards from the top of the coil. When the current passes through the coil, a deflecting torque is produced owing to the reaction between the permanent magnetic field and the magnetic field of the coil. Since the pole faces of the permanent magnet are shaped so as to give a radial field and the air gaps between the magnetic poles and iron cylinder are small, the flux density becomes uniform in a radial direction. Hence, the torque causing the coil to rotate turns out to be proportional to the current and constant for all positions of the moving coil as long as its sides are within the pole arcs of the magnet. The magnitude of the torque, therefore, can readily be known by the current of the coil multiplied by a constant.

The level of the coil can be adjusted by raising or lowering the support rod, which is held in place by the screws (9) during run. The centering of the coil is also adjusted by the levelling screws (10) of the stand (12). When the instrument is out of measurement, the support rod is lowered so that the coil becomes mounted on the iron cylinder (7), setting the suspension wire relaxed. The suspension carries a small mirror (13) below the coil upon which a light beam is cast. The beam of light is reflected onto a scale or to a recording photographic paper upon which the deflection is recorded.

The current is supplied from the potentiometer (14), the connection of which is illustrated in Fig. 2. A micro-ammeter (15) is inserted into the cir-

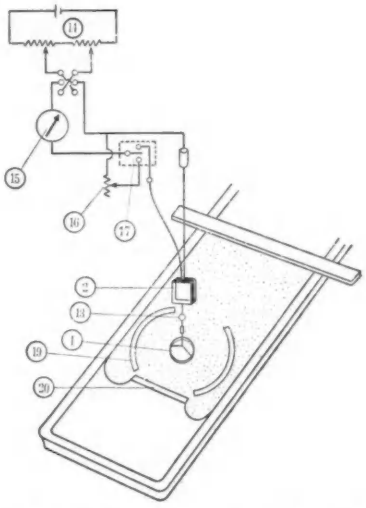

Fig. 2. Schematic illustration of the equipment.

cuit in series with the moving coil (2). In order to avoid the effect due to the eddy current which appears in the coil of the ammeter (15) at the instant of closing the circuit, the coil (2) of the ring provides a resistance (16) parallel with it, the magnitude of which is adjusted to be the same as that of the coil (2). The changeable switch (17) offers the alternative connections of the circuit either to the resistance (16) or to the moving coil (2), the operation of which will briefly be described later.

The ring is a shallow cylinder of platinum, the upper half of which is treated with paraffin, whereas the lower half is left unconditioned. The size of the ring is 3.0 cm. in diameter and 0.3 cm. in height. The moment of inertia of the suspending system was 1.12 g. cm^2. The torsion constant of the suspending wire was 0.016 dyne. cm.

The stand (12) of the instrument was laid on the cabinet (18), only the suspending system being enclosed in it. The instrument was so set that the ring was placed towards one end of the trough, the size of which was $60.0 \times 15.0 \times 10.0$ cm. The ring was provided with a guard (19) of a pair of arc, which was placed in the trough concentric to the ring. The top of the guard was just the same height as the brim of the trough and coated the top face with paraffin for water-repellency.

Determination of Instrumental Constant

The determination of the constant relating the current passed through the moving coil (2) to the deflecting torque applied to it was made as follows. The torsion wire, of which the torsion constant was previously determined, was attached to the moving coil instead of to the ring, and the lower end of the wire was fixed to the ground. The knob (11) was carefully levelled so as to put the wire in proper tension between the coil and the ground. The varying amount of current was let into the coil from the potentiometer, and the respective deflection of the coil was read on the scale by means of a lamp and scale system. As shown in Fig. 3, linear plots were obtained in the current-deflection curve, showing the following equation to be valid

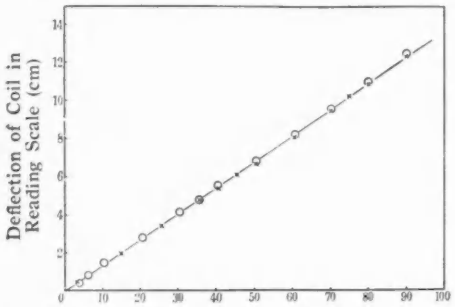

Fig. 3. Current-deflection curve of the moving coil. Circles and crosses represent the plots belonging to different run of measurement.

$$\theta = L \cdot m \tag{1}$$

where θ is the deflecting angle, m, the current, and L, a constant. Since the deflecting torque,* T, is directly proportional to the deflecting angle θ, the following equation holds

$$T = k \cdot \theta \tag{2}$$

where k is the torsion constant of the wire attached below the coil. Hence it turns out from the above equations that the torque is proportional to the current as seen in the following equation

$$T = (L \cdot k)m = p \cdot m \tag{3}$$

where p, being equal to $L \cdot k$, is a constant relating the current to the deflecting torque. In the present apparatus, p was calculated to 0.115 dyne. cm., when m was expressed in microammeter.

Procedure of Operation

The surface of water was cleaned by sweeping with moving barriers. After the ring was lowered so as just to touch the surface of water, the material under test was spread on the surface of the water. By raising carefully the support rod (4) and adjusting the levelling screws (10) for centering the coil, the ring (1) was allowed to be free in suspention. After adequate time was allowed for the equilibrium to be attained, the current was applied to the moving coil (2) of the ring. Prior to the measurement, the current was sent into the circuit turning the switch (17) so that the circuit was closed through the resistance (16), not through the coil (2). In this instant, only the ammeter was actuated by the amount of current which would be applied to the coil in case of measurement. At the time of measurment, the switch (17) was changed to the opposite side so that the current was sent into the coil (2), and the torque was now supplied to the ring without being affected by the eddy current due to the motion of the coil of the ammeter (15).

The deflection of the ring was measured on the scale, or if necessary, recorded on the photographic paper of the rotating drum. Since the deflecting torque of the ring is constant irrespective of the position of the ring if only the current passed through the coil is held constant, the creep curve under constant shear stress can readily be obtained under a constant current throughout the experiment.

If the potentiometer is so adjusted that the deflection of the ring is fixed to a certain value throughout the experiment, and the respective current is measured with time, the stress relaxation curve can readily be obtained.

In calculating the physical constants for the surface viscoelasticity, the film was considered as a mathematical plane. The surface shear modulus of rigidity (G) and surface viscosity coefficient (η) were obtained as follows, respectively, provided that the torque due to the moment of inertia of the rotating system could be ignored,

$$G = \frac{1}{4\pi}\left(\frac{1}{r_1^2} - \frac{1}{r_2^2}\right)\frac{p \cdot m}{\theta} \tag{4}$$

$$\eta = \frac{1}{4\pi}\left(\frac{1}{r_1^2} - \frac{1}{r_2^2}\right)\frac{p \cdot m}{\dot{\theta}} \tag{5}$$

where r_1 is the outer radius of the ring, and r_2 the inner radius of the guard coaxial to the ring, respectively.

In the present experimental condition, the stress as well as the strain applied to the film was not uniform throughout the film but varied with the distance from the center of the ring. The stress, S, applied to the outer radius of the ring was given by the following equation, when the moment of inertia of the ring might be ignored.

$$S = \frac{p \cdot m}{2\pi r_1^2} \tag{6}$$

In our usual experimental condition, in which the film resistance is sufficiently large compared with that of water, the water effect is negligibly small, and the immersion depth of the ring does not matter. However, if the film resistance is so small as to be comparable to that of pure water, the immersion depth would have to be taken into account.

* Since the torsion constant of the suspending wire was suffiiciently small compared with that of the wire attached below the coil, proportionat constant between T and θ was simply taken as k, neglecting the deflecting torque due to the suspension wire.

Discussion

Strictly speaking, the deflecting torque, T, should be expressed as follows, taking the torque due to the moment of inertia of the rotating system into consideration

$$T = p \cdot m - I\ddot{\theta} \qquad (7)$$

where I represents the moment of inertia, and $\ddot{\theta}$, the acceleration of the motion of the ring. The author, however, expressed the deflecting torque, T, simply as $p \cdot m$ in equation (4) and (5), neglecting the term $I\ddot{\theta}$. This was because of the fact that, in our usual experiment, $I\ddot{\theta}$ was sufficiently small compared with $p \cdot m$, since very slow creep was mainly subjected to our experiment and the value of I is comparatively small. However, if it were the case, in which $I\ddot{\theta}$ could not be neglected against $p \cdot m$, the correction for the moment of inertia should, of course, be made.

The electromagnetic driving technique very much extended the range of measurement with satisfactory precision. The upper limit of the stress available might be decided by the permissible strength of the current through the wire, in order that over-heating might not occur through the coil. On the other hand, the lower value of the stress might be limited by the extent, to which the stress applied by the current can practically cover the second ary torque due to the torsional drag of the suspension wire, or to the asymmetry of the rotating system, since the present apparatus must satisfy the condition that the deflecting torque is independent of the position of the coil. Using a changeable shunt for the micro-ammeter, the apparatus permitted the measurement over a range of stress from about 3×10^{-3} to about 1×10^{1} dyne per cm. without changing any element of the coil. Such an extremely wide application of the stress is a practical advantage over the previous instrument using a torsion wire, in which a fairly large number of wires must be interchanged in order to apply such a wide range of stress.

The standard deviation of a set of data which appeared in the deflection-current curves was consistently less than 2% and the error inherent to the apparatus was considered to be practically satisfactory. The absolute values of visicosity or elasticity obtained with a different run of experiment using real films however, were found to fluctuate to a considerable extent. This may be due to some uncontrollable experimental conditions which affect the formation of the structure of solid films, and is, of course, not an inherent fault of the apparatus.

Another advantage of this equipment lies in the remote control of operation, which is readily available using a pair of wires. The remote control increases not only the ease of operation, but also serves to provide the vibration-free experimental condition, which is essential for the study of surface films.

In addition to the static measurement, the determination and the analysis of the dynamic modulus is also an important problem of the study. If the alternating current of proper frequency would be introduced into the coil of this apparatus, and the response of the ring would be detected with reference to the input stress, the present apparatus would also be accessible to the dynamic measurement of the film.

Summary

In order to establish the standard set of surface rheometry, which involves the rheological measurement of films at liquid surface, a new type of surface rheometer was devised using electromagnetic driving technique. The advantage of this apparatus lies not only in its ease of operation and simplicity of construction, but also in its accessibility to various sorts of measurement. In addition, the wide range of measurement and remote control of operation provide a practical advantage for the experiment of surface films.

The author wishes to express his hearty thanks to Prof. Taro Tachibana for his helpful advice and encouragement.

Department of Chemistry, Faculty of Science, Ochanomizu University, Tokyo

Spectrochemical Study of Microscopic Crystals. VI.[1] *Light Absorption of Non-planar Quadri-co-ordinated Complexes*

By Shoichiro YAMADA and Ryutaro TSUCHIDA

(Received June 16, 1954)

In the former reports,[1,2] the present authors studied dichroism in the visible and ultra-violet of metallic quadri-co-ordinated complexes possessing planar configuration, and established the common rules on the dichroism. It is known that some metals such as copper (II) and cobalt (II) form non-planar quadri-co-ordinated complexes in addition to planar ones: e.g., $Cu(H_2O)_4^{++}$ in the crystal of $CuSO_4 \cdot 5H_2O$ is square,[3] and $CuCl_4^{--}$ in the crystal of Cs_2CuCl_4 has a distorted-tetrahedral configuration.[4] Complexes with distorted-tetrahedral configuration would probably show more or less remarkable anisotropy of light absorption, whereas complexes with regular-tetrahedral configuration would exhibit very slight or no anisotropy. Measurements of pleochroism may, therefore, be expected to throw some light upon the nature of chemical linkages as well as upon the configuration. For the above purpose Cs_2CuCl_4, Cs_3CoCl_5 and $K_2Co(NCS)_4 \cdot 4H_2O$ have been studied. In the present work absorption spectra of the above compounds in the crystalline state have been quantitatively determined, and the results of the measurements have been discussed in relation to the configuration of the complex ions.

Experimental

Materials.—Cesium cobaltous pentachloride was prepared in blue tabular crystals by spontaneous evaporation at a room temperature of aqueous solution of cobaltous chloride and excess of cesium chloride.[5] The crystals, which belong to the tetragonal system, show straight extinction and very slight dichroism. Measurements of absorption spectra were made on the face (100) with polarized light having its electric vector along the directions of extinction.

Crystals of cesium tetrachloro-cuproate were obtained by evaporating at a room temperature an aqueous solution of cesium chloride and cupric chloride.[4] The orange, tabular crystals thus obtained show a dichroism; they appear orange with electric vector parallel to the b-axis, and yellow with that perpendicular to the above. Optical measurements were performed in the (101) face with reference to the above two directions.

Potassium tetrathiocyanato-cobaltoate tetrahydrate was prepared in blue prismatic crystals by the method of v. Grotthus.[6] The crystals of the orthorhombic system show a definite dichroism in the prism face; they appear blue with the electric vector along the direction of elongation and pale blue with that perpendicular to the above. Dichroism measurement was carried out in the prism face with reference to the above two directions. The absorption spectrum was also determined with its solution in 99% alcohol containing potassium thiocyanate.[7]

Measurements.—Quantitative measurements of absorption spectra of crystals were made at room temperature by Tsuchida-Kobayashi's microscopic method[8] with polarized light in the region covering 7500 to 2400Å. α represents the absorption coefficient of a crystal. Molecular absorption coefficients of a crystal, k, were calculated from the relation, $k = 10\alpha M/\rho$, where M and ρ denote formula weight of a complex compound and density of a crystal, respectively.

Absorption spectrum in solution was determined with a Beckman DU quartz-spectrophotometer. ε represents extinction coefficient of the solution.

Results and Discussion

Cesium Tetrachlorocuproate.—According to the result of the crystal structure analysis,[4] the crystal consists of cesium ions and $CuCl_4^{--}$ anions having configuration of flattened tetrahedron. The maximum of the band at the longest wave-length could not be determined, since the band extends into the infra-red beyond the region of the measurement. Comparison of the absorption curve (Fig. 1) with previously reported data of other cupric complex compounds and analogy to cobaltic and chromic complexes indicate that the band with its maximum in

1) Part V of this series, S. Yamada and R. Tsuchida, This Bulletin, **27**, 156 (1954).

2) R. Tsuchida, S. Yamada and H. Yoneda, *J. Chem. Soc. Japan* **69**, 145 (1948); S. Yamada, *J. Am. Chem. Soc.*, **73**, 1182 and 1579 (1951); S. Yamada and R. Tsuchida, This Bulletin, **26**, 72 (1953).

3) C. A. Beevers and H. Lipson, *Proc. Roy. Soc.*, London A**146**, 570 (1934).

4) L. Helmholz and R. F. Kruh, *J. Am. Chem. Soc.*, **74**, 1176 (1952).

5) H. M. Powell and A. F. Wells, *J. Chem. Soc.*, **1935**, 359.

6) T. v. Grotthus, "Gmelins Handb. d. anorg. Chem.," 8. Aufl., 1932, **58**), 431.

7) The authors are indebted to the Analytical Laboratory of our department for the measurement of the solution with a Beckman spectrophotometer.

8) R. Tsuchida and M. Kobayashi, "The Colours and the Structures of Metallic Compounds," Osaka, 1944, p. 180.

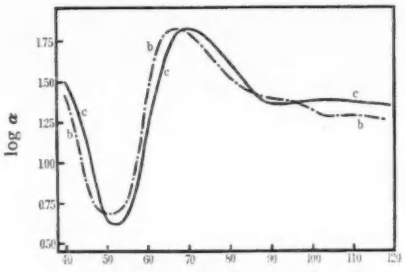

Fig. 1. Absorption spectra of Cs_2CuCl_4.

the infra-red region (band A) is considered to be due principally to electronic transitions of co-ordination electrons around the core of the metal atoms, and the band with its maximum at ν=about 70×10^{13}/sec. (band B) may be due largely to the existence of the negative ions in trans-positions.[9]

It is seen from the result of the crystal structure analysis that the b-absorption, absorption with electric vector parallel to the b-axis, is more abundant with the z-component than with the x-component

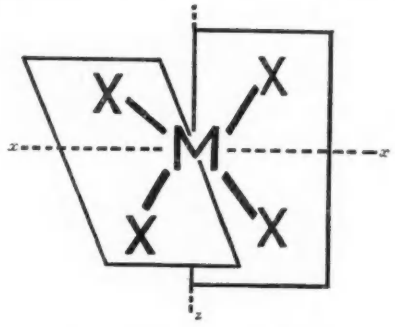

Fig. 2. Flattened-tetrahedral configuration of quadri-co-ordinated complexes.

(Fig. 2.), and that the c-absorption is richer in the x-component. From the configuration of the complex anion, anisotropy is expected for the crystal. The expectation is satisfied by the present measurement, which indicates that for the band B and also possibly for the band A the Z-absorption is bathochromic to the X-absorption. (Table I)

TABLE I

ABSORPTION MAXIMA OF Cs_2CuCl_4 IN THF CRYSTALLINE STATE

	ν,10^{13}/sec.	logα	M
b-abs.	67.0	1.82	9.11×10^4
c-abs.	70.0	1.82	9.11×10^4

The qualitative absorption spectrum of the compound was reported by Helmholz et al.[4] with the solid suspended in the mineral oil, but their results are not in good agreement with ours where a single crystal is used instead of powdered solid in oil.

Tricesium Cobaltous Pentachloride.—According to the X-ray analysis of the crystal,[5] the crystal consists of $CoCl_4^{--}$ cesium and chloride ions, $CoCl_4^{--}$, being regular-tetrahedral. Therefore, very slight or no anisotropy of light absorption can be anticipated for the crystal of the compound. Actually very slight anisotropy of absorption was observed (Fig. 3. and Table II). Slight dichroism may

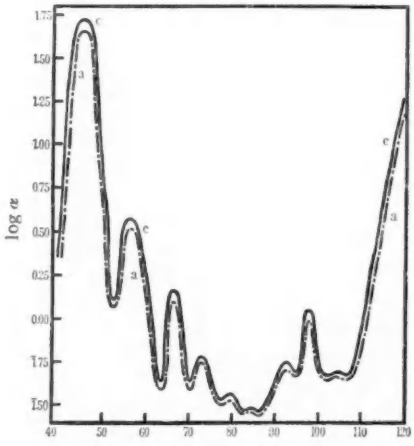

Fig. 3. Absorption spectra of Cs_3CoCl_5.

be attributed to the dissymmetrical crystalline field. The above result lends a further support to the regular-tetrahedral configuration of the quadri-co-ordinated complex in this crystal.[5] Recently Katzin et al.[10] reported reflection spectra with powdered solid of dipyridinium and dicesium tetrachloro-

TABLE II

ABSORPTION MAXIMA OF THE CRYSTAL OF Cs_3CoCl_5

ν,10^{13}/sec.	45.0	56.8	66.6	73.2	80.0	84.3	92.8	98.0
logα_a	1.65	0.51	0.10	$\bar{1}$.75	$\bar{1}$.53	$\bar{1}$.43	$\bar{1}$.69	$\bar{1}$.57

9) R. Tsuchida, This Bulletin, **13**, 436 (1938), Such a kind of band was named "third absorption band". See also, F. Basolo, *J. Am. Chem. Soc.*, **70**, 2634 (1948); ibid., **72**, 4393 (1950).

10) L. I. Katzin and E. Gebert, *J. Am. Chem. Soc.*, **75**, 2830 (1953).

11) A. v. Kiss and M. Gerendas, *Z. physik. Chem.*, **A180**, 117 (1938).

cobaltoates, both containing $CoCl_4^{--}$ ions. Their results, however, were only qualitative and limited within the visible region, although the absorption maxima reported by them generally coincide with the results of our present measurement. A. v. Kiss et al.[11] also reported absorption spectra of aqueous solution containing cobaltous chloride and great excess of chloride ions in the visible and ultra-violet. They recorded a number of sharp peaks. Most of the absorption peaks which have been found in the present measurement almost correspond with those reported by them. There were reported, however, other peaks in their work which have not been observed in our measurements.

Inspection of absorption spectra of the crystal leads us to the idea that the absorption bands of the complex anion between $\nu=45$ and 85×10^{13}/sec. may form one series. As reported in our recent communication,[12] wave numbers of the absorption peaks in the above series can be expressed by the following equation,

$$\tilde{\nu}=\nu_0+am-bm(m+1), \qquad (1)$$

where $\tilde{\nu}$ represents the wave-number of a peak, $\tilde{\nu}_0$ the wave-number of the band head, a and b constants, and m positive integer including zero (Table III). The following

TABLE III

A SERIES OF ABSORPTION PEAKS OF Cs_2CoCl_5 IN THE CRYSTALLINE STATE

m in eq.(1)	0	1	2	3	4	5
$(\tilde{\nu})$obs	15.0	18.9	22.2	24.4	26.7	28.0
$(\tilde{\nu})$cal	15.0	18.8	22.0	24.6	26.6	28.1

values have been obtained for a and b: $a=4.37\times10^2$/cm. and $b=2.92\times10^2$/cm. The expression of the form (1) may be derived readily in the approximation, using a familiar expression for an anharmonic oscillator[13] and assuming (a) that the absorption peaks correspond to transitions from the ground electronic state with vibrational quantum number zero to the excited electronic state with m as the vibrational quantum number, and (b) that the vibrational frequency is altered very little in the electronic transitions. Judging from the order of the vibrational frequency and considering that the measurement was made at room temperature, the former assumption may be permissible. The intensity relation of the absorption series may be understood qualitatively on the basis of the above assumed mechanism of the transition.[14] Using the above derived constants and assuming the above mechanism of the transition, the dissociation energy of the complex ion is estimated,[15] in the rough approximation, as 40.2 kcal. per mol. The value thus obtained seems reasonable,[16] favouring the above assumption. The fact that the band peaks can be correlated with electronic-vibrational transitions supports the view that the series of band peaks is due principally to transitions of the coordination electrons of the complex anion.[17,18] A similar fine structure had been reported by Shibata et al.[19] with solution of several metallic compounds at the temperature of liquid air, and an equation had been given to represent wave-numbers of absorption peaks in the fine structure.

Potassium Tetrathiocyanato-cobaltoate Tetrahydrate.—The compound in the crystalline state shows bands at $\nu=50$ and about 100×10^{13}/sec. and one more band in the infra-red; no measurement of the latter band was made in the present work. From comparison of the absorption curves (Fig. 4. and

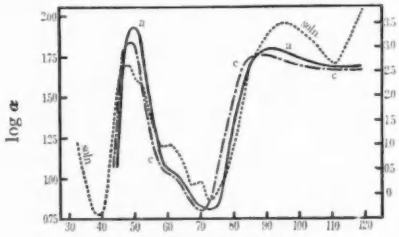

Fig. 4.
Absorption spectra of $K_2Co(NCS)_4\cdot4H_2O$.

TABLE IV

ABSORPTION MAXIMA OF $K_2Co(NCs)_4\cdot4H_2O$

	ν,10^{13}/sec.	logα	M	ν,10^{13}/sec.	logα	M
a-abs.	49.8	1.98	2.18×10^5	91	1.79	1.46×10^5
c-abs.	49.2	1.84	1.58×10^5	88	1.76	1.36×10^5

12) S. Yamada and R. Tsuchida, *J. Chem. Phys.*, **22**, 1273 (1954).

13) See, for example, G. Herzberg, "Spectra of Diatomic Molecules," Van Nostrand Company, New York, 1950, p. 151, etc.

14) For example, Ref. 13), p. 193, etc.

15) See, for example, K. S. Pitzer, "Quantum Chemistry," Prentice-Hall, New York, 1953, p. 255. The equation for diatomic molecules is tentatively assumed in the present estimation.

16) From spectroscopic study, Shibata et al. (Ref. 19) reported 48 kcal. for the dissociation energy of ($CoCl_2$ · acetone).

17) R. Tsuchida, This Bulletin, **13**, 388 (1938).

18) A similar conclusion was formerly drawn by v. Kiss et al, (Ref. 11).

19) Y. Shibata and K. Harai, *J. Chem. Soc. Japan*, **56**, 1 (1935).

Table IV) with that of tricesium cobaltous pentachloride, it is considered that the absorption band at $\nu = 50 \times 10^{13}$/sec. corresponds to the band at $\nu = 45 \times 10^{13}$/sec. in Cs_3CoCl_5, being due mainly to co-ordination electrons, and that the band stretching from ν = about 80×10^{13}/sec. further into the ultra-violet may correspond to "specific band,"[20] which is principally due to the NCS^- ions in co-ordination. The absorption spectrum of cobaltous thiocyanate in aqueous solution containing excess of potassium thiocyanate was reported by Kiss et al.[21] Their data roughly coincide with our result, but differ in detail, probably because their measurements were made with the mixed solution, involving much more complicated factors as compared with ours. It is seen that the crystal of the compound shows the corresponding band peaks in the shorter wave-length than does the solution.

According to the result of the crystal analysis,[22] the crystal consists of potassium ions, $Co(NCS)_4^{--}$ anions and molecules of crystallization water, $Co(NCS)_4^{--}$ ions being determined as tetrahedral. The crystal has been found to exhibit a marked dichroism. That is, as to the band at $\nu = 50 \times 10^{13}$/sec. a-absorption is hyperchromic and hypsochromic to c-absorption, and with the specific band a-absorption is hypsochromic to c-absorption. In consequence, it is readily concluded that the configuration of the anion, $Co(NCS)_4^{--}$, in this crystal deviates considerably from regular-tetrahedron. It is most likely that the complex anion should possess a configuration of distorted-tetrahedron. From analogy to dicesium tetrachlorocuproate, it is supposed that the a-absorption of this crystal corresponds to the X-absorption and that the c-absorption corresponds to the Z-absorption of the $Co(NCS)_4^{--}$ ion.

It is to be noted that there can be found a series of sharp bands with this compound in alcoholic solution as in the crystal of tricesium cobaltous pentachloride. Some of the peaks in the shorter wave-length may be covered under the specific band, since the specific band comes very close to the band series. Though peaks which appear separated from the specific band seem to be rather small in number, wave-numbers at the series of peaks can be represented by the equation of the form (1). The following values have been obtained for a and b; $a = 4.8 \times 10^3$/cm. and $b = 4 \times 10^2$/cm., dissociation energy of the complex being estimated, in the same way as in tricesium cobaltous pentachloride, approximately as 34 kcal.

General Considerations.—It seems of significance that those series of sharp peaks in the above two compounds can be expressed by the equation of a similar form and may reasonably be correlated with electronic-vibrational transitions directly related to the co-ordination linkages in the quadri-co-ordinated complex ions. There have been reported very few metallic complexes which show at room temperature a corresponding electronic absorption band consisting of a series of sharp peaks. One such example, besides the above two compounds, may be found with potassium permanganate in aqueous solution.[23]

The appearance at room temperature of a fine structure in an electronic absorption band of such a kind is probably due to many factors. But the following may be cited as one of the principal factors.[24] Since to a first approximation the only vibrations for which Δv, v being the vibrational quantum number, differs from zero in polyatomic electronic spectra are the totally symmetrical vibrations, the electronic absorption spectra of those complex ions, which have a very small number of totally symmetrical vibrations, will show a simplified vibrational structure. Thus $CoCl_4^{--}$ in the crystal of $CsCoCl_5$ and $M_nO_4^-$ in aqueous solution of potassium permanganate, both being regular-tetrahedral, have only one totally symmetrical vibration and, moreover, contain only simple ions as ligands. Therefore, their electronic absorption might be expected to be more simple than in other complexes of more complicated structure. As for $K_2Co(NCS)_4 \cdot 4H_2O$, $Co(NCS)_4^{--}$ in this crystal has been presumed, from dichroism measurement, to have flattened tetrahedral configuration. This, however, might be ascribed, at least partly, to the effect of the crystalline field upon the complex ion, and the complex ion in alcoholic solution might be assumed to be nearly regular-tetrahedral. In agreement with the assumption seems to be the fact that the crystal of this compound has been found to be slightly hypsochromic to the solution, and that the splitting of the absorption band is less marked in the crystalline state.

Another point which deserves attention

20) R. Tsuchida, This Bulletin, **13**, 471 (1938).
21) A. v. Kiss and P. Csokan, *Z. physik. Chem.*, A**186**, 239 (1940).
22) G. S. Zhdanov and Z. V. Zvonkova, *Zhur. Fiz. Khim.*, **24**, 1339 (1950); *C. A.*, **45**, 6001e (1951).
23) B. Lange and C. Schusterius, *Z. physik. Chem.*, A**159**, 295 (1932).
24) For example, see G. R. Harrison, R. C. Lord and J. R. Loofbourow, "Practical Spectroscopy," Prentice-Hall, New York, 1948, p. 291.

may be the fact that the above three complex compounds all involve relatively weak linkages. The weakness of the linkage seems to have some relation to the appearance of the electronic band with a fine structure.

It is of significance that there have been found complex-ions with distorted-tetrahedral configurations, intermediate between planar and regular-tetrahedral ones, in contrast to the generally accepted fact that as to magnetic properties there may usually be drawn a sharp line between tetrahedral and planar hybridization. Quadri-co-ordinated cupric and cobaltous complexes are expected to be square when ordinary hybridization of bond orbitals is assumed.[25] In fact this is found not to be the case. One of the reasons for the above fact may be that the linkages between the metal atom and the ligands are too weak to enter into planar hybridization of an ordinary type.[26]

The configuration of complex molecules would naturally be closely related to the hydbridization of bond orbitals in the molecule. The existence of these distorted-tetrahedral complexes, therefore, points to the possibility that the hybridization of bond orbitals, intermediate between tetrahedral and planar ones, may occur with the $CuCl_4^{--}$ and $Co(NCS)_4^-$ ions in these crystals. It is noteworthy that the same central metallic ion has been found to form complexes of different configurations with ligands of varying natures on the one hand, and that with the same ligands different metallic atoms as a centre form complexes of different configurations on the other. Thus it is readily recognized[27] that the natures of both metal atoms and ligands are in close relation to the state of hybridization, the stability of the bonds, and the configurations of the complex ions.

25) R. Tsuchida, *J. Chem. Soc. Japan*, **60**, 245 (1939); R. Tsuchida, M. Kobayashi and H. Kuroya, *Rev. Phys. Chem. Japan*, **13**, 151 (1939); N. V. Sidgwick and H. M. Powell, *Proc. Roy. Soc. London*, A**176** 153 (1940); L. Pauling, "The Nature of the Chemical Bond", Cornell Univ. Press, Ithaca, New York, 1940.

26) Since the configurations of the above complex ions were determined in the crystalline state, we could not remove another possibility that those complex ions would be non-planar only in the crystalline state where electrostatic forces of surrounding ions on the complex ions might be so strong and the linkages in the complexes so weak that the planar configuration would not be held.

27) N. V. Sidgwick, *J. Chem. Soc.*, **1941**, 433; D. P. Mellor and D. P. Craig, *J. Proc. Roy. Soc. N. S. Wales*, **74**, 474 and 495 (1940); D. P. Mellor, *Chem. Revs.*, **33**, 137 (1943); L. G. Van Uitert and W. C. Fernelius, *J. Am. Chem Soc.*, **76**, 379 (1954).

Summary

Absorption spectra of crystals of dicesium tetrachlorocuproate, tricesium cobaltous pentachloride and potassium tetrathiocyanatocobaltoate tetrahydrate have been quantitatively determined in the visible and ultraviolet region by the microscopic method with polarized light.

In accordance with the flattened-tetrahedral configuration of tetrachlorocuproate anion, the crystal of Cs_2CuCl_4 exhibits anisotropy of light absorption.

It has been found that crystals of Cs_3CoCl_5 are almost isotropic, supporting the regular-tetrahedral configuration of the $CoCl_4^{--}$ ion in this crystal.

It has also been found that $K_2Co(NCS)_4 \cdot 4H_2O$ in the crystalline state shows a marked dichroism. It is concluded from this observation that $Co(NCS)_4^{--}$ ions in this crystal are distorted-tetrahedral, just like the $CuCl_4^{--}$ ions in the crystal of Cs_2CuCl_4.

It has been found that Cs_3CoCl_5 in the crystalline state and $K_2Co(NCS)_4 \cdot 4H_2O$ in alcoholic solution show their second absorption band with a series of sharp peaks, which have been shown to be correlated with electronic-vibrational transitions. This fact is in harmony with the idea on the origins of the absorption bands of metallic co-ordination compounds proposed by one of the authors.

The authors wish to thank the Ministry of Education for a grant.

Department of Chemistry, Faculty of Science, Osaka University, Nakanoshima, Osaka

*Syntheses of Tetracyclohexylsilane and Methylcyclohexylsilanes**

By Motonori KANAZASHI and Michio TAKAKUSA

(Received June 22, 1954)

Preparation of tetracyclohexyl-silane[1] and germane[2,3,4] were attempted by several workers with the lithium compound or the Grignard reagent unsuccessfully. Even tricyclohexylalkylsilanes[1,5] could not be obtained due to a large steric hindrance of the cyclohexyl group. The present authors succeeded in making syntheses of these compounds by hydrogenation of methylphenylsilanes and found that the steric hindrance in these molecules was conquerable, though it had a fairly large effect in the case of substitution reaction. In this work, trimethylcyclohexylsilane, dimethyldicyclohexylsilane, methyltricyclohexylsilane, and tetracyclohexylsilane were prepared.

Experimental**

Methylphenylsilanes.—These compounds were prepared from chlorobenzene and corresponding methylchlorosilane by the Wurtz-Fittig reaction in benzene solution.

Trimethylphenylsilane: b.p. 170–171°, n_D^{20} 1.4901, d_4^{20} 0.8687. MR_D: obsd. 50.03, calcd. 50.10.

Dimethyldiphenylsilane: b.p. 101–104° at 2.5 mm Hg., n_D^{20} 1.5593, d_4^{20} 0.9877 MR_D: obsd. 69.45, calcd. 69.92.

Methyltriphenylsilane: m.p. 65–67°.

Tetraphenylsilane: m.p. 229–231°.

Raney Nickel Catalyst.—The catalyst was prepared from Raney nickel alloy, containing 38% of nickel, according to the direction of Adkins' so-called "W-6"[6], except that washing was done in hydrogen atmosphere under 300 mm. in water column instead of 1.5 atm.

Hydrogenation of Methylphenylsilanes.—Hydrogenation was carried out in a stainless-steel shaking type autoclave, 300 cc. in capacity under the condition shown in Table I. Methylcyclohexane was used as a solvent. The catalyst was supplied in two portions as the reaction did not proceed smoothly with an exception of trimethylphenylsilane.

TABLE I

HYDROGENATION OF METHYLPHENYLSILANES

Material	g. (mol.)	Catalyst g. (wt. %)	Solvent g.	Pressure atm.	Temperature °C.	Time hrs.	H_2 (c)	Product	Yield %
		(a)			(b)				
Me_3SiPh	30 (0.2)	4.5(15)	70	110–150	100–140(108)	2	2.98	I	67
Me_2SiPh_2	32.1(0.15)	5 (15)	70	80–100	85–170 (90)	7	5.9	II	62
$MeSiPh_3$	27.4(0.1)	5 (18)	70	60–100	80–170(100)	6	9.0	III	61
$SiPh_4$	51 (0.15)	10 (20)	80	50–100	80–150(100)	7	12.0	IV	63

(a) In the case of trimethylphenylsilane, "W-2" Raney nickel catalyst was used.

(b) The starting temperature of absorption was shown in brackets.

(c) Moles of hydrogen absorbed, to one mole of reactant.

Separation and Purification of Methylcyclohexylsilanes.

Trimethylcyclohexylsilane (I). Out of the hydrogenation mixture[a] a fraction boiling at 67–69° (25 mm.) was collected after removal of the reaction solvent by a fractionating distillation.

Dimethyldicyclohexylsilane (II). A fraction boiling at 94–103° (3–3.5 mm.) was collected.

Methyltricyclohexylsilane (III). A crystalline part was filtered out of the concentrated reaction mixture[a], washed with ethanol-methylcyclohexane mixture and recrystallized from methylcyclohexane[b].

Tetracyclohexylsilane (IV). An aimed product was extracted from the solid phase of the reaction mixture and recrystallized twice with decahydronaphthalene[c], washed with methylcyclohexane and dried in vacuum.

* Presented at the 7th. Annual Meeting of the Chemical Society of Japan held in Tokyo, April, 1954.

1) W. H. Nebergall and O. H. Johnson, *J. Am. Chem. Soc.*, **71**, 4022 (1949).

2) H. Bauer and K. Burschkies, *Ber.*, **65** 956 (1932).

3) O. H. Johnson and W. H. Nebergall, *J. Am. Chem. Soc.*, **70**, 1706 (1948).

4) O. H. Johnson and W. H. Nebergall, ibid., **71**, 1720 (1949).

5) N. W. Cusa and F. S. Kipping, *J. Chem. Soc.*, **1933**, 1040,

** All temperatures reported here were uncorrected.

6) H. Adkins and H. R. Billica, *J. Am. Chem. Soc.*, **70**, 695 (1948).

a) The catalyst was removed by filtration prior to these treatments.

b) This compound was dissolved in hot methylcyclohexane easily, contrasting with the case of IV.

c) This compound was hardly soluble in various solvents:

The solvent recovered from the reaction mixture was fractionated through a 30 cm. distillation column packed with stainless-steel helices, but hardly any benzene or cyclohexane were found in all cases.

Infrared Absorption Spectra.—The spectra were measured using a Perkin-Elmer Model 12-C Spectrometer with a rock salt prism of Government Chemical Industrial Research Institute, Tokyo. Two samples, trimethylphenylsilane and dimethyldiphenylsilane, were run in a potassium bromide cell 0.0125 mm. thick, without using a solvent. The other samples were measured in carbon tetrachloride solution.

$MeSiPh_3$, in about 20% carbon tetrachloride solution, cell thickness 0.1 mm.

I–III, in about 10% 0.1 mm.

IV, in about 3% 0.2 mm. and 1 mm.

Results and Discussion

All these phenylsilanes absorbed the theoretical amount of hydrogen and hydrogenation products were formed. Their physical constants and analytical data are given in Table II.

TABLE II

PHYSICAL CONSTANTS AND ANALYSES OF METHYLCYCLOHEXYLSILANES

Compound	b.p. °C.	b.p. mm.Hg.	n_D^{20}	d_4^{20}	Molar ref. Obsd.	Molar ref. Calcd.(a)	Analyses C Found	Analyses C Calcd.	Analyses H Found	Analyses H Calcd.	
I	67–9	25	1.4477	0.8163	51.24	51.30	(b)		(b)		(c)
II	101–3	3–3.5	1.4850	0.9136	71.50	72.32	74.01	74.91	12.61	12.57	(d)
	m.p.(°C.)										
III	73.0–73.2						78.21	77.99	12.39	12.40	
IV	279–281						79.97	79.91	12.40	12.30	(e)

(a) Calculated from bond refractivities reported by E. L. Warrick, *J. Am. Chem. Soc.*, **68**, 2455 (1946).

(b) Analyses of this compound were unsuccessful due to its explosibility in the combustion tube.

(c) Mass spectra. Parent peaks: mass 156, 157 and 158 (peak height 131, 20.2 and 6.0, respectively).

(d) Mass spectra. Parent peaks: mass 224, 225 and 226 (peak height 52.8, 11.0 and 2.8, respectively).

(e) Analysis. Si %: found 7.71, calcd. 7.79.

Mass-spectrometric data are available for identification of liquid products. The mass of trimethylcyclohexylsilane consisting of the most abundant isotopes of carbon, hydrogen, and silicon, i.e. $C_9{}^{12}H_{20}{}^{1}Si^{28}$, is 156 and this peak was found in the parent group of the spectra of I.[d] Besides, the relative heights of these three peaks (see Table II (c)) accord with those calculated for $C_9H_{20}Si$ based on the known isotopic abundance ratios[7] of involved elements. Other remarkable peaks are: "73, 74, 75" (corresponding to Me_3Si^+), "141, 142, 143" ($Me_2C_6H_{11}Si^+$), and "135, 136, 137" (Me_2PhSi^+). The presence of the last group (135–137), with absence in the intermediate region (p.e. from 152 to 155, or from 137 to 140), reveals contamination of unreacted trimethylphenylsilane, and at the same time shows that no incomplete hydrogenation products were formed (see Table III). The similar results were derived from mass spectra of II, but unreacted dimethyldiphenylsilane was not found.

TABLE III

POSSIBLE PRODUCTS IN HYDROGENATION OF TRIMETHYLPHENYLSILANE AND THEIR MASSES. (Some of fragments of these to be found in mass spectra are also listed)

$Me_3C_6H_{11}Si^+$	156	157	158
$Me_3C_6H_9Si^+$	154	155	156
$Me_3C_6H_7Si^+$	152	153	154
$Me_3C_6H_5Si^+$	150	151	152
$Me_2C_6H_{11}Si^+$	141	142	143
$Me_2C_6H_9Si^+$	139	140	141
$Me_2C_6H_7Si^+$	137	138	139
$Me_2C_6H_5Si^+$	135	136	137
Me_3Si^+	73	74	75

Infrared spectra of the four products and the three materials are given in Fig. 1. The quite identical spectra were obtained for the three methylcyclohexylsilanes. They also accord with spectrum of dicyclohexylsilane reported by West and Rochow[8], except absence of the absorption bands of Si—H[8], in 4.7–4.8 μ and 10.6–10.7 μ, and presence in 7.11 μ and 8.0 μ. Absorption bands in 7.11 μ and 8.0 μ are assigned to methyl group bonded to silicon as reported by Young et. al.[9] The

ether, ethanol, carbon tetrachloride, benzene, cyclohexane, and methylcyclohexane. This compelled us to choose a high-boiling solvent for extraction and recrystallization.

d) It is impossible to calculate the ordinary molecular weight from the masses and the relative heights of the parent peaks strictly, unless numbers of included atoms are postulated.

7) G. T. Seaborg and I. Perlman, *Revs. Modern Phys.*, **20**, 585 (1948).

8) R. West and E. G. Rochow, *J. Org. Chem.*, **18**, 303 (1953).

9) C. Young, P. C. Servais, C. C. Currie and M. J. Hunter, *J. Am. Chem. Soc.*, **70**, 3758 (1948).

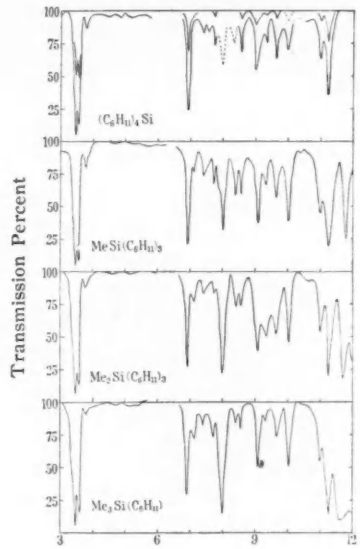

Wave Length in Microns
Fig. 1 (A).
Infrared spectra of cyclohexylsilanes.

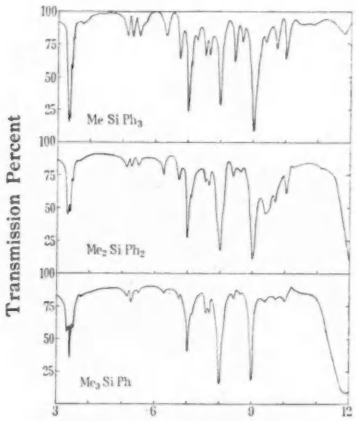

Wave Length in Microns
Fig. 1 (B).
Infrared spectra of methylphenylsilanes.

spectrum of tetracyclohexylsilane is identical with that of dicyclohexylsilane except the absorption bands of Si—H. In these spectra, the absorption assigned to alkene or phenyl group was not found, 3.2–3.4 μ, 7.0 μ and 9.7–9.8 μ. Further discussions, p.e. on the characteristic bands of cyclohexyl bonded to silicon or on the inverted isomerism, could not be made for the lack of data to which to refer.

All these results give a sufficient support to the identification of the prepared substances.

Steric hindrance of cyclohexyl group in organosilicon compounds was first discussed by Kipping and Cusa.[5] Their attempt to introduce one phenyl and three cyclohexyl groups to one silicon atom with Grignard reagent resulted in formation of phenyldicyclohexylcyclohexoxysilane. The reaction involving cyclohexyllithium and silicon tetrachloride[1] was studied by Nebergall and Johnson, and only tricyclohexylchlorosilane was obtained. Concerning it, the following reactions were also reported;

$$(C_6H_{11})_3SiCl + LiAlH_4 \longrightarrow (C_6H_{11})_3SiH$$
$$(C_6H_{11})_3SiH + X_2 \longrightarrow (C_6H_{11})_3SiX$$

where X is Br or I,

$$(C_6H_{11})_3SiCl + KOH \longrightarrow (C_6H_{11})_3SiOH$$
$$(C_6H_{11})_3SiOH + Ac_2O \longrightarrow (C_6H_{11})_3SiOAc$$

but the halogen atom was not substituted for by any alkyl groups. These facts should be attributed to the steric hindrance of the cyclohexyl group. The steric hindrance in organosilicon compounds is small, compared with carbon compounds because of the larger size of silicon and the longer distance in which silicon is bonded to carbon or other atoms.

Steric effects of *tert*-butyl[10], isopropyl[11], cyclohexyl[12], *o*-tolyl[13], and 1-naphthyl[14] have been discussed in previous literatures in silico-organic chemistry. The *t*-butyl has the largest effect of them and the results lead to the natural conclusion that the extent of the group in the surrounding space of silicon atom is a sole factor. From this point of view, cyclohexyl and isopropyl or other secondary alkyl groups have almost equal effects, as far as cyclohexyl is combined with

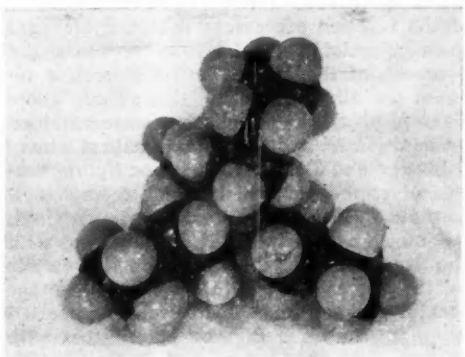

Fig. 2.
Stuart model of tetracyclohexylsilane.

10) L. J. Tyler, L. H. Sommer and F. C. Whitmore, *J. Am. Chem. Soc.*, **69**, 981 (1947); **70**, 2876 (1948); L. H. Sommer and L. J. Tyler, ibid., **76**, 1030 (1954).
11) H. Gilman and R. N. Clark, *J. Am. Chem. Soc.*, **69**, 1499 (1947); C. Eaborn, *J. Chem. Soc.*, **1952**, 2840.
12) Loc. cit.
13) H. Gilman and G. N. R. Smart, *J. Org. Chem.*, **15**, 720 (1950); **16**, 424 (1951).
14) H. Gilman and C. G. Brannen, *J. Am. Chem. Soc.*, 4640 (1951); A. D. Petrov and V. S. Chugunov, *Doklady Akad. Nauk, S. S. S. R.*, **77**, 815 (1951); P. S. Sanin and A. D. Petrov, *Zhur. Obschei Khim.*, **22**, 1124 (1952).

silicon in *e*-bond. And free rotation around C—C bond in it is somewhat prevented because of its ring-form structure.

The stuart model of tetracyclohexylsilane is constructed without much jostling, but the free rotation around the Si—C bond and the inverted isomerism of the cyclohexane ring is prevented entirely as shown in Fig. 2. The inversion is possible with difficulty in models of the other three compounds. The difficulty is diminished with the number of cyclohexyl groups, but these inverted isomers involving *p*-bond seemed to be more unstable than the original isomers involving no *p*-bond. (See Fig. 3.) It is of much theoretical interest to determine whether the inverted

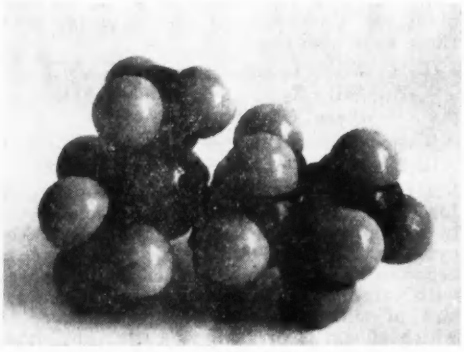

Fig. 3 (1).

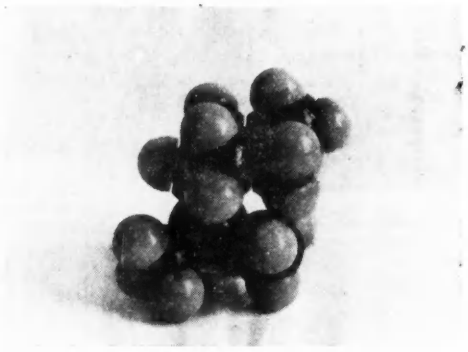

Fig. 3 (2).

Fig. 3. The two forms of stuart models of cyclohexyltrimethylsilane.
Left: Cyclohexyl bonds to silicon in *e*-bond and Si-cyclohexyl rotation is free.
Right: Cyclohexyl bonds to silicon in *p*-bond and the rotation is prevented.

isomer is present or not in the real substance, but this fact is not known from the infrared spectra of these compounds.

Now it is clear that the steric hindrance in them is not essential, or, not a subject of the structures themselves but a subject of the reaction processes; that is, cyclohexyl in a tricyclohexylsilyl group prevents the approach of the active centre of such a reagent as alkyllithium to the silicon atom. Therefore, syntheses of them were attained by addition of hydrogen, the smallest atom.

Ipatiev and Dolgov reported on hydrogenation of triphenylcarbinol[15] and tetraphenylmethane[16]. In both cases, tricyclohexylmethane was produced. Consideration with the Stuart model shows that it is impossible to introduce the fourth cyclohexyl to the central carbon atom in tricyclohexylmethyl group as shown in Fig. 4. This agrees with the results of Ipatiev and Dolgov. The difference in these and our results is explained by differences of atomic sizes and bond lengths. Ipatiev and Dolgov also studied analogous reaction of tetraphenylsilane under high pressure at high temperature without a catalyst[17]. In this experiment, hydrogenation did not take place, and the cleavage of

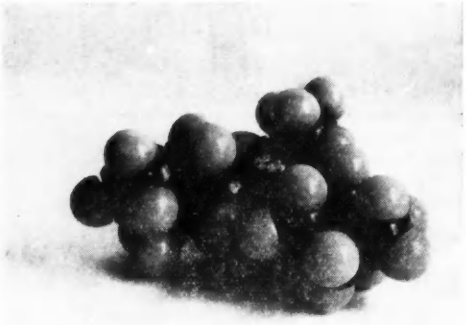

Fig. 4.
Stuart model of tricyclohexylmethyl.

Si—Ph bond with liberation of benzene was observed.

Studies on the steric hindrance of cyclohexyl group in organosilicon compounds are continued and syntheses of hexacyclohexyldisilane, hexacyclohexyldisiloxane and *t*-butyltricyclohexylsilane are under investigation now in this laboratory.

Summary

For new organosilicon compounds containing cyclohexyl group were prepared by hydrogenation of corresponding phenylsilanes. They are: trimethylcyclohexylsilane, dimethyldicyclohexylsilane, methyltricyclohexylsilane, and tetracyclohexylsilane. Physical

15) V. N. Ipatiev and B. N. Dolgov, *Compt. read.*, **183**, 304 (1926).
16) V. N. Ipatiev and B. N. Dolgov, ibid., **185**, 210 (1627).
17) V. N. Ipatiev and B. N. Dolgov, *Ber.*, **62**, 1220 (1929).

constants and infrared absorption spectra of these compounds were measured and discussions on the steric hindrance were done with Stuart models.

The authors are indebted to Mr. S. Saeki and Mr. T. Yoshimoto for the infrared spectra and Mr. H. Sakai for the mass spectra reported in this paper. They are also grateful to Dr. O. Simamura and Dr. T. Yamada for their helpful advice and encouragement during this work.

Electrotechnical Laboratory, Agency of Industrial Science & Technology
Nagata-cho, Chiyoda-ku, Tokyo

The Nature of the Hydrogen-Bond. I. The Delocalization Energy in the Hydrogen-Bond as Calculated by the Atomic-orbital Method

By Hiroshi TSUBOMURA

(Received June 21, 1954)

Until quite recently it has been assumed that the energy of the hydrogen-bond is mainly electrostatic. Such an assumption seems to be very valid in regard to the experimental evidence that this bond is formed only between molecules which contain polar groups. Also the energies of the electrostatic interaction between hydrogen-bonded molecules calculated by some authors[1,2] agreed fairly well with experimental values of the bond energies and were taken as evidences for the above mentioned assumption.

We face to some difficulties, however, if we try to explain the strengths of hydrogen-bonds of various molecules only from the electrostatic point of view. Let us consider, for example, acetone and ethyl ether. Both act as proton-acceptors in the hydrogen-bond and according to the electrostatic theory we are forced to conclude that the proton-accepting strength of the former is greater than that of the latter since the carbonyl group of the former is much more polar than the C-O group of the latter. But it is known experimentally that the accepting strength of acetone is nearly equal to, or rather less than that of ethyl ether.[3] It is also known that nitriles are moderate proton-acceptors in spite of the strong polarity of their C≡N group.[3]

These phenomena strongly suggest that other sources of the interaction energy exist in the hydrogen-bond. Quite naturally what we can obtain experimentally as the energy of a hydrogen-bond may be, from a theoretical point of view, interpreted as the algebraic sum of the following terms: (1) Electrostatic energy, (2) Dispersion force, (3) Exchange repulsion, (4) Delocalization energy due to the electron-transfer from a proton-acceptor to a proton-donor. Hence, even if the calculated value of the electrostatic energy of a hydrogen-bond agrees with the experimental dissociation energy, we cannot say that the former is the dominant part of the latter. It only shows that the algebraic sum of (2), (3) and (4) is practically zero. Therefore, a complete clarification of the energy of the hydrogen-bond would not be attained until we were able to calculate or estimate these terms precisely.

Unfortunately it is extremely difficult to calculate non-empirically the energy of a hydrogen-bond as the sum of the above mentioned terms. For the energy of a hydrogen-bond is of the order of several kilocalories, that is 0.01 atomic unit, and, to calculate it exactly, we should calculate numerous energy integrals which appear in the course of calculation within the error of, at most, 0.001 atomic unit. Practically, it is almost impossible to carry out such accurate calculations. Nevertheless, it seems important for the discussion of the nature of the hydrogen-bond to calculate, even approximately, each of the above-mentioned terms. The author's aim in this paper is to clarify the nature and to estimate the magnitude of the fourth term, that is, the delocalization energy.

The importance of this term has been quite recently recognized. In 1951, C.A. Coulson[4]

1) N. D. Coggeshall, *J. Chem. Phys.* **18**, 978 (1950).
2) J. A. Pople, *Proc. Roy. Soc.*, **A205**, 11 (1951).
3) M. Tsuboi, *Kagaku-no-Ryôiki (J. Japanese Chem.)*, **7**, 611 (1953).
4) C. A. Coulson, "Valence", Oxford Univ. Press (1952). p. 305

described a study of the magnitude of the contribution of various resonance hybrids in the hydrogen-bonded water molecules, and stated that the contribution of the hybrids which is related to the charge delocalization is considerably great. Nukasawa, Tanaka and Nagakura[5] have also emphasized the importance of this term and have proposed that it may conveniently be estimated by use of a second order perturbation theory in terms of molecular orbitals and with some empirical values of the ionization potentials and the excitation energies. Though it seems that their method is very convenient and significant for the qualitative discussion of the problem, it may be also important to carry out an exact non-empirical calculation and to decide whether their qualitative conclusion is correct or not. In this paper the results of the calculations of the hydrogen-bonded water molecules by the atomic orbital method are given.

The Basis of the Calculation

The structure of the two hydrogen-bonded water molecules has been assumed to be that shown in Fig. 1; namely, the two water molecules lie in a

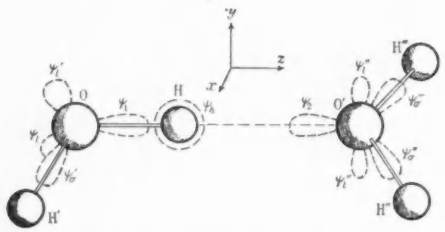

Fig. 1. The assumed structure of the hydrogen-bonded water molecules.

common plane and the hydrogen atom of the proton-donating molecule is situated on the straight line which connects the two oxygen atoms and

$$\psi_1 = 1/2(s+\sqrt{3}z)$$
$$\psi_{\sigma'} = s/2+\sqrt{2}/3x-z/2\sqrt{3}$$
$$\psi_{1'} = -s/2+x/\sqrt{6}+z/\sqrt{12}=y/\sqrt{2}$$
$$\psi_{1'} = -s/2+x/\sqrt{6}+z/\sqrt{12}-y\sqrt{2}$$

where s, x, y, and z denote the $2s$, $2p_x$, $2p_y$, and $2p_z$, AO's of O, and s', x', y', and z', denote those of O', respectively.

5) K. Nukasawa, J. Tanaka and S. Nagakura, *J. Phys. Soc. Japan*, **8**, 792 (1953).
6) J. A. Pople, *Proc. Roy. Soc.*, **A202**, 323 (1950).
7) S. Maeda, *Busseiron-Kenkyu*, **70**, 101 (1954). In this paper, S. Maeda reports his results on the SCF LCAO MO calculation of the water molecule. By the transformation of his SCF MO, he obtained as the equivalent AO'S of the oxygen atom approximately tetrahedral ones. It seems that his result also supports the validity of employing the tetrahedral AO's in the present calculation.

which, at the same time, coincides with the symmetry axis of the proton-accepting molecule. The individual atoms constituting these molecules have been designated in the way shown in this figure. The O-H and O-O' distances have been taken to be 0.96 Å and 2.70 Å, respectively.

In the present calculation, it is assumed, as is usual, that each of the oxygen atoms has four s, p-hybridized AO's, two of which are directed to the two hydrogen atoms and form electron-pair bonds with the 1s-AO's of the hydrogen atoms, respectively, while each of the remaining two AO's directed toward the opposite side to the O-H bonds, is occupied by two spin-antiparallel electrons and has no influence upon the O-H bonds.

The coefficients of hybridization of $2s$ and $2p$ AO's in these AO's have a strong influence on the electronegativity of oxygen atoms, and therefore on the energy of the hydrogen-bond. The best way is, of course, to make the variation treatment with inclusion of these coefficients. But, since the hydrogen-bond is a week perturbation, one may expect a good result by use of orbitals with constant hybridizations, if the coefficients of the hybridization are properly chosen. The result of the equivalent molecular orbitals obtained by J.A.Pople[6] has shown that the two bonding AO's and the two lone-pair AO's of the oxygen atom in a water molecule can be described by orbitals nearly tetrahedral. Relying upon this result, tetrahedral orbitals have been adopted for the present work. In this case, however, the hydrogen atom of the proton donor finds itself in the middle of the directions of the two lone-pair AO's of the proton acceptor in our assumed configuration of the two water molecules. As the inclusion of the two lone-pair AO's in the calculation complicates the problem, they have been transformed into a $2p_y$ AO and a diagonally hybridized AO (ψ_2) directed to the H atom. Then, only the latter is to be included in the calculation since the $2p_y$ AO is owing to its anti-symmetric character, unable to interact with the 1s AO of the hydrogen atom. Consequently, the valence AO's of the oxygen atoms we assumed here are as shown in Fig. 1, and their explicit forms are given by the following formulas:[7]

$$\psi_2 = (1/\sqrt{2})(s'-z')$$
$$\psi_{\sigma''} = (1/2)(s'+\sqrt{2}x'+z')$$
$$\psi_{\sigma'''} = (1/2)(s'-\sqrt{2}x'+z') \qquad (1)$$
$$\psi_{1''} = y.$$

Since the complete treatment of the problem is extremely tedious, and since the aim of the author is not to carry out a precise calculation for the particular case of water, but to discuss the magnitude and the nature of the delocalization energy for the hydrogen-bond in general, the problem was reduced to the variation treatment of the energy of four electrous over the three atomic orbitals, ψ_1, ψ_2 and ψ_h, in the potential field of the nuclea and of the remaining electrons which are distributed over the inner-shells and lone-pairs of oxygen atoms and other O-H bond-

orbitals. Such a treatment will give a fairly good result if the assumed distribution of these electrons agrees with the true one for the ground state of the system. According to Pople's result[6], the coefficients of the valence AO's of oxygen and hydrogen in the localized MO of the O-H bond of a water molecule are nearly the same. Hence, it is not so dangerous to replace the potentials of the bonding electrons for the OH′, OH″, and OH‴ bonds (See Fig. 1) by those of the six electrons which occupy, one by one, the valence AO's of the oxygen atoms, $\psi_{\sigma'}$, $\psi_{\sigma''}$, $\psi_{\sigma'''}$, and the 1s AO's of the three hydrogen atoms. Furthermore, the potentials induced by these hydrogen 1s-electrons may be assumed to cansel those of the atomic nuclea of hydrogen, in view of the large distances between these hydrogen atoms and the centres of the orbitals, ψ_1, ψ_2 and ψ_h. Thus, in the present calculation, we assume a core potential arising from the following nuclea charges and electronic clouds.

for O, $+8e$, $(\psi_{1s0})^2$, $(\psi_{\sigma'})^1$, $(\psi_{l'})^2$, $(\psi_{l'})^2$,
for O′, $+8e$, $(\psi_{1s0'})^2$, $(\psi_{\sigma''})^1$, $(\psi_{\sigma'''})^1$, $(\psi_{2p\pi O'})^2$
for H, $+e$. (2)

The Method of the Calculation

Based on these considerations, five resonance hybrids shown in the following formulas are assumed.

(A) O—H.....O (D) O^- H——O^+
(B) O^- H^+....O (E) O H^- O^+ (3)
(C) O^+ H^-....O

Eigenfunctions for these can be written as follows:

$$\Psi_A=N_A(\phi_1-\phi_2) \qquad \Psi_D=N_D(\phi_4-\phi_5)$$
$$\Psi_B=N_B\,\phi_3 \qquad \Psi_E=N_E(\phi_7-\phi_8), \quad (4)$$
$$\Psi_C=N_C\,\phi_6$$

in which N_A, N_B, etc., are the normalizing factors and the ϕ's are the four-electron determinantal wave functions:

$$\phi_1=(1\alpha^1\cdot h\beta^2\cdot 2\alpha^3\cdot 2\beta^1) \qquad \phi_5=(1\alpha^1\cdot 1\beta^2\cdot h\beta^3\cdot 2\alpha^4)$$
$$\phi_2=(1\beta^1\cdot h\alpha^2\cdot 2\alpha^3\cdot 2\beta^1) \qquad \phi_6=(h\alpha^1\cdot h\beta^2\cdot 2\alpha^3\cdot 2\beta^1)$$
$$\phi_3=(1\alpha^1\cdot 1\beta^2\cdot 2\alpha^3\cdot 2\beta^1) \qquad \phi_7=(1\alpha^1\cdot h\beta^2\cdot h\alpha^3\cdot 2\beta^1) \quad (5)$$
$$\phi_4=(1\alpha^1\cdot 1\beta^2\cdot h\alpha^3\cdot 2\beta^1) \qquad \phi_8=(1\beta^1\cdot h\beta^2\cdot h\alpha^3\cdot 2\alpha^4),$$

where, for example,

$$(1\alpha^1\cdot h\beta^2\cdot 2\alpha^3\cdot 2\beta^1)=\begin{vmatrix} (1\alpha)^1 & (h\beta)^1 & (2\alpha)^1 & (2\beta)^1 \\ (1\alpha)^2 & (h\beta)^2 & (2\alpha)^2 & (2\beta)^2 \\ (1\alpha)^3 & (h\beta)^3 & (2\alpha)^3 & (2\beta)^3 \\ (1\alpha)^4 & (h\beta)^4 & (2\alpha)^4 & (2\beta)^4 \end{vmatrix},$$

and $1=\psi_1$, $2=\psi_2$, $h=\psi_h$, α, and β are the two spin functions.

By use of these functions, the matrix elements H_{AA}, H_{BB}, etc. were calculated and the lowest root of the secular determinant,

$$|H-S.E|=0$$

was determined. This gives the energy of the O-H...O system in the ground state.

The Hamiltonian is given by the kinetic energy operator plus the three bare-nuclea field potentials and potentials caused by the electrons whose configuration is shown in (2). For ψ_1 and ψ_h, however, the core potential of O′ was set equal to

(potential of the neutral oxygen atom)$-$
$$2\int\psi_{2}^{*}(\mu)(e^2/r_{\nu\mu})\psi_2(\mu)d\tau_\mu,$$

and the former was ignored. The values of integrals were taken, if possible, from Kotani, Amemiya and Simose's table[8], and in other cases either directly calculated or estimated by the overlap approximation. Some of the directly culculated integrals were given in the Appendix. Slater-type atomic orbitals were used, and the effective nuclea charge of oxygen for the valence shells were taken to be 4.55. The coulombic integrals between AO's of O and O′ were calculated by the point-charge approximation.

In the calculation of $(\phi_k \mid H \mid \phi_j)$, the terms which arise by twice or more exchanges of electrons were ignored. Also, the exchange integral and overlap integral over ψ_1 and ψ_2 were neglected throughout the calculation. All the remaining terms were thoroughly included.

For comparison, the lowest energy of the O-H bond in a free water molecule was also determined. In this case, three resonance hybrids, A′, B′, and C′, similar to the types, A, B and C in (3) may be assumed. The bond eigenfunctions for them are:

$$\Psi_{A'}=N_{A'}(\phi_1'-\phi_2')$$
$$\Psi_{B'}=N_{B'}(\phi_3') \quad (6)$$
$$\Psi_{C'}=N_{C'}(\phi_3')$$

in which the ϕ''s are of the following form, when one uses the same abbreviated formula as used before,

$$\phi_1'=(1\alpha^1\cdot h\beta^2) \qquad \phi_6'=(h\alpha^1\cdot h\beta^2).$$
$$\phi_2'=(1\beta^1\cdot h\alpha^2) \quad (7)$$
$$\phi_3'=(1\alpha^1\cdot 1\beta^2)$$

	A	B	C	D	E
A	−E	0.43−0.70E	0.56−0.70E	0.37−0.26E	0.21−0.32E
B		−(1.28+E)	0.75−0.32E	−(0.17+0.38E)	0.31−0.23E
C			−(0.92+E)	0.36−0.12E	0.34−0.24E
D				−(2.55+E)	−(0.53+0.56E)
E					−(2.25+E)

$=0$ (8)

	A′	B′	C′
A′	−E	0.42−0.69E	0.58−0.69E
B′		−(1.29+E)	0.71−0.31E
C′			−(0.90+E)

$=0$ (9)

8) Kotani, Amemiya and Simose, *Proc. Phys.-Math. Soc. Japan*, **20**, Extra Number 1, **22**, Extra Number.

Results and Discussion

The calculated matrix elements for the O-H . . . O system and for the free molecule are given in (8) and (9), respectively.

As may be seen from these equations, the zero point of the energy was taken at the value of H_{AA} for (8) and at the value of H_{AA}' for (9). Since in absolute value $H_{AA} \neq H_{AA}'$, the zero points of these two equations are not the same. (The calculated values are, $H_{AA}=12.298$, $H_{AA}'=5.429$, in atomic unit.)

TABLE I

	Lowest eigenvalue	C_A^2	C_B^2	C_C^2	C_D^2	C_E^2
(1)	0.3015	0.705	0.088	0.194	0.007	0.008
(2)	0.2756	0.715	0.098	0.187	/	/
(3)	0.2787	0.721	0.088	0.190	/	/

In Table I, (1) shows the result of the solution of the secular equation (8), (2) shows that of the three-dimensional secular equation obtained by dropping the terms, H_{DX}'s and H_{EX}'s, and (3) shows that of the secular equation (9)·C_A^2, C_B^2, etc. are the coefficients for the resonance hybrids, A, B, etc. for the lowest eigenvalue.

From this table, it can be seen that C_C^2 is always larger than C_B^2. This difference occurs mainly for the reason that in the secular determinant, (8) and (9), H_{CC} is larger than H_{BB}, and it means that the structure of O^+H^- contributes more to the ground state of the molecule than the structure of O^-H^+. This is contradictory to the usual chemical concept that the O-H bond is characterized, to a certain extent, by the O^-H^+ structure. Hence, in order to examine the validity of the results here obtained, the dipole moment of the water molecule was calculated. From the supposition of the AO's of the oxygen atom in a valence state, on which the present calculation is based' it is conceivable that the dipole moment of the water molecule consists of two bond dipoles and a lone-pair dipole[9] as shown in Fig. 2. By use of the

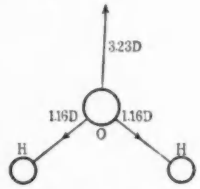

Fig. 2.

coefficients for the lowest-energy-state bond eigenfunction listed in the third row of Table I, the O-H bond moment was calculated to be 1.79D (O^+H^-). The main part of this moment, however, does not arise from the fact that C_C^2 is larger than C_B^2, but it arises from the resonance hybrid indicating homopolar bond (type A). As the calculated lone-pair dipole moment is 3.23 D and directs in the opposite side to the O-H bonds, the total moment amounts to 1.17 D, a value somewhat smaller than the experimental one, 1.84 D. On the contrary, if one assumes, as Pople assumed, that C_B^2 is a little larger than C_C^2, the calculated dipole moment will approach to the experimental value. Therefore, it can be concluded that in the present calculation H_{BB} has been a little underestimated compared to H_{CC}. It seems difficult, however, to avoid errors of this degree in view of the approximation of the method employed in the present work. Further discussions on the validity of the present calculation will be made later in this paper.

The energy of the delocalization due to the D- and E-structures may be given by the difference of the lowest eigen-values listed in the first and second rows of Table I, which amounts to 0.0259 AU., that is, 8.1 kcal./mol. On the other hand, the calculated electrostatic energy of the hydrogen-bond between two water molecules given by Pople[2], is 5.95 kcal./mol. A comparison of these two values allows us to conclude that the delocalization energy is of the same order of magnitude as, or rather larger than, the electrostatic energy.

From a survey of the features of the secular equations, (8) and (9), one can obtain some knowledge on the general character of the delocalization energy. First, we have seen that the inclusion of the D- and E-structures modifies the lowest energy of the system by only 0.0259 AU., a very small value compared to each matrix element. Therefore the problem can be, to some degree of exactness, treated by the second-order perturbation theory for the ground-state of the O-H group with inclusion of the higher energy states, D and E. The ground state of the O-H group may be given by a wave function

$$\Psi_O = c_A\Psi_A + c_B\Psi_B + c_C\Psi_C \qquad (10)$$

The second-order perturbation energy will then be,

$$(\Delta E)_{OD} = (H_{OD} - S_{OD}\cdot E)^2/(H_{OO} - H_{DD}),$$
$$(\Delta E)_{OE} = (H_{OE} - S_{OE}\cdot E)^2/(H_{OO} - H_{EE}). \qquad (11)$$

It will be interesting to calculate the perturbation energy by use of (11), and compare the results with the exact value. As a rough approximation H_{OO} in (11) may be replaced

9) J. A. Pople, ref. 6. C. A. Coulson, ref. 4.

by H_{AA} since the major part of Ψ_0 consists of Ψ_A. Correspondingly, we get,

$$(\Delta E)_{AD}=(H_{AD}-S_{AD}\cdot E)^2/(H_{AA}-H_{DD}),$$
$$(\Delta E)_{AE}=(H_{AE}-S_{AE}\cdot E)^2/(H_{AA}-H_{EE}), \quad (12)$$

where, for the E, 0.28 may be used. (See (3) of Table I).

The numerical results are:

$$(\Delta E)_{AD}=0.0346\text{AU.}=11\text{ kcal./mol.},$$
$$(\Delta E)_{AE}=0.0066\text{AU.}=2\text{ kcal./mol.},$$

The sum of these two values, 13 kcal./mol., is considerably larger than the true one, 8.1 kcal./mol. This may result from the negative value of $(H_{BD}-S_{BD}\cdot E)$, and $(H_{DE}-S_{DE}\cdot E)$.

From the above equations we can see that the delocalization energy becomes the greater, as the differences between H_{DD} or H_{EE} and other diagonal matrix elements decrease, and it is clear that these differences become the smaller,the larger the electron affinity of O and the smaller the ionization potential of O'*.

We can also see that the energy depends on the resonance integrals, $(H_{DX}-S_{DX}\cdot E)$ and $(H_{EX}-S_{EX}\cdot E)$. (Here X designates the elements A, B and C.) From the survey of the explicit forms of these terms, it can be seen that all of these terms, except $(H_{CE}-S_{CE}\cdot E)$, are approximately proportional to the overlap integral between ψ_2 and ψ_h, denoted hereafter by S_{2h}. Therefore it may be concluded that the delocalization energy increases with increasing S_{2h}. In general, S_{2h} depends on the distance between H and O', the formal charge of O' and the hybridization factor of ψ_2. Concerning the last factor it can be easily shown that S_{2h} has a maximum at a certain hybridization factor α. $(1>\alpha>0)$

Therefore, if one confines his attention within the influence of the overlap integral, he can conclude that the delocalization energy for a proton-acceptor which has an s, p-hybridized lone-pair orbital is, if the hybridization factor is appropriate, larger than the delocalization energy for a proton-acceptor which has pure s- or p-lone-pair orbital. It is interesting to note that, from the electrostatic point of view, a conclusion similar to that mentioned above can also be drawn, concerning the relation between the strength of hydrogen-bonds and the hybridization of the lone-pair of the proton-acceptor[10].

Eqs. (11) also suggest the limit of the accuracy for the obtained value of the delocalization energy. Namely, its accuracy is approximately the same as the accuracy of such terms as $(H_{AA}-H_{DD})$, $(H_{AD}-S_{AD}\cdot E)$, etc. As for the validity of these values, of course, there are many points to be discussed. For example, it is a question whether or not Slater-type AO's give reasonable results for the energy of interaction between atoms which are so separated as in this case. S. Maeda, in private communication, has pointed out that, when we used SCF AO's, the overlap integral, S_{2h}, will become much larger than the value calculated by use of Slater AO's. Also, when we calculate such terms as $(H_{AA}-H_{DD})$, some error will enter into the result on account of the fact that the same screening constant is used for both neutral and ionized states[11]. The correction of this error will increase our value of the delocalization energy.

Influence of the Formal Cahrge at O'

Thus far, it has been assumed that the proton-accepting oxygen atom has no formal charge. This assumption may be valid in many cases where the accepting molecule has only single bonds, because it has been recently accepted that even for a bond, usually thought to be polar, the main part of its polarity arises from the atomic dipole and the bond itself is for many cases nearly homopolar. But when the molecule with which we are concerned is a conjugated double-bond system, such as, for example, phenol or benzoquinone, the oxygen atoms will definitely carry a considerable positive or negative charge. In such cases the formal charge will not only modify the electrostatic interaction energy between proton-donors and proton-acceptors but will also modify the contribution of the delocalization energy by its effect of reducing the ionization potential of the lone-pair of the proton-acceptor and by increasing the overlap integral between the hydrogen 1s AO and the lone-pair AO. The increase of this overlap integral is caused by the change of the screening constant of the oxygen atom due to the formal charge. For instance, the same calculations were made for the case when the oxygen atom, O' has -0.2e formal charge. In this case the matrix elements corresponding to those given in (8) are a little modified and the following results are obtained.

$$H_{AA}-H_{DD}=2.33\text{AU.},$$
$$H_{AD}-S_{AD}\cdot E=0.39\text{AU.}-0.26E.$$

By use of these values and Eq. (12), the second-order perturbation energy arising only from the D-structure is calculated to be 13.5 kcal./mol., showing a 2.7 kcal. increase in comparison with the former result. On the other hand the increase of the electrostatic energy due to the same formal charge is about 1 kcal./mol.

* This has been already pointed out by Nukasawa, Tanaka and Nagakura[9].

10) W. S. Fyfe, *J. Chem. Phys.*, **21**, 2 (1953).

11) W. Moffitt, *Proc. Roy. Soc.*, **A210**, 236 (1951).

Comparison with the Experimental Facts

From the present results of calculation, it has been concluded that the delocalization energy amounts to about 8 kcal./mol. for the hydrogen-bond between water molecules. On the other hand the calculated electrostatic energy for the bond is about 5 kcal./mol. The experimental value of the heat of sublimation for ice is 12.2 kcal./mol., and if one tentatively assumes that about one fourth of this value is attributed to the interaction of non-neighbors, the energy of the hydrogen-bonds may be estimated to be about 9 kcal./mol. Since two hydrogen-bonds exist per one water molecule, the energy of the single hydrogen-bond is estimated to be about 5 kcal./mol. Hence, in order to assume that the theoretical and experimental energy values are consistent, one should consider that a repulsive energy of the order of 8 kcal./mol. is present in the hydrogen-bond. It may be easily understood that this repulsive energy is provided by the difference between exchange repulsion and the dispersion force, since the O-O distance for the hydrogen-bonded molecules must be shortened by the attractive electrostatic and charge-transfer forces, compared to the equilibrium O-O distance which would be attained when only usual dispersion force and exchange repulsion are present.

From the present results, it seems that the disagreement between the order of the experimentally found proton-accepting strengths of some proton-acceptors and the electrostatically predicted ones may be explained by taking into account the delocalization energies. For example, as is described before, the proton-accepting strengths of diethyl ether, acetone and acetonitrile are known to be as follows:

diethyl ether≒acetone>acetonitrile.

In these compounds, it can be concluded that the delocalization energy for the hydrogen-bond grows stronger from right to left in the above formula, and thus compensates or overwhelms the increase of the electrostatic energy from left to right. For, as is concluded previously, the delocalization energy increases as the ionization potential of the lone-pair of the accepting molecule decreases, and the lowest ionization potentials of these molecules, which may be considered to correspond to those of the lone-pairs, are as follows:

diethyl ether[12]>acetone[13]>acetonitrile[12].

The delocalization energies depend, however, not only on the ionization potentials but also on various other terms, for example, the overlap integral between hydrogen and lone-pair AO's which have not yet been clarified for such complex molecules. Hence a precise argument on these points remains to be made in future.

Summary

The delocalization energy for the hydrogen-bonded water molecules has been calculated non-empirically by use of the atomic orbital method, with a simplified model. The delocalization energy thus calculated amounts to about 8 kcal./mol. which is rather greater than the calculated electrostatic energy that has been usually considered to be the most important source of the binding force. The proton-accepting strengths of ether, acetone and acetonitrile have been discussed by use of this result.

Appendix

Some of the integrals calculated by the author are listed below in atomic unit. The notations are the same as those used by J. F. Mulligan (*J. Chem. Phys.*, **19**, 347 (1951)). s, σ, and π are the 2s, 2pσ, and 2pπ AO's of the atom O, and s', σ', and π', are those of the atom O', respectively.

Overlap integrals		Bare nuclea-field-potential energy integrals		Coulomb integrals	
S(s,s')	0.00594	(H: s',s')	0.6066	(s's': hh)	0.6029
S(s,σ')	0.00867	(H: $\sigma'\sigma'$)	0.6208	($\sigma'\sigma'$: hh	0.6078
S(σ,σ')	0.01260	(H: $\pi'\pi'$)	0.5995	($\pi'\pi'$: hh)	0.6011
S(π,π')	0.00156	(H: s'σ')	0.1166		
		(H: hs')	0.1616		
Exchange integrals		(H: hs')	0.1761		
(Approximate value)		(O': hh) =	(s's': hh)		
(hs': hs')	0.0359	(O': hs')	0.2502		
(hσ': hσ')	0.0483	(O': hσ')	0.1715		

The author wishes to thank Professor K. Kozima heartily for his valuable advice.

Tokyo Institute of Technology
Ohokayama, Meguro-ku, Tokyo

12) J. D. Morrison and A. J. C. Nicholson, *J. Chem. Phys.*, **20**, 1221 (1952).

13) T. M. Sugden and W. C. Price, *Trans. Farad. Soc.*, **44**, 116 (1948).

The Densities of Polyvinyl Alcohol Film at Moist States

By Hiroshi TADOKORO, Syuzo SEKI and Isamu NITTA

(Received July 9, 1954)

Introduction

Although there exist a considerable number of papers on the sorption of water vapor by high polymers, only a few works have been carried out about the density of high polymers at moist states, and this phenomenon seems to present an important problem for a course of further studies on the mechanism of water sorption. Such density investigations have already been made with wool (A. T. King[1]), native cellulose fibers (E. Filby and O. Maass,[2] A. J. Stamm and M. Seborg[3]) and regenerated cellulose fibers (P. H. Hermans[4]), whereas there, is, as far as the present authors are aware, none yet with synthetic polymers. The synthetic high polymers, whose crystallinity can be changed more or less easily by heat- or mechanical treatments, have an advantage in such density studies, because the density stands in close relation with the crystallinity, which in turn governs the feature of water sorption. The present study was undertaken as a preliminary investigation of such a problem in connection with our previous works[5,6] on the sorption of water vapor by polyvinyl alcohol (PVA), bearing in mind that there might be some analogy between this substance and cellulose.

Experimental

a) Density Measurements.

i) *Sample*: The sample used was purified by the following procedures. The powdered specimen of PVA (average degree of polymerization: 2100) was dissolved in water at about 80°C. The 1% aqueous solution of sodium hydroxide was added to exclude residual acetyl groups on standing overnight. This solution was then neutralized with hydrochloric acid, and dialysed with distilled water for two weeks in order to eliminate inorganic salts, and then PVA was precipitated by adding methanol-acetone mixture. The films used for experiment were cast from about 2.5% aqueous solution of the purified PVA, on a glass plate placed horizontally in an air thermostat at 50° ±5°C. This took about five hours. The films were about 0.05 mm. thick, and were cut in pieces about 1 mm. × 5 mm.

ii) *Apparatus and procedures*: About 500 mg. sample in a weighing bottle was dried at about 60°C. under a high vacuum (10^{-4} mm. Hg atm. or below), until its weight became constant within ±0.2 mg. This procedure required about 10 days. The dry sample in the weighing bottle was placed in a small desiccator, in which the relative humidity was controlled by an aqueous solution of sulfuric acid of a definite concentration This desiccator was thermostated at 25°±0.05°C. The sorption equilibrium required about three weeks.

The density measurements were made by the flotation method, by using carbon tetrachloride-benzene mixtures as the flotation media. In this case, a minute amount of water contained in the medium will cause a serious uncertainty on the data. So we have taken special precautions to remove the trace of water, by drying benzene with metallic sodium and carbon tetrachloride with potassium hydroxide. One measurement of density took about 15 minutes. When the specimen was suspended stationarily, another one was then immersed in addition after a short time, and it was found that the latter specimen behaved almost in the same way as the former. Thus, it was confirmed that the adsorbed water in the sample was not appreciably transferred to the flotation medium during the measurement. The density of the flotation medium was determined by use of the bicapillary pyknometer.[8]

All of the density measurements were duplicated with different specimens, and the two corresponding readings coincided with each other within ±0.06% except the sample containing 45.5% water.

The density of the sample in water was measured with the ordinary 10 cc. bottle type pyknometer at 25° ±0.05°C. and found to be 1.312 ±0.003 g./cc.

b) Desorption Measurements.—The sample for these measurements was prepared in the same way as that used for the density measurements, in this case the thickness and size being about 0.02 mm. × 17 mm. × 50 mm.

The apparatus was similar to that described in a previous paper[9] with some modifications to

1) A. T. King, *J. Text. Inst.*, **17**, T53 (1926); **18**, T274 (1927).
2) E. Filby and O. Maass, *Canad. J. Res.*, **7**B, 162 (1932).
3) A. J. Stamm and M. Seborg, *J. Phys. Chem.*, **39**, 133 (1935).
4) P. H. Hermans, "Contribution to the Physics of Cellulose Fibers," Elsevier Publishing Co., Inc., Amsterdam—New York, 1946, p. 73; "Physics and Chemistry of Cellulose Fibers," same publisher, 1949, p, 206.
5) I. Nitta, S. Seki and Y. Yano, *Ann, Report Inst. Fiber Res. (Osaka Univ.)*, **5**, 33 (1950).
6) I. Nitta, S. Seki, Y. Yano and S. Tajima, ibid., **6**, 13 (1952).
7) I. Nitta, S. Seki, H. Chihara, K. Kuriyama and S. Nakajima, ibid., **7**, 24 (1953).
8) M. R, Lipkin, A. D. Davidson, W. T. Harvey and S. S. Kurtz, Jr., *Ind. Eng. Chem, Anal. Ed.*, **16**, 55 (1944).
9) I. Nitta, S. Seki, M. Momotani and K. Satô, *J. Chem. Soc. Japan*, **71**, 378 (1950).

meet the present requirements. The relative humidity was controlled as mentioned above.

About 200 mg. of the sample was suspended from a quartz spring balance (sensitivity: 0.153 mm./mg.) by a glass string. The accuracy of the travelling microscope was ±0.01 mm., and the temperature of desorption was 25° ±0.05°C. The sample was dried under high vacuum (10^{-4} mm. Hg or below) at 60° ±0.05°C. and then the weight of th bone-dry sample was determined.

Fig. 1 shows that the time required to reach

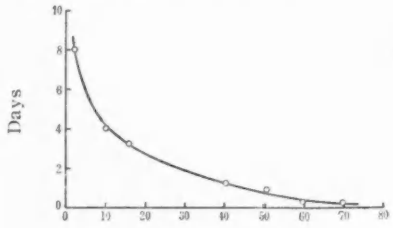

Final Relative Humidity %

Fig. 1. Relation between time required for desorption equilibrium and final relative humidity.

the desorption equilibrium depends to a remarkable degree upon the relative humidity, indicating that the desorption rate under low relative humidity is very low. The rate-determining process should be the diffusion of water molecules in the polymer film.

Results and Discussion

The densities of the PVA film at moist states are shown in Fig. 2*, and those for native cellulose[3] and regenerated cellulose[4] are also shown for reference. Each density curve showed a conspicuous maximum at about 1.5, 2.5 and 4.5% water content for PVA, native cellulose and regenerated cellulose, respectivery.

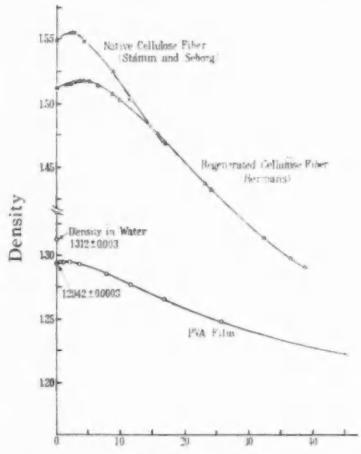

Water Content %

Ffg. 2. Density-water content curves.

* The density of PVA sensibly depends on the temperature and the duration of drying, heat- and mechanical treatments, degree of polymerization, etc. In connection with these, the experiments of the effect of heat treatment on densities are now in progress in this laboratory.

The existence of such a maximum has been explained differently by several investigators. Filby and Maass[2] attempted to explain the maximum for native cellulose by assuming a compression of the bound water in the specimen under about 100,000 atm. pressure, whereas Stamm and Seborg[3] estimated this pressure as about 3440 atm. However, this compression hypothesis seems to be superficial and to be only a formal interpretation. On the other hand, Hermans' interpretation[4] is based on the assumption that the apparent volume V_a per 1 g. of polymer in moist state, consists of the following three parts:

$$V_a = (1+a)/d_a = \varphi_w + a + \varepsilon_a,$$

where a is water content in g. per 1 g. bone-dry polymer, d_a, density of the moist polymer whose water content is a g., φ_w, the net volume of the polymer, which should be equal to the specific volume of the polymer measured in water, and ε_a is the volume of the empty space which can be ultimately filled with water molecules but cannot be permeated by the molecules of the flotation medium. As the water content a increases, the empty space ε_a will diminish in proportion and will disappear at last, thereafter the increase in V_a will become equal to the volume of water sorbed and the slope should be 45°. Fig. 3 shows the V_a curves against the water

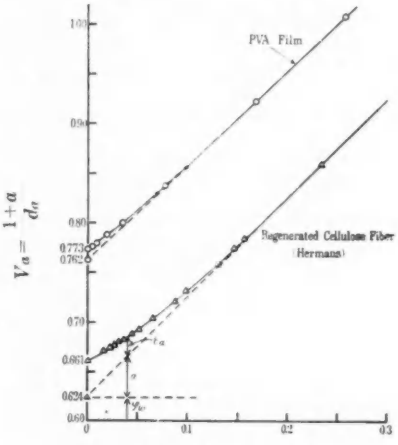

Water Content (a)

Fig. 3.

Relation between V_a and water content.

content a for our PVA data together with those for regenerated cellulose by Hermans.[4] In the case of PVA, the slope of the dashed straight line is slightly less than that of regenerated cellulose, whose slope is exactly 45°. This is presumably due to the fact that the interaction of PVA with water is larger than that of cellulose. As to this phenomenon, further study should be made to discover whether the water molecule may infiltrate the crystalline part of PVA or not.

In order to elucidate the nature of the empty space a little more, we calculated the so-called pore size distribution of the PVA film as well as regenerated cellulose fiber from our data of desorption isotherm and of Hermans, by means of Foster's method.[10] The desorption isotherms for PVA and regenerated cellulose[4] are shown in Fig. 4,

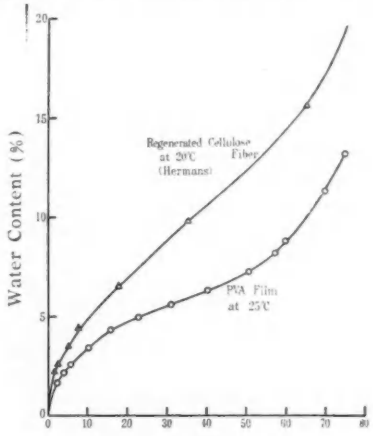

Fig. 4. Desorption isotherms.

and the pore size distribution curves are shown in Fig. 5. $V(\phi)$ in Fig. 5 stands for the

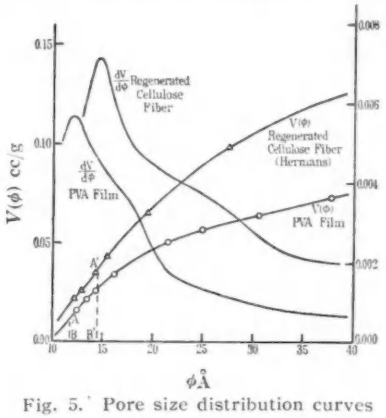

Fig. 5. Pore size distribution curves

integrated volume of pores whose diameter is smaller than ϕ. Although the variation of surface tension with the radius of curvature has been recently discussed theoretically by many authors,[11-15] we did not take this effect into our calculation, as these theories seem to be not yet quite decisive. By differentiating $V(\phi)$ with respect to ϕ the size distribution of the pore was obtained.

The empty volumes $\varepsilon_{a=0}$'s of the present sample and the related substance[3,4] are shown in Table I. In Fig. 5 the pore volumes corresponding to $\varepsilon_{a=0}$'s for PVA and regenerated cellulose are indicated by AB and A'B' respectively. It may be supposed that the pores of the diameter smaller than 11.7 Å. for PVA and 14.5 Å. for regenerated cellulose candot be inhabited by the molecules of the flotation medium, the mixture of carbon tetrachloride and benzene being used as the flotation medium for PVA, and that of carbon

TABLE I

DENSITY DATA AND CRYSTALLINITY

Material	$\varepsilon_{a=0}$ (cc./g.)	Wathr content of max. density (%)	Amorphous part fraction* (%)
PVA film	0.011	1.5	~7** (Nitta Seki, Yano and Tajima[3])
Native cellulose fiber	0.017	2.5	32 (Hailwood and Horrobin[15])
Regenerated cellulose fiber	0.037	4.5	65 (Hailwood and Horrobin[15])

* By sorption method.

** This is the data of the powder specimen which has the same degree of polymerization as the present sample.

10) A. G. Foster, *Discussions Faraday Soc.*, No. 3, 41 (1948).
11) R. C. Tolman, *J. Chem. Phys.*, **17**, 333 (1949).
12) J. G. Kirkwood and F. P. Buff, ibid., **17**, 338 (1949).
13) V. K. LaMer and G. M. Pound, ibid., **17**, 1337 (1949).
14) G. C. Benson and S. Shuttleworth, ibid., **19**, 130 (1951).
15) G. M. Pound and V. K. LaMer, ibid., **19**, 506 (1951).

tetrachloride and nitrobenzene for regenerated cellulose.[7] By use of the covalent and van der waals radii, the diameters of the molecules of the flotation media were estimated as follows:

carbon tetrachloride	~6.6 Å.
benzene	~7.3 Å.
nitrobenzene	~8.5 Å.

In spite of the boldness of the assumptions made above, the maximum diameters given above of the pore unaccessible for the molecules of the flotation media may be said to be in the same order of magnitude with the estimated geometrical sizes of these molecules, though the latter come out somewhat smaller. As the sources of such disagreement, the following factors may be pointed out.

(1) The water and nitrogen* sorption areas of polyvinyl acetal (acetal content 9.6%) measured previously by us were 65.9 m.²/g. and 6.0 m.²/g., respectively.[7] From this it may be reasonably assumed that while water molecules can break into the small space between the PVA molecular chains, nitrogen molecules cannot.[17,18] Accordingly, this fact seems to suggest that the geometrical size of the free molecule is not necessarily a decisive factor, but the mode of interaction between sorbent and sorbate must be also taken into account. Moreover, it may be possible that the pore size will vary as the water content increases.

(2) The filling-in of the pores with flotation medium is, quite probably, a matter out of equilibrium during the measurements of the present case.

(3) The Foster method assumes the Kelvin equation. It is now open to question whether this macroscopic equation can be applied to such a small pore of the molecular dimension.[11-15]

Finally, we may consider the relation among the maximum density of Fig. 2, the quantity $\varepsilon_{\alpha=0}$ and the crystallinity determined by the sorption method.[6,16] As shown in Table 1, the water content at which the density shows maximum, and the empty volumes $\epsilon_{\alpha=0}$'s increase in the following order:

PVA < native cellulose < regenerated cellulose

and the % amorphous region measured by the sorption method also increases in the same order.[6,16] This fact may be explained by assuming that mainly the amorphous region of these polymers is accessible to water and has nearly the same fraction of the empty volume.

Summary

(i) The densities of PVA film at moist states were measured at 25°C. with flotation method by using carbon tetrachloride-benzene mixtures. The density against water content curve shows a conspicuous maximum at about 1.5% water content.

(ii) The water desorption expriment was carried out using the same specimen. The pore size distributions of PVA film and regenerated cellulose fibers were calculated by the Foster method from our desorption date and Hermans' data, respectively.

(iii) The results are discussed and compared with those of other investigators obtained with native and regenerated cellulose.

The authors express their sincere thanks to Kurashiki Rayon Co. Ltd. for kindly giving them the PVA samples used for this work, to Dr. K. Hirabayashi and Mr. Y. Sone of the Institute for Chemical Research of Kyoto University, and to Messrs. H. Chihara and K. Suzuki of this laboratory for helpful advice and criticism.

Department of Chemistry, Faculty of Science, Osaka University, Osaka

16) A. J. Hailwood and S. Horrobin, *Trans. Faraday Soc.*, **42B**, 84 (1946).

* These two molecules have nearly the same molecular diameter (N_2: ~4.1 A, H_2O: ~4.0 A.).

17) K. W. Mooney, A. G. Keenan and L. A. Wood, *J. Am. Chem. Soc.*, **74**, 1367, 1371 (1952).

18) T. M. Shaw, *J. Chem. Phys.*, **12**, 391 (1944).

*Electron Diffraction Investigation on Tribromotropolone**

By Masaji KUBO, Masao KIMURA and Katsumi KIMURA

(Received May 28, 1954)

In a series of researches by one of the present writers and his collaborators,[1-7] measurements were made of the dipole moments of tropolone and a number of its derivatives using benzene solutions. The positions of various substituents in these tropolone derivatives were determined from a comparison of the observed moments with the theoretical moment calculated for various conceivable positions of the substituents. In this determination, an assumption was tacitly made that in analogy to ortho and para positions in benzene only carbon atoms 3 (ortho), (para) and 7 (ortho') are to be considered for the positions of substituents such as halogen atoms or a nitrogroup. One of the present writers and his collaborator[8] calculated π-electron distribution using the molecular orbital treatment and thereby revealed that carbon atoms 3, 5 and 7 have a greater share of π-electrons than carbon atoms 4 (meta) and (meta'). This suggests that electrophilic atoms and radicals preferentially attack hydrogen atoms at ortho, ortho' and para positions.

Although the conclusions derived from these physico-chemical considerations were found to be in conformity with the results of organic synthesis,[8] it is most desirable that this new type of ring compounds be provided with a more direct experimental proof in favor of the adequacy of the aforementioned assumption. The present investigation was undertaken in order to verify that the three bromine atoms of tribromotropolone are substituted for the hydrogen atoms of tropolone at ortho, ortho' and para positions. This compound is comparatively complicated for an electron diffraction experiment. Fortunately two of the present writers[10] as well as Heilbronner and Hedberg[11] have already carried out an electron diffraction study on tropolone and elucidated the geometrical configuration of the molecule of this compound. It is anticipated because the atomic number of bromine is high that the positions of bromine atoms in tribromotropolone can be determined by electron diffraction method accurately enough to give a decisive conclusion.

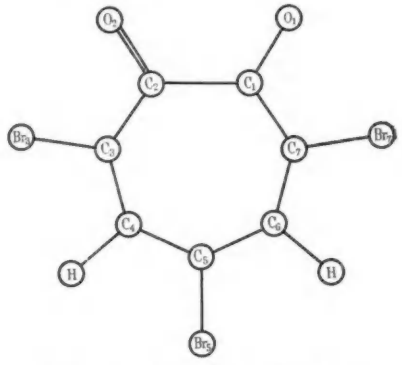

Fig. 1. *o*, *o'*, *p*-Tribromotropolone.

Material and Experimental Method.—A sample of tribromotropolone (m.p. 126°) was synthesized and purified in the laboratory of organic chemistry, Tohoku University. It was evaporated at a temperature 20—30° higher than its melting point and then passed through the high temperature nozzle described in a paper by one of the present writers and his collaborator.[12] The gas molecules ejected into a vacuum chamber interfered with an electron beam having a wavelength of about 0.06 Å. The wavelength was calibrated by means of gold foil. The camera length was 11 cm.

Experimental Results.—The visual intensity curve obtained is shown in Fig. 2. The q-values for the maxima and minima are given in Table I. From the visual intensity curve, a preliminary radial distribution function was calculated. The interatomic distances thus evaluated were used to obtain a preliminary theoretical intensity curve for

* Read before the scientific meeting of the Chemical Society of Japan held on April 4, 1952.

1) M. Kubo, T. Nozoe and Y. Kurita, *Nature*, **167**, 688 (1951).

2) Y. Kurita, T. Nozoe and M. Kubo, This Bulletin, **24**, 10 (1951).

3) Y. Kurita, T. Nozoe and M. Kubo, ibid., **24**, 99 (1951).

4) Y. Kurita, T. Mizuno, T. Mukai and M. Kubo, ibid., **26**, 192 (1953).

5) Y. Kurita, T. Nozoe and M. Kubo, ibid., **26**, 242 (1953).

6) Y. Kurita, S. Seto, T. Nozoe and M. Kubo, ibid., **26**, 273 (1953).

7) Y. Kurita and M. Kubo, ibid., **27**, 364 (1954).

8) Y. Kurita and M. Kubo, ibid., **24**, 13 (1951).

9) See papers by T. Nozoe and his collaborators published for the most part in the *Proc. Japan Acad.* and *Science Repts. Tohoku Univ.* Series I since 1950.

10) M. Kimura and M. Kubo, This Bulletin, **26**, 250 (1953).

11) E. Heilbronner and K. Hedberg, *J. Am. Chem. Soc.*, **73**, 1386 (1951).

12) M. Kimura and M. Aoki, This Bulletin, **26**, 429 (1953).

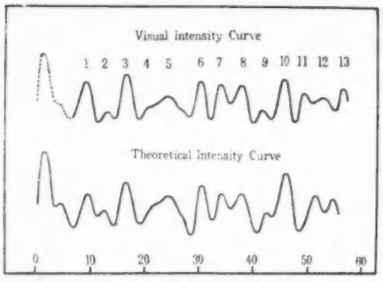

Fig. 2. The visual intensity curve and the theoretical intensity curve of tribromotropolone.

TABLE I

THE q-VALUES FOR THE MAXIMA AND MINIMA OF DIFFRACTION HALOS

Max.	Min.	q obs.	Max.	Min.	q obs.
1		9.42		8	35.64
	2	11.01	8		37.90
2		12.86		9	39.38
	3	14.45	9		41.62
3		16.36		10	43.36
	4	18.63	10		45.30
4		20.58		11	47.13
	5	22.48	11		49.20
5		24.39		12	50.88
	6	27.82	12		53.00
6		30.02		13	54.20
	7	31.61	13		56.30
7		33.73			

the range below $q=8$. As shown in Fig. 2, the visual intensity curve is extended to the region of small q-values by means of this theoretical intensity curve. The final radial distribution curve,

$$rD(r)=\sum_{q=1}^{\max} I_q \exp(-aq^2)\sin\left(\frac{\pi}{10}qr\right), \qquad (1)$$

obtained from the visual intensity curve supplemented by the dotted curve is shown in Fig. 3. In this equation, notations have their usual significances. The constant a was chosen to give $\exp(-aq^2)=0.1$ at the maximum q-value. The atomic distance evaluated from this radial distribution curve are given in the third column of Table II. They

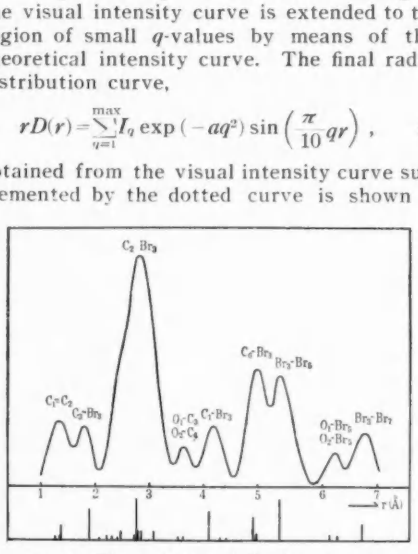

Fig. 3. The radial distribution curve of tribromotropolone.

TABLE II

INTERATOMIC DISTANCES IN TRIBROMOTROPOLONE

Atom pairs	Z_iZ_j/r_{ij}	Distances (exp.)	Distances (theor.)
Br_3–Br_5	38	5.40 A	5.40 A
Br_3–C_2	38	2.80	2.76
Br_3–C_3	28	1.82	1.88
Br_3–C_1	26	4.15	4.10
Br_3–C_6	21	4.96	4.92
Br_8–Br_7	15	6.77	6.74
C_1–C_2	13	1.36	1.36
Br_7–O_1	8	2.80	2.86
Br_8–O_2	8	2.80	2.79
C_1–C_3	8		2.47
C_1–C_4	7		3.08
Br_5–O_1	5	4.96	4.98
Br_7–O_2	5	4.96	4.92
Br_5–O_1	4	6.23	6.28
Br_5–O_2	4		6.14
O_2–C_1	4		2.22
Br_3–H_4	4	2.80	2.74
O_1–C_1	3	1.36	1.36
O_1–C_2	3		2.32
O_2–C_2	3		1.26
O_1–O_2	2		2.42
O_1–C_3	2	3.64	3.64
O_1–C_4	2		4.42
O_2–C_4	2		3.54
O_2–C_5	2		4.30
C_4–H_4	1		1.09
C_3–H_4	1		2.07

are assigned to atom pairs given in the first column. The designation of the atom pairs is evident from Fig. 1. In the second column, the values of Z_iZ_j/r_{ij} are given in arbitrary unit. The atom pairs contributing predominantly to each peak in the radial distribution curve are also given in Fig. 3. It will be seen from Table II and Fig. 3 that the majority of peaks in the radial distribution curve are due to interatomic distance involving a bromine atom or between bromine atoms. Therefore it is possible to determine definitely the location of three bromine atoms relative to each other and also to the tropolone ring. The interatomic distances obtained from the radial distribution curve can adequately be explained if we consider that the three bromine atoms are substituted for hydrogen atoms of tropolone at otho, para and ortho′ positions. If a bromine atom were in meta or meta′ position instead of at para position, the peak at 5.40

Å would be absent and the peak at 3.00 Å should be higher than the peak attributable to C_2–Br_3 distance. If each of three bromine atoms were bonded separately to one of three carbon atoms which, in turn, are bonded together consecutively, even though a peak at 5.40 Å could appear the peak at 3.00 Å would be much higher than it is in actuality and agreement could never be attained with the observed data. Thus it is confirmed that the sample of tribromotroplone under investigation is an *o*, *o*', *p*-derivative.

The radial distribution function of tribromotropolone is not suitable for the determination of the geometrical configuration of a tropolone ring. This is because the only distance obtainable for the determination of ring structure from the radial distribution curve is C–C bond distance equal to 1.36 Å whereas a number of parameters are required for the definite detrmination of the geometrical configuration of the molecule of this compound. In addition the mean amplitudes of various normal modes of vibration will appreciably affect the form of theoretical intensity curves. Considering possible errors inherent in the visual intensity curve, it seems impossible to determine the configuration of the molecule under investigation unless some simplifications be made. Therefore we assumed as follows. (1) The cycloheptatriene ring has a plane regular heptagon form with the length of its edge equal to 1.36 Å, as already mentioned. (2) All three C–Br bonds have the same length and are directed outward from the ring along the lines bisecting the respective ∠CCC angles so that both Br(para)-Br(ortho) and Br(para)-Br(ortho') distances are equal to 5.40 Å, as revealed by the radial distribution curve. (3) The C–H distance is equal to 1.09 Å. (4) The C–O distance is equal to 1.36 Å, while C=O distance is 1.26 Å long, as found in a tropolone molecule.[10]

A theoretical intensity based on these assumptions,

$$I(q)=\sum_i{}'\sum_j \frac{Z_iZ_j}{r_{ij}} \sin\left(\frac{\pi}{10}qr_{ij}\right), \qquad (2)$$

in which a constant factor is omitted, has been calculated for a rigid model and is given in Fig. 3. The interatomic distances calculated for this model are given in the last column of Table II. The vertical bars in Fig. 3. are drawn in proportion to Z_iZ_j/r_{ij}. It will be seen that the agreement of the theoretical intensity curve with the visual intensity curve is satisfactory and that the vertical bars in Fig. 3. are in good accord with the heights of peaks in the radial distribution function.

We do not intend to assert that this theoretical intensity curve is the only possible form in agreement with experiment. For instance, the C–C distances in the ring could be a little longer or they might not be exactly equal. Despite these minor reservations, we believe that the problem of the positions of bromine atoms relative to the tropolone ring is undoubtedly settled.

Summary

Tribromotropolone of melting point 126° was investigated in gaseous state by electron diffraction method. The two Br–Br distances equal to 5.40 Å and 6.77 Å respectively were found as distinct isolated peaks in the radial distribution curve. These distances together with the known configuration of tropolone ring already studied gave decisive evidence that in this molecule three bromine atoms are substituted for hydrogen atoms of tropolone at ortho, ortho' and para positions. This conclusion is in good agreement with the prediction of molecular orbital treatment of tropolone and proves the adequacy of the assumption made in the structural determination by dipole moment data, i.e. that electrophilic atoms and groups substiute hydrogen atoms of tropolone at ortho, ortho' and para positions but not those at meta and meta' positions.

We express our deep appreciation to Prof. Nozoe and his collaborators at Tohoku University for providing us with the material used in this experiment and also to the Ministry of Education for supporting this research.

Chemical Department, Faculty of Science, Nagoya University, Nagoya

Dependence of the Molecular Polarization of Carbon Dioxide on Pressure

By Masaji KUBO and Tadashi UCHIDA

(Received June 8, 1954)

One of the present writers[1] has proposed a theoretical formula for the pressure effect on the dielectric constant of gases on the basis of the mutual action of dipoles, namely

$$\left(\frac{\varepsilon-1}{\varepsilon+2}\right)\frac{M}{d}=P=a+\frac{b}{T}+\frac{3ab^2\rho}{8\pi N\beta^3T^2}, \qquad (1)$$

where ρ is the concentration of gas molecules in moles per cc or the reciprocal of molecular volume. The symbol β denotes the radius of the action sphere of molecules. All others have their usual significances. This theoretical equation indicates that the molecular polarizations of nonpolar substances are independent of pressure even when raised to a few hundred atmospheric pressures. The constancy of molecular polarization is in agreement with experiments on hydrogen, nitrogen, methane and air. For polar substances, the equation predicts that the molecular polarization at constant temperature increases linearly with the reciprocal of molecular volume. The results of ammonia conform to this relation. The value of molecular radius which is calculated from the pressure dependence of molecular polarization agrees well with those values obtained from the viscosity of the gas or from the constant b in the van der Waals equation of state. Somewhat exceptional behavior is exhibited by carbon dioxide. Although this gas is nonpolar, the molecular polarization increases slightly but definitely with pressure. It was suggested that this behavior might be due to effects other than dipole-dipole interaction, such as quadrupole interactions, which were neglected in the derivation of the aforementioned theoretical equation. Since then knowledge of the electronic structure of carbon dioxide molecule has been extended to such a degree that it is now possible to give a quantitative interpretation of the pressure dependence of the molecular polarization of this gas. In the present paper the results of a theoretical treatment on this problem will be given.

MacCormack and Schneider[2] used experimental second virial coefficient data for carbon dioxide to investigate the intermolecular potential of this molecule on the basis of a Lennard-Jones model. It was found that the derived force constants varied with temperature, the low temperature data yielding higher values of the collision diameter. They interpreted the results in terms of partial binary association and suggested a T-shaped configuration for the resulting dimer having a separation between the centers of monomeric units, viz. C-C distance, equal to 3.91 Å. A conceivable dimer configuration with the two monomeric molecular axes aligned in parallel was proved to be unstable. The suggested dimer formation could explain adequately the increase of collision diameter at lower temperatures and the dimer configuration led to a Coulomb interaction energy to compare favorably with the heat of dimerization obtained from the temperature dependence of the equilibrium constant of dimerization. The equilibrium constant was obtained from the second virial coefficient observed experimentally at lower temperatures and the coefficient calculated for a monomeric gas on the basis of the Lennard-Jones parameters from the high temperature data. The value of the equilibrium constant K_p of dimerization at 100°C. was found to be equal to 4.51×10^{-4} atm^{-1}.

The T-shaped dimer has no center of symmetry and hence should have a finite overall moment μ, which contributes to orientation polarization. If the degree of association is denoted by w, the molecular polarization P of the gas is given by

$$P=(1-w)P_{mono}=(w/2)P_{di}. \qquad (2)$$

Inasmuch as the dimer is a loose complex, it is reasonable to suppose that the electronic polarization is unaffected by dimerization. Therefore

$$P=P^\circ+(w/2)(P_{ori}+\Delta P_A), \qquad (3)$$

where P° ($=P_{mono}$) is the molecular polarization of unassociated carbon dioxide, i,e., the limiting value of molecular polarization at approaching zero pressure and P_{ori} is the orientation polarization of dimers,

$$P_{ori}=\frac{4\pi N}{3}\left(\frac{\mu^2}{3kT}\right). \qquad (4)$$

The quantity ΔP_A is the increase of atomic

1) M. Kubo, *Sci. Papers Inst. Phys. Chem. Research* (Tokyo), **27**, 295 (1935); This Bulletin **13**, 167 (1938). Cf. S. Glasstone, *Ann. Repts. Progr. Chem.*, **33**, 130 (1936); P. W. Bridgman, *Revs. Mod. Phys.*, **18**, 70 (1946).

2) K. E. MacCormack and W. G. Schneider, *J. Chem. Phys.*, **19**, 849 (1951).

polarization of dimers over twice the atomic polarization of monomers. Since the force field in monomeric units, viz. CO_2 molecules, will not be altered appreciably by the formation of the loose dimer, the assumption may be made that the vibrational modes of monomeric units remain practically unaffected by dimerization. A carbon dioxide molecule has four $(3\times3-5=4)$ normal vibrations, while the T-shaped dimer molecule has twelve $(3\times6-6=12)$ normal modes. Therefore ΔP_A will be the sum of contributions from four $(12-2\times4=4)$ modes of intermonomer vibrations.

By definition, the equilibrium constant is given as

$$K_p=\frac{p[(CO_2)_2]}{p^2(CO_2)}=\frac{(w/2)}{(1-w)^2p}, \qquad (5)$$

where p denotes the total pressure. Solving this equation for w and expanding the solution in a power series in K_pp, one obtains

$$w=2K_pp(1-4K_pp+\cdots\cdots). \qquad (6)$$

On introducing this in Equation 3, it becomes

$$P=P^\circ+K_pp(1-4K_pp)(P_{ort}+\Delta P_A). \qquad (7)$$

The molecular polarization P can be measured as a function of pressure p and the molecular polarization P° at approaching zero pressure has been obtained accurately ($P^\circ=7.35$ cc.).[3] As has already been mentioned, $K_p=4.51\times10^{-4}$ atm^{-1} at 100°C.[2] Therefore Equation 7 contains only one unknown parameter, $P_{ort}+\Delta P_A$, which can be obtained from experimental data. On the other hand, P_{ort} can be calculated if the dipole moment of a dimer can be estimated and ΔP_A will be obtained if the frequencies, the reduced masses and the effective charges of the four intermonomer vibrations mentioned above are evaluated properly. Subsequently the authors give a comparison of the sum of these two calculated quantitise with the experimental value of $P_{ort}+\Delta P_A$.

The dielectric constant of carbon dioxide at high pressures has been measured by many investigators. Inasmuch as one of the present writers reviewed available data on this problem in his previous reports,[1] references to earlier works need not be comprehensive. The measurements of Keyes and Kirkwood[4] and of Uhlig, Kirkwood and Keyes[5] carried out in the Massachusetts Institute of Technology were revised at the same laboratory by Keyes and Oncley[3] using a new cell. The extensive data by Michels and Michels[6] were critically examined by Keyes and Oncley, who corrected them for the "origin failure" ascribed to a variable displacement of the internal parts of the condenser when subjected to stresses induced by the presence of a high pressure gas. The adjusted data were found to be in good agreement with those obtained by themselves.

In Fig. 1. a plot is made of the molecular

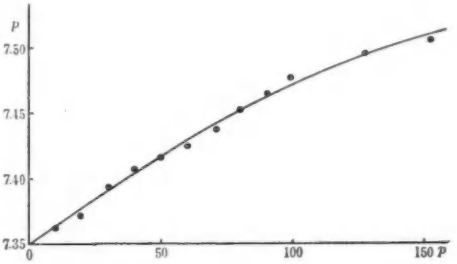

Fig. 1. Dependence of the molecular polarization P(cc.) of carbon dioxide upon pressure p(atm.).

polarization obtained by Keyes and Oncley against pressure rather than against P°/v as is done in the original report, where v denotes the molecular volume.* To convent molecular volume data to pressure, Michels and Michels' p-v-T data[7] were used. The old density data obtained by Amagat and the new by MacCormack and Schneider[8] gave practically identical results. The full line in Fig. 1. depicts the value of P calculated by Equation (7) with $P_{ort}+\Delta P_A=3.30$ cc. Over the entire pressure range studied, the points lie very close to the parabolic line within experimental errors as is expected from Equation (7). If experimental points lie on a parabola, one can give an empirical equation with three constants capable of fitting the curve to experimental points. It should be noted that in Equation (7) there are only two adjustable parameters, viz., P° and $P_{ort}+\Delta P_A$. This indicates that the explanation of the change of polarization with pressure in terms of partial association is adequate.

3) F. G. Keyes and J. L. Oncley, *Chem. Revs.*, **19**, 195 (1936).
4) F. G. Keyes and J. G. Kirkwood, *Phys. Rev.*, **36**, 754, 1570 (1930).
5) H. H. Uhlig, J. G. Kirkwood and F. G. Keyes, *J. Chem. Phys.*, **1**, 155 (1933).
6) A. Michels and C. Michels, *Phil. Trans. Roy. Soc. London*, **231**, 409 (1933).
* Since P° is equal the real volume per mole of molecules regarded as conducting spheres, P°/v is the ratio of the real volume of molecules to the total volume which they occupy.
7) A. Michels and C. Michels, *Proc. Roy. Soc. London*, A**153**, 201 (1935); A. Michels, C. Michles and H. Wouters, ibid., **153**, 214 (1935).
8) K. E. MacCormack and W. G Schneider, *J. Chem. Phys.*, **18**, 1269 (1950).

Estimation of the Dipole Moment of a Dimer

The geometrical configuration of the dimer of carbon dioxide proposed by MacCormack and Schneider[2] is given in Fig. 2. As regards the

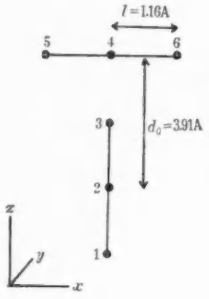

Fig. 2. Geometrical configuration of the dimer of carbon dioxide. Black circles and white circles stand for carbon and oxygen atoms respectively.

charge distribution in a monomeric unit, it may be assumed that each oxygen atom carries $-\kappa e$, while the carbon atom carries $+2\kappa e$. Here e denotes the absolute value of an electronic charge. In a dimer the electric field of each of the three point charges in a monomeric unit polarizes each of the three atoms of the partner monomer. The vector sum of eighteen ($2\times3\times3=18$) induced moments is equal to the over-all moment μ of a dimer. Straightforward calculations yield that the moment is directed antiparallel to the positive z-axis with the following value:

$$\mu=(\alpha_C+2\alpha_O)\kappa e\left[\frac{1}{(d_0-l)^2}+\frac{1}{(d_0+l)^2}-\frac{2d_0}{(d_0^2+l^2)^{3/2}}\right], \quad (8)$$

$$[\ ]=5.59\times10^{14}\ \text{cm}^{-2}.$$

Here α_C and α_O denote the polarizabilities of carbon and oxygen atoms respectively. In this case $\alpha_C+2\alpha_O$ is equal to the polarizability α of a carbon dioxide molecule. This molecule is fairly anisotropic, the polarizability in the direction parallel to the molecular axis $\alpha_\parallel$ ($=4.05\times10^{-24}$cm^3.) being greater than that perpendicular to the axis $\alpha_\perp$ ($=1.95\times10^{-24}$ cm^3).* If the relative position of the two monomeric units in a dimer is taken into account, it is reasonable to assume that α in this case is equal to $(\alpha_\parallel+\alpha_\perp)/2$ rather than $(\alpha_\parallel+2\alpha_\perp)/3$. Hence $\alpha=3.00\times10^{-24}$ cm^3.

Carbon dioxide has been treated from the molecular orbital point of view by Mulliken,[9] Moffitt,[10] Mulligan[11] and Shull.[12] The last author discussed in detail the off-center electron distribution of a carbon atom, which distribution he stated could hardly be interpreted as an ionic character of a C-O bond. Subtracting the terms due to this off-center distribution, he was left with a net equivalent charge distribution in which each of the oxygen atom carries $-0.40e$, i.e., $\kappa=0.40$.

On introducing the values of α and κ in Equation (8), one obtains $\mu=0.322$ D, which corresponds to the orientation polarization at 100°C. given by

$$P_{ori}=\frac{4\pi N}{3}\left(\frac{\mu^2}{3kT}\right)=1.694\ \text{cc}. \quad (9)$$

Contribution of the Four Intermonomer Normal Vibrations to Atomic Polarization

The dimer molecule has a symmetry C_{2v} with symmetry elements of $C_2(z)$, $\sigma_v(xz)$ and $\sigma_v(yz)$. Normal vibrations can be classified into four symmetry types as shown in Table I. Of the four intermonomer normal vibrations mentioned in the foregoing section, one belongs to type A_1, two to type B_2, and one to type B_2. The four normal vibrations in question are shown in Fig. 3.

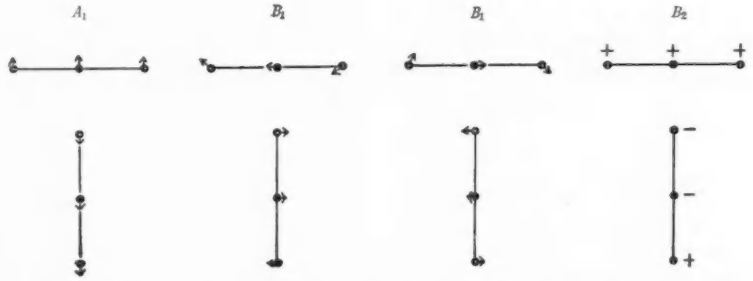

Fig. 3. Intermonomer normal vibrations of the dimer of carbon dioxide.

* Taken from Landolt-Börnstein, Zahlenwerte und Funktionen, 6th ed. 1951, Band I, 3 Teil, p. 511.

9) R. S. Mulliken, *J. Chem. Phys.*, **3**, 720 (1935); *Revs. Mod. Phys.*, **14**, 204 (1942).

10) W. Moffitt, *Proc. Roy. Soc. London*, A**196**, 524 (1949).

11) J. F. Mulligan, *J. Chem. Phys.*, **19**, 347 (1951).

12) H. Shull, *Proc. Natl. Acad. Sci. U. S.*, **38**, 400 (1952).

TABLE I

CLASSIFICATION OF VARIOUS NORMAL VIBRATIONS OF THE DIMER OF CARBON DIOXIDE INTO SYMMETRY TYPES

Symmetry types	Symmetry coordinates	No. of normal vibr.	Translation and rotation	Genuine normal vibr.	Intramonomer vibr.	Intermonomer vibr.
A_1	$z_1,\ z_2,\ z_3,\ z_4,\ z_5+z_6,\ z_5+z_7$	6	T_z	5	4	1
A_2	y_5-y_6	1	R_z	0	0	0
B_1	$x_1,\ x_2,\ x_3,\ x_4,\ x_5-x_6,\ z_5-z_6$	6	$T_x,\ R_y$	4	2	2
B_2	$y_1,\ y_2,\ y_3,\ y_4,\ y_5+y_6$	5	$T_y,\ R_x$	3	2	1
Total number		18	6	12	8	4

The contribution of a normal mode of vibration to the atomic polarization is given by[13]

$$Q=\frac{1}{3}\left(\frac{Ne_{eff}^2}{3\pi M_{eff}\nu^2}\right)=\frac{4\pi Ne_{eff}^2}{9k_0}, \qquad (10)$$

in which N is Avogadro's number, e_{eff} is the effective charge, ν is the vibrational frequency, M_{eff} is the effective mass associated with the vibration, and k_0 is the force constant. The factor 1/3 was introduced to take into account all the possible orientation in space of a molecule having a linear oscillator. Therefore if the effective charge and the force constant for a particular normal vibration are known, the contribution of the normal vibration to the atomic polarization can be calculated.

Normal Vibration of Type A_1.—Let q denote the increase of C-C distance over its equilibrium value. Apparently q is the normal coordinate of this vibration. The dipole moment which points along the direction of negative y-axis can be calculated in the same manner as in the derivation of Equation (8), even when the vibration is excited. This yields immediately the effective charge given by

$$e_{eff}=\frac{d\mu}{dq}=-2\alpha\kappa e\left[\frac{1}{(d_0-l)^2}+\frac{1}{(d_0+l)^2}-\frac{2d_0^2-l^2}{(d_0^2+l^2)^{5/2}}\right], \qquad (11)$$

$$[\ ]=2.99\times10^{22}\ \mathrm{cm}^{-3}.$$

It should be mentioned here that the polarizabilities of carbon and oxygen atoms enter the equation in the form of $\alpha_C+2\alpha_O$ and no assignment to individual atoms is required.

To obtain the force constant of this vibration, the potential function V was constructed out of the attraction term of Coulomb interactions and the repulsion term of the Lennard-Jones potential assumed to be proportional to the inverse twelfth power of the separation d $(=d_0+q)$, viz.

$$V=\sum\frac{E_iE_j}{r_{ij}}+\frac{\lambda}{d^{12}}, \qquad (12)$$

where E_i denotes a charge in one of the monomeric units, E_j that in the other, r_{ij} the distance between them to be expressed as a function of l, d_0 and q. The values of E's are $+2\kappa e$ for carbon atoms, and $-\kappa e$ for oxygen atoms.

The constant λ was chosen so as to give a minimum of V at $d=d_0$, namely

$$\lambda=2\kappa^2e^2\left[\frac{1}{(d_0-l)^2}-\frac{d_0-l}{[(d_0-l)+l^2]^{3/2}}-\frac{2}{d_0^2}+\frac{2d_0}{(d_0^2+l^2)^{3/2}}+\frac{1}{(d_0^2+l)^2}-\frac{d_0+l}{[(d_0+l)^2+l^2]^{3/2}}\right]\frac{d_0^{13}}{12}, \qquad (13)$$

$$[\ ]=1.60\times10^{-4}\ \mathrm{cm}^{-2}.$$

Through cumbersome but straightforward calculations, one obtains the following expression for the force constant:

$$k_0=\frac{d^2V}{dq^2}=2\kappa^2e^2\left[-\frac{2}{(d_0-l)^3}-\frac{1}{[(d_0-l)^2+l^2]^{3/2}}+\frac{3(d_0-l)^2}{[(d_0-l)^2+l^2]^{5/2}}+\frac{4}{d_0^3}+\frac{2}{(d_0^2+1^2)^{3/2}}-\frac{6d_0^2}{(d_0^2+l^2)^{5/2}}-\frac{2}{(d_0+l)^3}-\frac{1}{[(d_0+l)^2+l^2]^{3/2}}+\frac{3(d_0+1)^2}{[(d_0+l)^2+l^2]^{5/2}}\right]+12\times13\frac{\lambda}{d_0^{14}}, \qquad (14)$$

$$[\ ]=-2.51\times10^{22}\ \mathrm{cm}^{-3}.$$

In this equation, the right-hand side of Equation (13) was substituted for λ, leading to:

$$k_0=5.62\kappa^2e^2\times10^{22}\ \mathrm{erg/cm^2}. \qquad (15)$$

Introducing this value as well as that of effective charge in Equation (10), one obtains the following value for the contribution of this normal vibration to atomic polarization:

$$Q(A_1)=0.482\ \mathrm{cc}. \qquad (16)$$

13) J. H. Van Vleck, "The Theory of Electric and Magnetic Susceptibilities", Oxford Press, 1932, p. 363.

Normal Vibration of Type B_2.—The normal coordinate q of this vibration may be taken as one-half of the difference between y-coordinates of the two carbon atoms. One can determine the displacements of atoms from the plane of a dimer molecule in equilibrium under two conditions, that no translation and no rotation of the dimer molecule as a whole take place, and that the configuration of monomeric units remain unchanged. The result are shown in Table II, where ξ denotes

$Md_0/2ml=4.63$, M and m being the masses of a CO_2 molecule and an O-atom respectively.

TABTE II
DISPLACEMENT OF ATOMS FROM THE PLANE OF A DIMER MOLECULE

O-atom, 1	$(\xi-1)q$
C-atom, 2	$-q$
O-atom, 3	$-(\xi+1)q$
Atoms, 4, 5, 6	$+q$

It is obvious from symmetry considerations that the change of moment takes place in a direction parallel to z-axis. Calculations analogous to the foregoing yield the following result:

$$e_{eff}=\frac{d\mu_y}{dq}=-\alpha K e\left[\frac{2+\xi}{(d^0-l)^3}+\frac{2-\xi}{(d_0+l)^3}-\frac{4}{(d_0^2+l^2)^{3/2}}\right], \tag{17}$$

$$[\ ]=2.40\times10^{23}\ \text{cm}^{-3}.$$

Again the assignment of polarizability to individual atoms is not necessary. In this case, however, α should be equal to $\alpha_\perp$ rather than to $(\alpha_\parallel+\alpha_\perp)/2$, because all the y-components of induced moments are perpendicular to the molecular axes of monomeric units. The electrostatic and repulsive interactions being assumed as in Equation (12), the potential function of this normal vibration is calculated as:

$$V=V_0+\kappa^2e^2\left[\frac{(2+\xi)^2}{(d_0-l)^3}-\frac{(2+\xi)^2}{[(d_0-l)^2+l^2]^{3/2}}-\frac{8}{d_0^3}+\frac{8}{(d_0^2+l^2)^{3/2}}+\frac{(2-\xi)^2}{(d_0+l)^3}\right.$$
$$\left.-\frac{(2-\xi)^2}{[(d_0+l)^2+l^2]^{3/2}}\right]q^2-\frac{24\lambda}{d_0^{14}}q^2+\cdots. \tag{18}$$

$$[\ ]=4.35\times10^{23}\ \text{cm}^{-3}.$$

Mentioned should be made here that the third term in this equation due to repulsion is less than 4% of the second term due to electrostatic force and hence the assumed functional form of repulsive potential is rather trivial. The force constant is obviously twice the coefficient of q^2 in the right-hand side of Equation 18. The contribution of this normal vibration to atomic polarization can then be evaluated by the use of Equation (10),

$$Q(B_2)=0.212\ \text{cc.} \tag{19}$$

Normal Vibration of Type B.—There are two normal vibrations belonging to the symmetry type of B_1, both of which are infrared active. Unless some assumptions be made for the force field of the dimer molecule, it is difficult to evaluate the effective charges and the force constants of these normal vibrations. Since the contributions of these vibration are rather minor portions of $P_{ort}+\Delta P_A$ compared with the first term, the writers gave up tedious efforts to evaluate the values of Q and simply assumed that every normal vibration contributes nearly the same amount to atomic polarization. This assumption may be justifiable to some extent because each of the vibrations of symmetry types A_1 and B_2 contributes to ΔP_A an amount of the same order of magnitude as that of the other vibration. The sum of P_{ort} (=1.694 cc.), $Q(A_1)$ (=0.482 cc.), $Q(B_2)$ (=0.212 cc.) and $2Q(B_1)$ (=0.694 cc.), i.e., $P_{ort}+\Delta P_A$ is equal to 3.08 cc. It can be seen that this order of magnitude compares favorably with 3.30 cc. obtained experimentally from the pressure dependence of molecular polarization.

In conclusion, mention should be made of the dielectric constant of ethylene studied by David, Hamann and Pearse.[14] The values of the Clausius-Mosotti function at high pressures were found to exceed the value at the limiting zero pressure. In view of the similarity between the behavior of carbon dioxide and ethylene in this respect, it may be suggested that ethylene also forms a T-shaped dimer molecule which, owing to π-electron transfer, has a finite electric moment.

Summary

The dependence of the molecular polarization of carbon dioxide upon pressure was explained by partial binary association suggested by MacCormack and Schneider on the basis of the second virial coefficient. The theoretical considerations indicate that molecular polarization increases with pressure and that the rate of increase of molecular polarization decrease as the pressure increases. The results of theoretical predictions agree with experiments quantitatively over the entire pressure range if a parameter contained in the theoretical formula is adjusted properly. This parameter can be interpreted as the molecular polarization of dimeric molecules plus the difference between the atomic polarization of dimers and twice the atomic polarization of monomers. The three quantities, the dipole moment of the dimer, the effective charges of four intermonomer normal modes of vibration and the force

14) H. G. David, S. D. Hamann and J. F. Pearse, *J. Chem. Phys.*, **19**, 1491 (1951).

constants of the same, were evaluated theoretically. A numerical value of the aforementioned parameter which is calculated from these three quantities compares favorably with that obtained from the dependence of molecular polarization on pressure.

Chemical Department, Faculty of Science, Nagoya University, Nagoya

A Microphotographic Research on Salt System: $NaNO_2$—KNO_3

By Kaoru SAKAI

(Received May 18, 1954)

Introduction

A considerable amount of microphotographic study on the metallic alloys has been made with the aid of a metallographic microscope, but little has been made on the salt systems. The reason seems to lie in some difficulties of observing directly the state of the etched surface of the salt ingot under the metallographic microscope, because its etched surface is liable to glitter dazzlingly all over the sample. W. M. Magden[1], S. F. Žemczužny[2], E. Shibata & H. Imai[3], A. Kofler[4] have reported microscopical technique of investigating binary salt systems, chiefly for the case of eutectics. But they were not successful in observing the microscopic structures of specimens in the case of solid solution except the silicates and the unhygroscopic salts because of some technical difficulties.

As the $NaNO_2$–KNO_3 system contains the hygroscopic salt ($NaNO_2$), the surfaces of etched specimens become stained during the process of polishing. Besides the specimens of this system are fragile and porous, therefore it is doubtful whether this system belongs to the solid solution type or to the eutectic type. If this system belongs to the former, the dendrite crystals of soild solution can not be observed microscopically by the usual technique, because they are not composed of pure salt like those in the eutectic case. So the author intended to improve the technique and succeeded in taking a clear microphotograph of this system.

Experimental

(1) Thermal Analysis and Electric Conductivity Measurement.—Kagan and Kamuischan[5] made the thermal analysis of the $NaNO_2$-KNO_3 system and found it to be a case of solid solution (It was found somewhat round in the neighbourhood of the temperature minimum 141.1°C, 46 5 Mol.% KNO_3); but it is not so sure unless the microscopical observations are made, because the heat capacities of the specimens are extremely small and the obtained cooling curves are so irregular that it is doubtful whether this system belongs to the solid solution type or to the eutectic type.

The author made a study on phase diagram of this system by means of thermal analysis and electric conductivity measurement by using an electric furnace of sufficiently large heat capacity. The cooling rate was ca. 1°C./45 sec. between 200–300°C., the same as in the research of Kasé[6]. Fig. 1 shows the results obtained. But the author failed to determine the accurate liquidus by these two methods alone because the cooling curves are of very slow slope.

Fig. 1 also shows that the solidus obtained by conductivity method* always lies under that of thermal data. Because in the practice of thermal

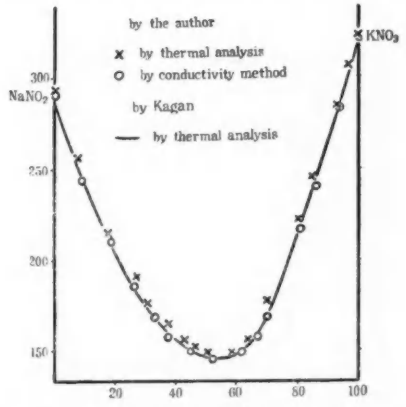

Fig. 1. Phase diagram of $NaNO_2$—KNO_3

1) W. M. Magden, *J. Chem. Soc.*, 458 (1930), 874 (1930).
2) S. F. Zemczuzny, *Z. anorg. Chem.*, **153**, 47 (1926).
3) E. Shibata, H. Imai, *J. Sci. Hiroshima Univ.* A**14**, 1 (1949).
4) A. Kofler, *Chem. Ber.*, **85**, 447 (1952).
5) M. Ya. Kagan and N. Kamuischan, *J. Applied Chem.* (U. S. S. R.) 5347 (1932); *Chem. Abstr.*, **27**, 15 (1933).
6) T. Kasé, *J. Applied Phys. Japan*, **7**, 213 (1938).
* The used apparatus is the same as that described in *J. Chem. Soc.* (Japan) Pure Chem. Sec. **75**, 64 (1954).

analysis the thermocouple is set in the centre of the melt, we cannot get rid of the thermal effect occuring from the segregation, but in the case of the electric conductivity there is little error from that source.

(2) Microscopic Method

(*a*) *Method of flattening the surfaces of salt ingots.*—To smooth the surfaces of ingots, it is usually necessary to polish them with the various grades of emery papers and the soft brushes made of flannel. But the ingots of this system are so fragile and porous that their surfaces are liable to be damaged during the process of polishing, and the more they include large amount of KNO_3, the more fragile and porous they become. So the following method is recommended. Mixes of $NaNO_2$ and KNO_3 in various proportions are prepared in a quartz crucible (Fig. 2) which is composed

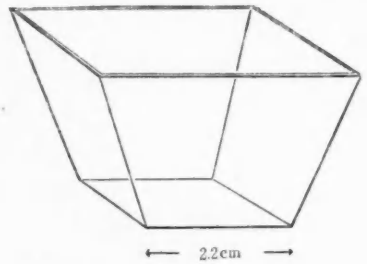

Fig. 2. Quartz crucible.

of five well-polished quartz plates. By the help of this crucible, we are now able to avoid all the troubles in cutting and polishing the surfaces of ingots, because the five surfaces of ingot facing the crucible plates are already as glassy as mirrors.

(*b*) *Method of etching.*—The surfaces of the obtained specimens are etched with etching solution. In this case the author used the saturated KNO_3 solution in 25% alcohol*, because in etching the surfaces of specimens it is recommended to use the saturated solution of the salt of smaller solubility of the two.

(*c*) *Microscopic operation.*—After the above treatment the etched surfaces are pressed on celluloid plates, slightly moistened with amylacetate in which a small amount of celluloid is dissolved. A few minutes later, the celluloid plates are carefully peeled off and examined microscopically.

When the quartz crucible does not react with salt ingot, we have now become able to study phase diagrams of almost all salt systems as easily as those of metallic alloy. Thus, the microphotographic method of studying salt systems can be applied not only to the unhygroscopic specimens but also to the hygroscopic, fragile and porous specimens such as mentioned above.

* E. Shibata used water as the solvent, but it is inadequate because of its high solubility.

Results and Discussions

The dendrite crystals of solid solution are found in the above inserted Photo. 1–5. The shapes of dendrite crystals closely resemble those of Cu-Ni[7,8], Cu-Sn[9] alloys, steel[10] and devitrified glass[11]. The dendrite structure of solid solution occurs in the state of imperfect equilibrium, and when the cooling rate is comparatively rapid, the diffusion of each ion of the mixed salts may be interrupted. So, if the specimens are annealed at the neighborhood of melting points, each ion of salts may diffuse slowly, and the concentration at each part of the melt may become uniform; then the dendrite crystals of soild solution may entirely disappear. See Photo. 6. If the $NaNO_2$—KNO_3 system belongs to a eutectic without any solid solution range, dendrite crystals should not disappear, and moreover, the areas occupied by dendrite crystals in the whole area ought to be varied as the composition changes. But it has been found out by this experiment that the areas of dendrite crystals are always constant on the whole. See Photos. 1–5. This fact also shows that this system belongs to a case of solid solution. And if the cooling rate can be limited within the proper extent to give rise to dendrite crystal, the size of dendrite may become maximum, when the cooling rate is minimum. It is proved by Photos. 1, 3, 4 and 5.

Summary

(1) The phase diagram of the $NaNO_2$–KNO_3 system was constructed by the thermal analysis and the electric conductivity measurements. The solidus on the whole is the same as found by Kagan.

(2) By the microphotographic method it was ascertained that this system belongs to a case of soild solution just as Kagan had inferred and that the nature of dendrite crystals in solid solution of the salts closely resembles those of alloys and devitrified glass.

(2) By the improved technique the microphotographic method of studying salt systems has now become able to apply to almost all salt systems.

7) I. Iitaka, *Bull. Inst. Phys. Chem. Res.* **13**. 1395 (1934).
8) S. H. Carpenter, J. M. Robertson, *Metals*, **1**, 223 (1939).
9) A. Sauveur, *Trans. Amer. Soc. for Steel Treating*, July, 1 (1923).
10) A. Sauveur, "Metallography and Heat Treatment of Iron and Steel", Chap. 3 (1933).
11) J. Sugie, Study of 'Glass Crystals', 8 (1943).

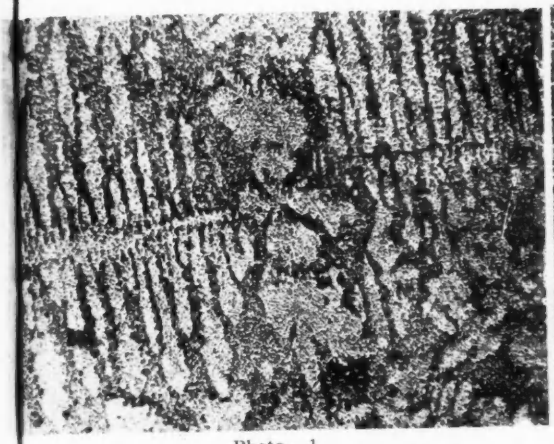

Photo. 1
×80, 24 wt. % KNO_3 (Rapid Cooling)

Photo. 2
×80, 31 wt. % KNO_3 (Medium Cooling)

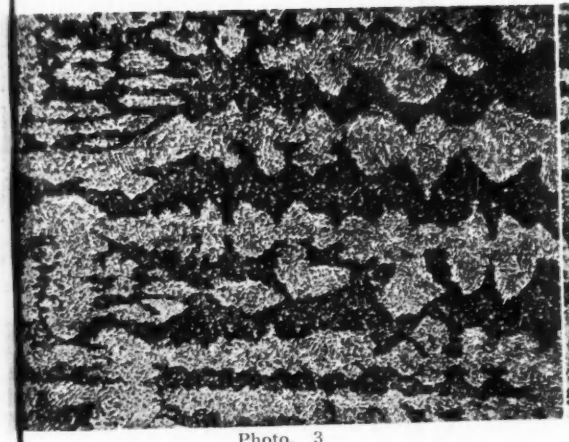

Photo. 3
×75, 51.5 wt. % KNO_3 (Slow Cooling)

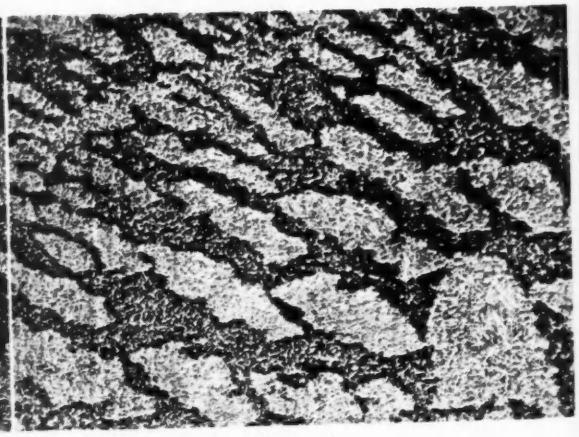

Photo. 4
×75, 65 wt. % KNO_3 (Slow Cooling)

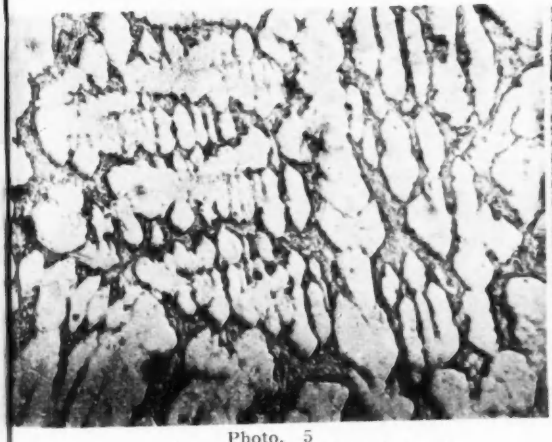

Photo. 5
×75, 82 wt. % KNO_3 (Slow Cooling)

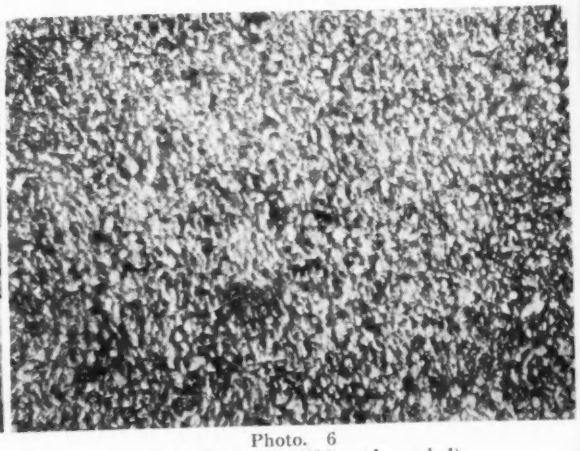

Photo. 6
×80, 82 wt. % KNO_3 (Annealed)

The author wishes to express his sincere thanks to Prof. Eiichi Shibata for his valuable advice and encouragement. This investigation was supported in part by a grant from the Ministry of Education.

Senior High School, Department of Education, Kanazawa University, Kanazawa

Sorption of Gases on Evaporated Nickel Films. I. Sorption of Oxygen

By Zenjirō ODA

(Received June 1, 1954)

Although the sorption of oxygen by evaporated metal films has been studied by various authors[1,2,3,4] there appears some discrepancies in the present view on the sorption mechanism and the structure of evaporated metal films.

The present work was undertaken to understand the behaviour of oxygen adsorbed on the surface more clearly and to examine the applicability of the Cabrera-Mott's theory of oxidation[5] for evaporated metal films.

Experimental

The rate of sorption was measured by a constant-volume method, employing slight modification of the apparatus used by Rideal and Trapnell[3]. A sensitive Pirani gauge and a McLeod gauge were used to measure the pressure ranging from 10^{-6} to 10^{-2} mmHg.

A U-shaped pure nickel filament 0.5 mm. in diameter and 11 cm. long was spot-welded to stem leads and sealed in a vacuum tube. Evacuating the system, the nickel filament was evaporated onto the inner wall of the bulb.

After the bulb was backed for 4 hrs. or longer, the trap was cooled with liquid oxygen and the filament was outgassed at about 1000°C. for half an hr. or longer. Immersing the bulb in melting ice, filament temperature was raised to 1300°C. and maintained at that temperature for a desired period with control of heating current. Since the film thus prepared on the wall of the bulb was unstable, it was kept at 0°C in vacuum for 20 min. before the gas was admitted. Electron diffraction study[6] showed that the films thus prepared consist of fine crystallites with their (110) planes slightly orientating parallel to the base.

The weight of the film was finally determined by weighing the bulb before and after the dissolution of the film.

In measuring the change of electrical resistance of the film in the course of sorption, the test tube described elsewhere[7] was attached to the adsorption apparatus.

Results and Discussions

Although the reaction temperatures were 0°, −78° and −183°C., the sorptions of oxygen were unchanged substantially and found to consist of two stages, i.e., an initial rapid process and a subsequent slow process.

(1) On admitting a known amount of gas to a clean film, a number of increments were consumed at the same very rapid rate and reached an equilibrium pressure of 10^{-6} mmHg. within 5 min.

(2) Subsequent increments were consumed at successively decreasing rate.

A typical example of these uptakes with a film at 0°C. is shown in Fig. 1, where the

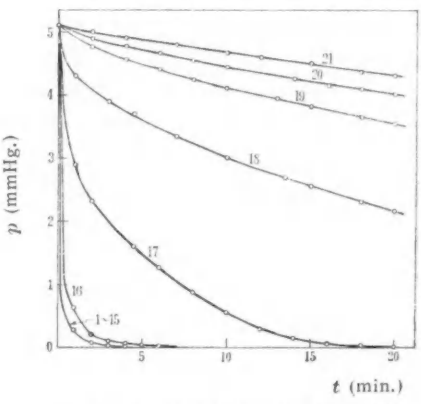

Fig. 1. Sorption of oxygen (T_s=0°C).

first fifteen increments are the rapid process, after which the rate of uptake falls with the number of increment.

1) O. Beeck, A. E. Smith and A. Wheeler, *Proc. Roy. Soc.*, (A) **177**, 61 (1941); O. Beeck, "Advances in Catalysis" II, Academic Press, New York (1950), p. 151.
2) J. A. Allen and J. W. Mitchel, *Disc. Farad. Soc.*, no. 8, 309 (1550).
3) E. K. Rideal and B. M. W. Trapnell, *Proc. Roy. Soc.*, (A) **205**, 409 (1951).
4) W. Scheuble, *Z. f. Phys.*, **135**, 125 (1953).
5) N. Cabrera and N. F. Mott, *Reports on Progress in Physics*. Vol. XII, 163 (1949).
6) K. Ono and Z. Oda, unpublished.
7) Z. Oda, *Oyōbutsuri* (*J. Appl. Phys., Japan*), **22**, 142 (1953).

TABLE I
RAPID SORPTION OF OXYGEN

Evap. time	Evap. amount[1]	Sorpt. temp.	No. of Ni atom	No. of sorbed O atom	Ni/O atomic ratio
min.	mg.	°C.			
30	7.1	0	7.34×10^{19}	4.44×10^{18}	16.5
30	6.7	0	6.91	4.58	15.1
45	8.4	0	8.67	5.34	16.2
15	2.7	0	2.79	2.36	11.8
30	5.3	−183	5.47	2.96	18.5
		0		4.66	11.7
30	6.3	0	6.51	4.56	14.4
30	6.2	−183	6.92	3.32	20.8
		0		5.08	13.6
30	5.3	0	5.47	2.70	20.3
30	4.2	0	4.34	2.20	19.7
30	8.1	0	8.36	4.72	17.7
30	11.2	−78	11.56	4.46	25.9
		0		5.32	21.7
30	11.0	−78	11.36	4.38	25.9
30	8.8	0	9.09	1.50	60.6[2]
30	5.6	−183	5.78	2.78	20.8
30	6.4	−183	6.61	3.70	17.8

1) The average thickness of film is 141Å/mg. using the bulk density of nickel.
2) run 22, which has been pre-sintered at 240°C. for 30 min.

I. Rapid Process

Sorption amount.—The amount of oxygen sorbed in this stage is given with that of nickel deposited in Table I, where allowance is made for the amount adsorbed by nickel filament. It is noticed that the amount sorbed at −78° and −183°C. were 85 and 60% as much as that at 0°C. respectively. Comparing the mean thickness of film and the corresponding atomic ratio of deposited nickel to sorbed oxygen (Ni/O), it is supposed that the oxygen would penetrate into the film as deep as 40 to 60 Å at this initial stage, if the film had a compact structure without any pores or cracks. However, this does not seem to be the case according to the data of Beeck.[1] The atomic ratio (Ni/O) at 0°C. sorption increases with the deposit, i.e., the oxygen sorbing capacity per unit weight of nickel decreases with increase of the deposit in these experimental regions. In run 22, in which the film was pre-sintered at 240°C. for 30 min. before gas admission, this ratio is about 60 and the sorbed amount is about 1/3 of that of the non-heat-treated films. Electron diffraction study[5] has suggested that the nickel film consists of fine crystallites which grow larger with film thickness and heat-treatment.

From these results, it is reasonable to explain the sorption process of oxygen on the basis of granular structure of film. If this is the case, oxygen will penetrate into the grain boundary at the rapid process and further diffuse in the crystallites with oxidation.

Low-temperature-adsorption of nitrogen.—As has been reported previously, the adsorption of nitrogen at −183°C. on the nickel film shows saturation at a pressure of 2×10^{-2} mmHg or higher. Comparing the number of nitrogen melecules sorbed at this saturation region with that of oxygen rapidly sorbed at −183°C. in Table II, the ratio

TABLE II
SORPTION AMOUNT OF O_2 AND N_2 AT −183°C.

Expt. No.	O_2 sorbed at rapid process moles/10 mg. Ni $\times10^{17}$	N_2 saturation adsorption moles/10 mg. Ni $\times10^{17}$
7	29.05	
9	27.98	
24	24.82	
15		5.20
23		4.06
mean	27.66	4.63

O_2/N_2 is found to be about 6. According to Beeck, one molecule of nitrogen can occupy two surface atoms of nickel. If this relation is applied to the present case, three oxygen molecules will correspond to one surface atom of nickel, so that it is reasonable to expect that even at the temperature of −183°C. oxygen can penetrate into the interior of crystallites to some extent.

Changes of electrical resistance.—It was also expected that the measurement of electrical resistance of film under sorption could furnish considerable insight into the behaviour of sorbed oxygen. After newly prepared film had been stabilized[8] to some extent, a known amount of gas was admitted and changes of gas pressure and film resistance were recorded

8) This stabilization process of evaporated nickel films was discussed in detail in ref. (7).

with time. Data obtained at 0° and −183°C. are shown in Figs. 2 and 3, respectively. It

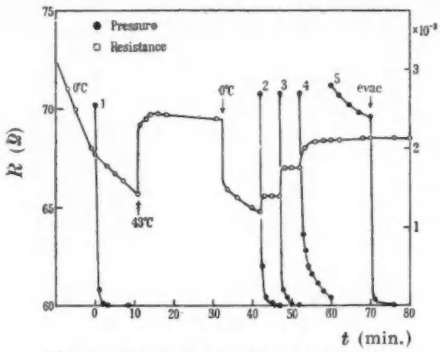

Fig. 2. Changes of electrical resistance with sorption (T_s=0°C)

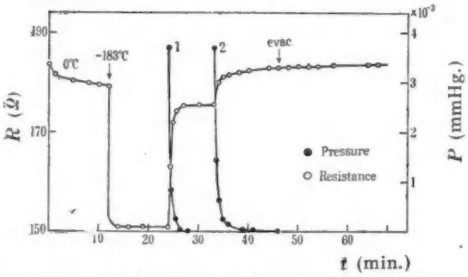

Fig. 3. Changes of electrical resistance with sorption (T_s=−183°C)

should be noticed that similar changes of resistance are observed with sorption at both temperatures.

On the other hand, adsorption of nitrogen and carbon monoxide which is considered to be chemisorbed on the surface gives rise to the increase of resistance within 1% and tend to restore its original value with desorption in the case of the former. Hence, the larger irreversible changes in resistance caused by oxygen uptake appear to account for the fact that oxidation proceeds even at −183°C. in the rapid process.

Estimation of thickness of oxide layer.—It is now possible to estimate the thickness of oxide layer formed in the rapid process at 0°C. from the data shown in Table I and electron diffraction patterns. The values calculated on suitable assumptions[9] are 5 Å and 4.5 A for thicker and thinner films, respectively. These values correspond to approximately 2 layers[10] of nickel atom. However, owing to the variety in size and mutual contact in actual films the effective surface of crystallite is supposed to be reduced and the oxide layer may correspondingly become thicker than ca. 10 Å.

II. Slow Process in Room-Temperature-Sorption

Pressure and temperature dependency of sorption rate.—Reducing the pressure stepwisely on the way of slow sorption, the rate of uptake also falls with pressure. Evaluating the rate of uptake $r_s\left(=-\frac{dp}{dt}\right)$ for each pressure range and plotting log r_s against log p, a straight line is obtained for each run. From the slope of these lines, the rate is well expressed as a function of pressure by the equation

$$-\frac{dp}{dt}=kp^{1/2}, \qquad (1)$$

where k is a constant. Integration of Eq. (1) gives

$$p^{1/2}=\text{const.}-kt/2, \qquad (2)$$

which represents a linear relation between $\sqrt{p}$ and t. In fact, as shown in Fig. 4, the

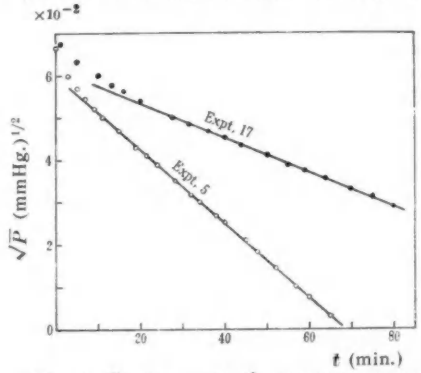

Fig. 4. Square root of pressure versus time (T_s=0°C)

data give a good agreement with Eq. (2) except for those in an early stage. Since the above rate versus pressure relationship inplies the sorption sites to be kept constant in course of one increment, it is naturally anticipated that deviations from linearity are observed at the early stage where the decrease

9) The following assumptions are made: (1) all crystallites composing a film are spheres of uniform size and their surfaces are entirely available for sorption. (2) Oxide layer has a composition of 1:1 atomic ratio and extends from surface to interior concentrically in each crystallite. From Table I O/Ni is given to be 1/20 for thicker films. Hence, atomic ratio of reacted metal to total one is given by

$$\frac{4.3\pi\left\{r_0^3-(r_0-r_1)^3\right\}}{4.3\pi r_0^3}=\frac{1}{20}$$

where r_0 and r_1 are the radius of original crystallite and the thickness of reacted layer, respectively. We set r_0=250 Å the magnitude roughly estimated from electron diffraction patterns. For thinner films, one may set O/Ni=1/12 and r_0=150 Å.

10) Estimated from distance between (110) planes (2.48 Å).

of sites is appreciable. Eq. (2) suggests that the dissociation of adsorbed molecules must take place faster than the migration of atoms, and so the dissociation is not a rate-determining step.

To obtain the activation energy E from the measured sorption rate itself, sorption rates were measured with a single film by changing the bulb temperature stepwisely without changing the other surface characters, and k was obtained from a stepwise $\sqrt{p}$ versus t plot. Temperature-dependency of the rate constant k in Eq. (2) is then given by

$$k = k_0 \exp(-E/RT),$$

Hence, by plotting log k against $1/T$ for each experiment, an activation energy of 12.6 ±1 kcal/mol. is obtained as a mean of three experiments.

Recovery of bare metallic surfaces.—The rapid sorption can be observed again by the film which has taken up sufficient gas to show no more rapid uptake, if it is kept in high vacuum at higher temperature than of sorption, but if the film is allowed to be evacuated at 0°C. one finds no such rapid sorption to recover. A few examples are shown in Fig. 5. The cause is considered to

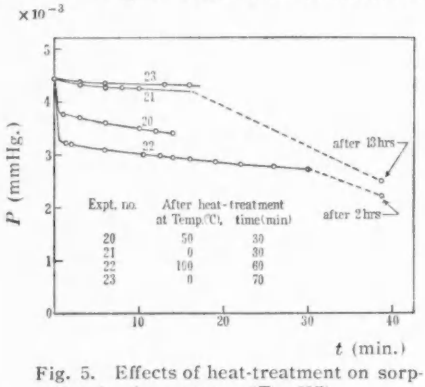

Fig. 5. Effects of heat-treatment on sorption in slow process (T_s=0°C)

be a recovery of bare metallic surfaces due to either the desorption of gas already sorbed or diffusion of metal ions through oxide layers or both. Since there is found no further liberation of gases in the closed system by raising the temperature, this recovery may be attributed to the latter mechanism.

From the above results, the most probable rate-determining step in this slow process is concluded to be the migration of metal ions to the oxygen atoms adsorbed on the oxide surface.

III. Slow Process in Low-Temperature-Sorption

Pressure dependency of sorption rate.—From the sorption rate versus pressure relationship obtained by the same method as described above, the rate of sorption at this temperature is expressed approximately by

$$-\frac{dp}{dt} = k'p, \qquad (3)$$

where k' is a constant. That is, the linear rate law can be applied to the present case.

Desorption and recovery of bare metallic surfaces.—When the temperature is raised to 0°C., rapid sorption occurs again after instantaneous desorption. However, this desorbed amount is far smaller for the case where the system is previously evacuated to 10^{-3} mmHg at −183°C. (1.55×10^{-3} mmHg−l.). than for the case without evacuation (5.55×10^{-3} mmHg−l.). As shown in Fig. 6, if the

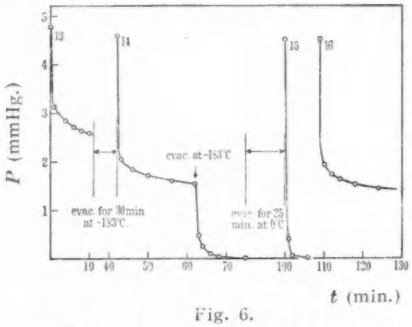

Fig. 6.
Effects of evacuation and temperature raising on sorption rate (T_s=−183°C)

sorption is stopped for half an hr. by evacuating the gas (Curve 13), the supplementary admission of gas (Curve 14) is attended with a more rapid uptake than that of curve 13 which has not been kept in high vacuum. In addition, when the bulb temperature is raised to 0°C. in high vacuum (point c) and allowed to stand for 25 min., subsequent admissions (Curves 15 and 16) at −183°C. are consumed at a rate as rapid as by the initial fresh film. These facts suggest that there occurs such a weak sorption at −183°C. that sorbed gas can be easily liberated even by low temperature evacuation. Therefore, the recovery of bare metallic surfaces observed in this figure is considered to be due to both the desorption and the enhancement of metal ion diffusion through oxide layers by raising the temperature.

Consequently, it is reasonable to consider that in the slow process of low-temperature-sorption, molecular adsorption takes place on the surface of oxide layers which have already

formed at the rapid process, and then these adsorbed molecules slowly dissociate to form oxide layers. The rate-determining step in this process may thus refer to either the adsorption of molecules or the dissociation of adsorbed molecules on the oxide surfaces.

IV. Considerations on the Basis of the Cabrera-Mott's Theory of Oxidation

As noticed above, oxygen can be taken up very rapidly with an almost constant rate in the initial stage of oxidation, but the rate falls abruptly after the oxide layer thickens to ca. 10 Å. Following the Cabrera-Mott's theory, the rate of formation of such a very thin oxide layer is given by

$$dx/dt = A \exp.(X_1/X - W/kT), \qquad (4)$$

where $X_1 = naV/kT$, a is the width of potential barrier between metal and oxide, V is the contact potential difference between metal and adsorbed layer, W is the energy required for a metal ion to migrate from a metal point to a vacant lattice point of oxide, A is a constant related only to the state of metal surface and the size of oxide, and k and T have the usual meanings.

If the oxide layer is very thin, i.e., $X \ll X_1$, the term X_1/X related to the strength of electrical field caused by shift of electron from metal to oxide is comparable to the term W/kT and so the apparent energy of activation becomes smaller. Therefore, in this stage the sorption which gives rise to the formation of vacant cation sites on the oxide surface is very much accelerated. While the rate of sorption is very rapid and appears to be almost independent of temperature, the amount rapidly sorbed is found to decrease as the temperature becomes lower. This is also explained by Eq. (4) as due to the fact that on account of predominance of W/kT to X_1/X with increasing X, the rapid process goes over into a slow one at smaller value of X with lowering the temperature.

In the slow process at room temperatures, the apparent energy of activation E is given by 12.6 kcal/mol. (0.57eV.), which must be represented from Eq. (4) by the following relation,

$$W - naV/X = E. \qquad (5)$$

Although the value of W for nickel has not been known, Cabrera and Mott have given 1.8 and 1.1 eV. for aluminum and copper, respectively. In the present case, also, the value of W is expected to be of the order of 1 eV. Hence, it is found that the field-dependent term naV/X has a large influence on the migration of metal ions even in the slow process.

Summary

While the sorptions of oxygen on the evaporated nickel films are very fast at the early stage and become slow at the later independently of the temperature, oxygen is suppoted to invade the interior even at the early stage of sorption. On the other hand, at the later stage the rate-determining step of low-temperature-sorption is different from that of room-temperature-sorption.

The author wishes to thank Mr. Y. Mizushima for helpful advice and discussion and also expresses his hearty thanks to Mr. T. Ichimiya for his interest and encouragement.

The Electrical Communication Laboratory,
Nippon Telegraph and Telephone
Public Corporation Tokyo

Dichroic Study on Polyvinylalcohol Fibre. IV. *A Theoretical Relation between the Intrinsic Double Refraction and the Dichroism*

By Yasuji KOBAYASHI and Saburo OKAJIMA

(Received July 13, 1954)

The relations between the stretching degree v relative to the isotropic state and the intrinsic double refraction Γ or the dichroism D of a cellulose fibre were already calculated by the authors.[1] Now in this paper the relation between Γ and the dichroic orientation is derived in a more general form.

A. Double Refraction. — The refractive index parallel to the fibre axis z of a refractive indicatrix, whose principal axis points to θ, φ is already calculated as (1), where θ and φ are the latitude and the azimuth.

1) S. Okajima, *J. Soc. Chem. Ind. Japan*, **43**, 351 (1940); S. Okajima and Y. Kobayashi, *J. Soc. Textile and Cellulose Ind. Japan*, **3**, 89 (1947).

$$n_z=\left(\frac{1}{n_\alpha^2}\sin^2\theta+\frac{1}{n_\Gamma^2}\cos^2\theta\right)^{-1/2}. \quad (1)$$

Now developing the right-hand side of (1) into a power series and neglecting the higher terms of $\Gamma_\infty=n_\Gamma-n_\alpha$, n_z is simplified as (2) or (2'),

$$n_z=n_\Gamma-(n_\Gamma-n_\alpha)\sin^2\theta, \quad (2)$$

$$=n_\Gamma\cos^2\theta+n_\alpha\sin^2\theta, \quad (2')$$

while the refractive index parallel to the x-axis of the above refractive indicatrix is given by (3) according to the previous calculation:

$$n_x=n_\alpha+(n_\Gamma-n_\alpha)\sin^2\theta\cos^2\varphi. \quad (3)$$

Now the refractive indices of the fibre $n_\parallel$ and $n_\perp$, parallel and perpendicular to the fibre axis are generally shown by (4) and (5) respectively:

$$n_\parallel=\int_0^{\pi/2}\int_0^{\pi/2}J_\theta n_z\sin\theta\,d\theta\,d\varphi\Big/\int_0^{\pi/2}\int_0^{\pi/2}J_\theta\sin\theta\,d\theta\,d\varphi, \quad (4)$$

$$n_\perp=\int_0^{\pi/2}\int_0^{\pi/2}J_\theta n_x\sin\theta\,d\theta\,d\varphi\Big/\int_0^{\pi/2}\int_0^{\pi/2}J_\theta\sin\theta\,d\theta\,d\varphi, \quad (5)$$

where J_θ is a distribution function of the mers.

Substituting the equations (2) and (3) into the equations (4) and (5) respectively,

$$n_\parallel=n_\Gamma-(n_\Gamma-n_\alpha)\cdot f(J_\theta), \quad (6)$$

$$n_\perp=n_\alpha+1/2\cdot(n_\Gamma-n_\alpha)\cdot f(J_\theta), \quad (7)$$

and $$\Gamma=n_\parallel-n_\perp=(n_\Gamma-n_\alpha)\cdot\{1-3/2\cdot f(J_\theta)\}, \quad (8)$$

where $f(J_\theta)=\int_0^{\pi/2}J_\theta\cdot\sin^3\theta d\theta$,

and $$\Gamma/\Gamma_\infty=f_o=1-3/2\cdot f(J_\theta), \quad (9)$$

as defined by P. H. Hermans[2].

From (6) and (7)

$$(n_\parallel+2n_\perp)/3=(n_\Gamma+2n_\alpha)/3=n_{iso}=\text{constant}. \quad (10)$$

The relation (10) was already proved experimentally by the authors[3] in the case of the cellulose fibre.

B. Dichroic Orientation f_D.—When the long axis of a particle of the dye-cellulose complex lies in the direction θ, φ, the coefficients of transparency of the particle, t_z and t_x, for the plane-polarized light vibrating parallel and perpendicular to z are

$$t_z=\beta-(\beta-\alpha)\cos^2\theta, \quad (11)$$

$$t_x=\beta-(\beta-\alpha)\sin^2\theta\cos^2\varphi, \quad (12)$$

where α and β are t_z and t_x at $\theta=0$, respectively, i.e., the principal coefficients of transparency.

The coefficients of light absorption, $K_\parallel$ and $K_\perp$, of a fibre for the plane-polarized light vibrating parallel and perpendicular to the fibre axis are also given by

$$K_\parallel=\frac{\int_0^{\pi/2}\int_0^{\pi/2}J_\theta\cdot k_z\cdot\sin\theta\,d\theta\,d\varphi}{\int_0^{\pi/2}\int_0^{\pi/2}J_\theta\cdot\sin\theta\,d\theta\,d\varphi}, \quad (13)$$

and

$$K_\perp=\frac{\int_0^{\pi/2}\int_0^{\pi/2}J_\theta\cdot k_x\cdot\sin\theta\,d\theta\,d\varphi}{\int_0^{\pi/2}\int_0^{\pi/2}J_\theta\cdot\sin\theta\,d\theta\,d\varphi}, \quad (14)$$

where

$$t_z=10^{-kz},\ t_x=10^{-kx},\ \alpha=10^{-k_\parallel},\ \beta=10^{-k_\perp}, \quad (15)$$

Now developing the right-hand sides of (15) and neglecting the higher terms of every k (k is very small), we obtain

$$\left.\begin{aligned}k_z&=k_\parallel\cos^2\theta+k_\perp\sin^2\theta\\ k_x&=k_\perp+(k_\parallel-k_\perp)\sin^2\theta\cos^2\varphi\end{aligned}\right\}. \quad (16)$$

Then k_z and k_x are of the same forms as these of n_z and n_x respectively and therefore substituting these relations into (13) and (14), $K_\parallel$ and $K_\perp$ can be given in the same forms as $n_\parallel$ and $n_\perp$ respectively, i.e.,

$$K_\parallel=k_\parallel-(k_\parallel-k_\perp)\cdot f(J_\theta), \quad (17)$$

$$K_\perp=k_\perp+1/2\cdot(k_\parallel-k_\perp)\cdot f(J_\theta), \quad (18)$$

and, therefore, the dichronic orientation f_D is

$$\begin{aligned}f_D&=(K_\parallel-K_\perp)/(K_\parallel+2K_\perp)\\ &=(k_\parallel-k_\perp)/(k_\parallel+2k_\perp)\cdot\{1-3/2\cdot f(J_\theta)\}\\ &=(k_\parallel-k_\perp)/(k_\parallel+2k_\perp)\cdot f_o\end{aligned} \quad (19)$$

and $$1/3\cdot(K_\parallel+2K_\perp)=1/3\cdot(k_\parallel+2k_\perp)=\text{constant}. \quad (20)$$

Therefore f_D is directly proportional to f_o. The same relation is already obtained by J. M. Preston,[4] where he assumed that $k_\perp$ is equal to 0 and the proportional constant $(k_\parallel-k_\perp)/(k_\parallel+2k_\perp)$ is equal to 1. Our observation on the ramie fibre, which is dyed with Kongo red, indicates that $k_\perp$ is not 0, although it is very small and difficult to be determined accurately and our old data give the constant 0.89. The latest data on the polyvinylalcohol fibre indicate that the possibility of still larger values of 0.95–1. The details will be described in the following paper.

2) P. H. Hermans "Contribution to the Physics of Cellulose Fibres", 1946.

3) S. Okajima and T. Iwamoto, *J. Soc. Chem. Ind. Japan*, **43**, 355 (1940).

4) J. M. Preston and P. C. Tsien, *J. Soc. Dyers and Col.*, **66**, 361 (1950).

As to the constancy of $k_{\parallel}+2k_{\perp}$, it holds good only when the fibre is dyed very lightly. The old data show some deviations from this relation as shown in Table I, but the latest ones prove this to be true as seen in Table II. In this case a sample of cellulose filament was dyed very lightly with Kongo red and $K_{\parallel}$ and $K_{\perp}$ were measured by using the filtered Hg-line. In order to prove the rule, $K_{\parallel}+2K_{\perp}$ are corrected by dividing by the diameter. The new samples were dyed very lightly but they are sufficient to obtain the exact values of $K_{\parallel}$ and $K_{\perp}$, when Hg-line is used, because this is absorbed so much by the dye as compared with the case where D-line is used.

TABLE I

THE ABSORBTION COEFFICIENT OF A POLYVINYL-ALCOHOL FIBRE DYED WITH KONGO RED

v	Diam., mm.	$K_{\parallel}$	$K_{\perp}$	$1/3\,(K_{\parallel}+2K_{\perp})$ / Diam.
1.00	0.1417	0.170	0.144	1.08
1.43	0.1185	0.174	0.108	1.10
1.69	0.1090	0.182	0.088	1.10
2.07	0.0985	0.196	0.060	1.07
3.08	0.0807	0.214	0.026	1.10
4.11	0.0700	0.224	0.020	1.26
4.99	0.0635	0.228	0.010	1.30

TABLE II

THE ABSORBTION COEFFICIENT OF A CELLULOSE FIBRE DYED VERY LIGHTLY WITH KONGO RED

v	Diam., mm	$K_{\parallel}$	$K_{\perp}$	$1/3\,(K_{\parallel}+2K_{\perp})$ / Diam.
1.00	0.1825	0.468	0.559	2.90
1.05	0.1816	0.485	0.551	2.91
1.14	0.1610	0.497	0.445	2.87
1.27	0.1495	0.525	0.394	2.93
1.38	0.1436	0.536	0.361	2.92
1.54	0.1333	0.559	0.300	2.90
1.66	0.1260	0.598	0.266	2.99
1.81	0.1230	0.567	0.215	2.70
1.90	0.1150	0.578	0.201	2.84
2.11	0.1130	0.578	0.183	2.78
2.21	0.1087	0.582	0.149	2.70
2.28	0.1056	0.594	0.132	2.71
2.40	0.1015	0.615	0.124	2.83
2.55	0.1020	0.611	0.124	2.81
2.56	0.1030	0.611	0.124	2.78
2.69	0.0981	0.671	0.108	3.01

Faculty of Engineering,
Tokyo Metropolitan University,
Tokyo

Some Optical Properties of Cellulose Hydrate

Saburo OKAJIMA, Yasuji KOBAYASHI and Tetsuya KIKUCHI

(Received July 13, 1954)

In the preceding paper[1] a linear relation between the intrinsic double refraction Γ and the dichroic orientation f_D of a fibre was derived as follows:

$$f_D=\frac{K_{\parallel}-K_{\perp}}{K_{\parallel}+2K_{\perp}}=\frac{k_{\parallel}-k_{\perp}}{k_{\parallel}+2k_{\perp}}\cdot\frac{\Gamma}{\Gamma_{\infty}} \qquad (1)$$

As is well known f_O, i.e. Γ/Γ_{∞}, indicates the orientation of the total molecules, while f_D mainly indicates that of the amorphous region. As to the orientations of the crystalline and amorphous regions, the former is higher than the latter according to the general views[2] at present. The above relation (1) was obtained on the tacit assumption of an equal orientation degrees in the crystalline and amorphous regions, but the linear relation is also expected even when the two regions have different orientation degrees, if f_O and f_D are always in proportion. This proportional constant being C, (1) becomes

$$f_D=((k_{\parallel}-k_{\perp})/(k_{\parallel}+2k_{\perp})\cdot C\cdot\Gamma/\Gamma_{\infty},\quad C\leqq 1.$$

In the range of the constancy of C, Γ/f_D is directly proportional to Γ_{∞}. As Γ_{∞} of a certain polymer changes with its crystallinity, Γ/f_D may possibly be a measure of the crystallinity of the polymer.

It is known that the crystallinity of a regenerated cellulose fibre is kept constant during the deformation. Accordingly a linear relation is expected between its f_D and Γ when C is also kept constant and it is actually confirmed experimentally as below. Then Γ_{∞} of the hydrate cellulose may be estimated from the experimental relation (1).

1) Y. Kobayashi and S. Okajima, This Bulletin, **27**, 471 (1954).

2) P. H. Hermans, "Contribution to the Physics of Cellulose Fibre, 1946; J. M. Preston and P. C. Tsien, *J. S. D. C.*, **66**, 361 (1950), etc.

A. Measurements of Γ and f_D of the Fixed Specimens

(1) Preparation of the Anisotropic Filaments.—A sample of the absorbent cotton on the market was purified by extracting with a boiling 1% NaOH solution and dissolved in a cuprammonium solution, from which cellulose was coagulated into an isotropic filament and regenerated as described previously.[3]

This isotropic filament of cellulose hydrate was stretched to various degrees, v, but in Exp. II the decoppering was carried out after being stretched to v which was calculated from the residual dry length relative to the isotropic dry state.

(2) Measurements of Γ and f_D.—The filaments were fixed to the frames as described previously[4] and Γ and f_D were measured with D-line.

An appropriate mixture of tricresylphosphate and dibutylphthalate was used as the mountant. The refractive index was 1.54, which is equal to n_{iso}[5] of the cellulose hydrate.

The dyeing was made with a 1% solution of Kongo red in 50% C_2H_5OH-H_2O and it was carefully controlled so that $K_{\parallel}$ did not go over 0.6 in any case.

Exp. I. A fresh and undried isotropic filament of cellulose was stretched and treated in succession as follows and used for the measurement of f_D.

(a) Dyed with Kongo red.
(b) Stretched to v in water at room temperature.
(c) Air-dried.
(d) Relaxed in water at room temperature.
(e) Air-dried again.

The filament was not allowed to shrink during the treatments (a)-(c) but it was free in (d) and (e). The specimen for Γ was prepared in the same way but a 50% C_2H_5OH-H_2O was used in (a) instead of the dye solution.

In Figs. 1 and 2 Γ and f_D are plotted against v and in Fig. 3 Γ against f_D. According to the

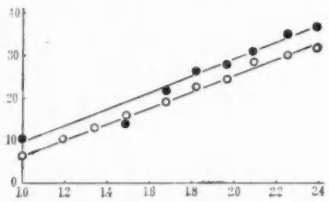

Fig. 1.
○ before Mercerization.
● after Mercerization.

figures Γ and f_D increase almost linearly with v and Γ-f_D is also linear as the theoretical relation (1) requires.

The specimens used for the above measurements

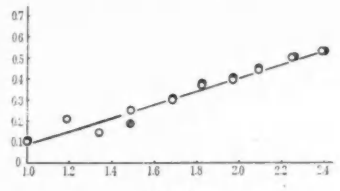

Fig. 2.
○ before Mercerization.
● after Mercerization.

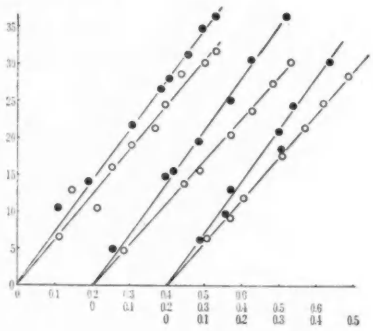

Fig. 3.
○ before Mercerization.
● after Mercerization.

were then washed free from the mountant, mercerized with an 18% NaOH solution at room temperature, regenerated by pouring into a boiling 0.5% acetic acid solution, washed thoroughly and again observed. Of course in these treatments the longitudinal shrinkage was prohibited, otherwise they would shrink and disorientate. As shown in Figs. 1-3, Γ increases after the mercerization, but f_D remains almost unchanged. Both measures are also in a linear relation but the slope grows steeper.

Exp. II. In this experiment an isotropic filament, which was not yet decoppered was stretched in a 5% NaOH solution and then regenerated, washed, and treated as in (c)-(e) of the preceding experiment. The specimens for f_D were dyed after fixing to the frame, while those for Γ were treated, of course, with a 50% C_2H_5OH aq. solution.

In order to observe the effect of the mercerization, separate specimens were mercerized in this case as they were fixed to the frames and then dyed or treated with the 50% C_2H_5OH-H_2O solution. In other words, the mercerization was given to the undyed specimens. Fig. 3 indicates that the result is similar to the above: the linear relation of Γ-f_D holds good and the slope increases after the mercerization also in this case.

Exp. III. The isotropic filament used in the above experiment was decoppered and then stretched as in Exp. I. But the undyed specimens were mercerized as in Exp. II. A similar result is obtained as shown in Fig. 3.

3) S. Okajima and S. Hayama, This Bulletin, **27**, 61 (1951).
4) S. Okajima and Y. Kobayashi, This Bulletin, **25**, 268 (1952); S. Okajima, Y. Kobayashi and R. Yamada, ibid., **26**, 235 (1953).
5) S. Okajima, *J. Soc. Chem. Ind. Japan*, **49**, 128 (1946); P. H. Hermans, "Contribution to the Physics of Cellulose Fibre", 1946.

B. Measurements of Γ and f_D of the Relaxed Specimens

In the foregoing measurements each specimen was treated in the fixed state to a frame. Now the measurements of Γ and f_D were carried out in the relaxed state. The specimens were cut into the pieces of 3-4 mm lengths after the treatments (a)-(e) mentioned below, and they were inserted into a thin-walled glass capillary in a line and dried at 60°C under the high vacuum (<0.001 mm Hg) as shown in Fig. 4, when one

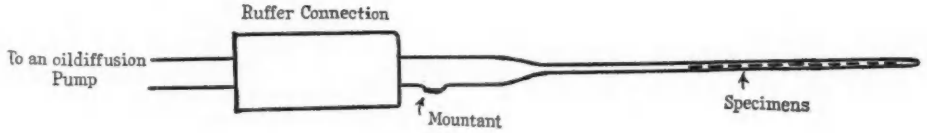

Fig. 4.

drop of the mountant was also placed in the capillary near the open end. After the specimens were dried completely they were mounted. For this purpose the capillary was bent slightly down at the rubber connection, then the mountant streamed down along the inner wall of the capillary and dipped the specimens. The capillary was closed by melting near the open end. $K_{\parallel}$, $K_{\perp}$ and Γ of the specimens in the closed capillary were measured as usual but from the outside of the capillary. Therefore the last drying and the measurements were carried out in the relaxed state in this case as compared with the treatments in A.

The stretching of the isotropic cellulose filament which was prepared as in A was carried out successively in the following order.

(a) Stretched in water at room temperature.
(b) Boiled in water.
(c) In Exp. IV, air-dried at room temperature. In Exps. V and VI, oven-dried at 100°C.
(d) Relaxed in boiling water.
(e) Air-dried again under no tension.

In these treatments (b) and (c) were carried out under tension, while (d) and (e) were carried out in the free state as described in each experiment.

Hg-line filtered through a Mazda's filtere VG1A was used for the following measurement of f_D. Of course the green light is absorbed so much by Kongo red, that the specimens must be dyed very lightly, otherwise $K_{\parallel}$ goes over 0.6. Then the specimens are, on the contrary, so transparent for Na-line, that the same dyed specimens can be used for the measurement of Γ. In Fig. 5 the points ● and ○ are the observed values of the dyed and undyed specimens respectively which show clearly that the effect of the dyeing is negligible. So the same specimens were used for the measurements of Γ and f_D in Exps. V and VI. Of course for this purpose the specimens must be dyed under the conditions which do not cause any disorientation due to swelling and contraction and the condition was accomplished by using the 50% C_2H_5OH aq. solution as the dyeing medium at room temperature.

A small discontinuity can be seen in the early stage of the deformation in Fig. 5, which was already pointed out previously.[6]

6) S. Okajima and Y. Kobayashi, This Bulletin **24**, 85 (1951).

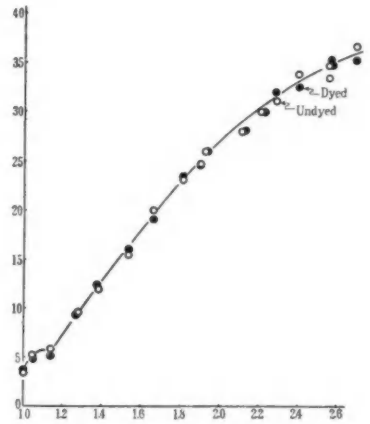

Fig. 5.

Exp. IV. Each specimen was cut into two parts, one of which was dyed with Kongo red as before to measure f_D, while the other half was used for the measurement of Γ after being treated with the alcohol solution. The relation between Γ and f_D is shown in Fig. 6.

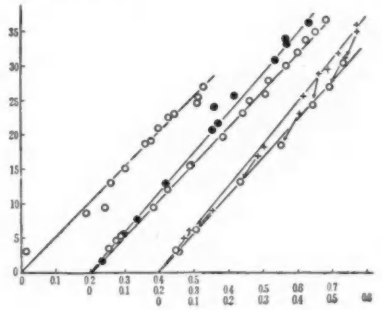

Fig. 6.
○ before Mercerization.
● after Mercerization.

Exp. V. Γ of the unmercerized and mercerized specimens were measured at first and after being dyed, again Γ and f_D were measured. The results

are similar to the above. The mercerization was carried out under tension to avoid the shrinking of the anisotropic filament.

Exp. VI. A part of the specimens were dyed, air-dried, fixed to the frame, vacuum-dried and $K_{\parallel}$, $K_{\perp}$ and Γ were measured as mentioned in A, except that the same dyed specimens were used for both measurements (VIa). These specimens were cut into pieces after 10 days' vacuum-drying and relaxing in boiling water and again observed in the free state (VIb). As shown in Fig. 6, the slope of the line Γ-f_D becomes less steep by this relaxation, although the linear relation holds goods also in this case.

C. Discussion

All the experimental results prove that a linear relation holds good between Γ and f_D as the theory requires. But the slope θ of the line is not necessarily constant and changes from case to case as shown in the acompanying table. In order to analyze the causes of this fluctuation, the following effects are considered:

(1) The mercerization increases the slop in all cases.

(2) Among Exps. I, II, III and VIa, where the specimens were observed in the fixed state, θ in Exp. II is $56\text{-}57\times10^{-3}$ and slightly smaller than the others. This is because the filament was decoppered under the stretched state. It is interesting to note that this θ increases also to the equal level of 70×10^{-3} after mercerization.

Exp. No.	State of the specimen	$\theta\cdot10^3$ Before merc.	After merc.
I	Fixed to the frame	60—62	69—70.5
II	" "	55.5—57	70—71.5
III	" "	58—59.5	70.5
IV	Relaxed	50	—
V	"	52	58
VIa	Fixed to the frame	60—61	—
VIb	Relaxed	55	—

(3) θ in Exps. I, III and VIa are also larger than those in Exps. IV, V and VIb. This seems to be related to the fact that the specimens in the former experiments are dried and observed in the fixed states, while in the latter cases they are in the relaxed states.

Now we consider the meaning of this θ. If the orientation degrees in the crystalline and amorphous regions of a fibre are not different from each other as assumed in the calculation of (1), the linear relation between Γ and f_D means at once the correctness of the formula (1). Then the inclination is equal to

$$\Gamma_\infty \div \frac{k_{\parallel}-k_{\perp}}{k_{\parallel}+2k_{\perp}}$$

and the fluctuation of this value is nothing but the variation of Γ_∞. Γ_∞ increases generally with the crystallinity, so the value of Γ_∞ indicates quantitatively the relative amount of the crystalline region. So the constancy of Γ_∞ through a series of the varying v is a new support for the specimens of view[7] that the crystallinity is kept constant during the stretching of the cellulose fibre.

As to the absolute value of Γ_∞, the authors[8] obtained 62.4×10^{-3}, while P. H. Hermans[5] 55×10^{-3}, J. M. Preston[9] 54×10^{-3} and A. Frey-Wyssling[10] 49×10^{-3}. These estimations contain some assumptions and the above θ appears to be very valuable for criticising these values of Γ_∞, but the problem is not so simple. The inclination θ is

$$\Gamma_\infty \div \frac{C\cdot(k_{\parallel}-k_{\perp})}{k_{\parallel}+2k_{\perp}}$$

and knowledge of C or $(k_{\parallel}-k_{\perp})/(k_{\parallel}+2k_{\perp})$ is necessary for this purpose, but it is yet poor. The term $(k_{\parallel}-k_{\perp})/(k_{\parallel}+2k_{\perp})$ is 1 and 0.89 according to Preston's view[11] and the authors' old data respectively, but our latest data show the possibility of a still greater value 0.96. This value was found repeatedly when a polyvinylalcohol fibre of the highest orientation which had been heat-treated after the highest stretching was observed. Considering that the real filament must fall short of the ideally parallel orientation and further that the ordinary polyvinylalcohol sample on the market contains some irregularities in the structure, then $(k_{\parallel}-k_{\perp})/(k_{\parallel}+2k_{\perp})$ of the ideal filament must be still greater than 0.96. But if Kongo red molecule has the structure

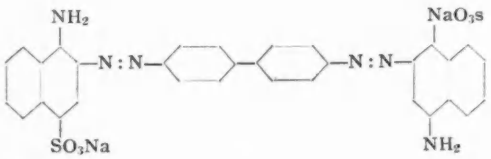

7) e. g. H. R. Kruyt, "Colloid Science" II, p. 55, 613 (1949).
8) K. Atsuki and S. Okajima, *J. Soc. Chem. Ind. Japan*, **40**, 360B (1937).
9) J. M. Preston, *Trans. Faraday Soc.*, **29**, 65 (1933).
10) A. Frey-Wyssling, *Helv. Chim. Acta*, **22**, 981 (1939).
11) J. M. Preston and P. C. Tsien, *J. S. D. C.*, **66**, 361 (1950).

and this molecule orientates parallel to a cellulose molecule by means of two NH_2-groups, then $(k_{\parallel}-k_{\perp})/(k_{\parallel}+2k_{\perp})$ may be smaller than 1 because the line connecting the two NH_2-groups is not parallel to the direction of the diazo groups. After all the value can be considered to exist between 1 and 0.96 and it is approximated to 1 in the following discussion.

Now Γ_∞ are 60×10^{-3} and $50\text{–}55\times10^{-3}$ according to the states of the specimens and nearly coincide with the hitherto obtained data by the present authors and the others mentioned above, then C can be considered to be nearly equal to 1 and θ is directly equal to Γ_∞. If C is much smaller than 1, Γ_∞ must also be smaller. This means that the orientation degree of the amorphous region is not especially lower than that of the crystalline region, provided, of course, the dichroism can indicate the orientation of the amorphous region only. But another concept is also possible. Because a simple estimation of $(K_{\parallel}+2K_{\perp})$ from the present degree of dyeing shows that about one molecule of Kongo red is absorbed to 10,000 glucose residues and such small quantities of the dye molecules are not necessarily considered to be absorbed only in the amorphous region but also on the surfaces of the crystallites where the orientations are more or less higher; in other words, the dye molecules seem to be distributed uniformly in the filament. Then C can be equal to 1.

The selective indication of the orientation in the amorphous region may occur only when the more intense dyeing was made and the absorbtion becomes decisively predominant in the amorphous region.

A similar linear relation between Γ and f_D can be seen also in the case of a polyvinylalcohol filament till $f_D=0.89$ or 0.96 as will be described in a separate report. In the case of the cellulose filament the line Γ-f_D is interrupted at $f_D=0.6$ by the breakdown of the sample. Of course it can not be decided at present which of the views is true, but it can be said that f_D is equivalent to f_0.

From these points of view the change of θ can be explained directly by the concept of the change in Γ_∞ and, therefore, the change in crystallinity as below:

(1) The mercerization followed by the hot-regeneration must be considered to increase the relative amount of the crystalline region. This confirms the result of Hermans,[12] who found it by means of the X-ray method. According to him the crystallinity increases by about 10% after the mercerization and our Γ_∞ increases also by the same amount.

(2) The crystallinity of the filament decoppered under tension is slightly lower than that regenerated in the free state. The cause may be that a too excessive strain appears in the filament due to the deswelling at the decoppering process. This strain is released when it is mercerized and the crystallinity increases to the normal level. Therefore the value of Γ_∞ is equal to 70×10^{-3}, irrespective of the slightly lower value of the original Γ_∞ in Exp. II.

(3) As is often mentioned, the relaxed specimens give the smaller value of Γ_∞. The effect of the relaxation may appear principally in the last drying operation. The filament highly dried under tension may cause the crystallization of the metastable portion, among which the smaller or more unstable crystals are destroyed again when the filament is treated in boiling water in the free state. And this recrystallization appears to become more stable if the filament has been dried at a higher temperature and for a longer period because Γ_∞ increases in the order IV to VIb (excepting VIa). They were relaxed similarly in boiling water after air-drying (IV), oven-drying for 1 hr. (V) and oven-drying followed by vacuum-drying for 10 days (VIb) and the larger portion of the crystals appears to survive after the relaxation in the above order.

Therefore the fluctuations observed in the hitherto obtained values of Γ_∞ by the different authors may be related to the small fluctuation of the crystallinity due to the slight difference in the conditions under which the specimens were treated.

(4) The mercerization was carried out before and after the dyeing in Exps. III and I respectively but Γ_∞ increases by the equal amount and arrived at the equal level after the treatment in both cases. Therefore such a crystallization is thought not to be disturbed by the dye molecules. This is very interesting when it is considered that the crystallization of a polyvinylalcohol filament due to heating is fairly disturbed by the dye molecules absorbed as will be reported in a separate paper.

Faculty of Engineering,
Tokyo Metropolitan
University, Tokyo

12) P. H. Hermans and A. Weidinger, *J. Polymer Sci.*, **6**, 533 (1951).

LETTER

Internal Vibrational Structure Found in the Low Temperature Fluorescence of Silver Nitrite Crystals

By Shoji MAKISHIMA and Takeshi TOMOTSU

(Received April 30, 1954)

As briefly reported in the previous letter[1] pure silver nitrite crystals show the strongest fluorescence among the common silver salts. Moreover they are distinguished from other salts by the fact that they have a structure in the fluorescence spectra at the liquid oxygen temperature. The structure is somewhat diffuse, the stripes appearing on a broad emission band as a repetition of the nearly equi-distant darkness (Fig. 1). The structure

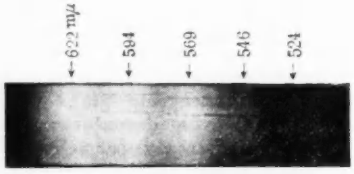

Fig. 1. Stripes of emission spectrum of solid $AgNO_2$.

vanishes at several ten degrees above the liquid oxygen temperature, although the fluorescence remains sufficiently strong. The structure is more distinct when the crystal is precipitated in the excess of nitrite ions. This suggests that the luminescence and its structure originate from some lattice defects. Upon examining the photometer curve it proved that the mean separation of the peaks in the structure is approximately 750 cm^{-1}. A comparison with the known Raman or infrared spectral data[2] concerning nitrites or nitrates makes us draw the conclusion that the structure is ascribed to the deformation vibration of NO_2 group. It seems very rare for an internal vibration with definite meaning to appear in the ordinary solid luminescence like this, because a silver nitrite crystal has no shielded electronic states which are characteristic of rare earths, uranyl salts or compounds containing π-electrons.

Almost the same luminescence characteristics are observed with $AgNO_3$ crystals containing a trace of NO_2^- or with $NaNO_2$ crystals containing a similar amount of Ag^+. A conclusion is reached, therefore, that the origin of the luminescence lies not in the whole lattice of $AgNO_2$, but in the localized bond between Ag and NO_2 group having a nature of an isolated molecule.

Silver nitrite possesses a considerable amount of the character of nitro-compound. This is easily predicted from the well-known fact, that the nitro-paraffins are formed together with the nitrite ester, when alkyl halides react with $AgNO_2$. In the state of a nitro-compound, silver is connected with the nitro-group by a perfectly covalent bond. So, the covalent nature is much more remarkable in the bond of $AgNO_2$ than in other silver salts. When the covalent part increases in the binding, a pair of anion and cation facing to the lattice defects bears the character of an isolated molecule. The interaction with the lattice vibrations is thus diminished, and it becomes possible to expect the appearance of the internal vibrational structure as well as the nonvanishing of the luminescence at higher temperatures. In fact, as shown below, silver nitrite has a higher vanishing temperature of fluorescence than any other salts tested. This agrees quite well with the non-appearance of the internal vibrations in the latter cases.

Salts	$AgNO_2$	AgCN	Ag_2SO_3	AgCl
Approx. vanishing Temp. °C	+90	−50	−90	−120

More detailed discussions may become possible, when the data concerning the temperatures of liquid hydrogen or helium are available, which, however are impossible in our laboratories.

The Institute of Science and Technology, University of Tokyo, Tokyo

1) S. Makishima and T. Tomotsu, This Bulletin, **27**, 71 (1954).

2) A. Langseth and E. Walls, *Z. phys. Chem.* B **27**, 209 (1934), D. Williams, *J. Am. Chem. Soc.* **61**, 2987 (1939), E. A. Miller and C. H. Wilkins, *Anal. Chem.* **24**, 1253 (1952).

Polymerization by Electric Discharge

By Kiyoteru OTOZAI, Sanshiro KUME, Shobun NAGAI, Tai YAMAMOTO, and Shouzow FUKUSHIMA

(Received June 8, 1954)

In the course of the study on the paper chromatography of poly ethylene oxide[1], we

found that the surface of the liquid polymer was covered by a membrane with the action of the electric discharge by "Tesla coil", the vacuum tester, when polymer was treated in vacuum. In order to ascertain the accelerating effect of the discharge on polymerization, anticipated from this phenomenon, we preliminarily examined the action of the discharge on some polymers and monomers of different type.

(1) **Polyethylene Oxide.** "Carbowax 4,000" was put in a glass ampule, evacuated continually, melted at 60°C., and exposed to the discharge for 10 minutes. With the action of the discharge the surface of the sample was covered with a colorless membrane, which was insoluble and remained fibrous in hot water. The reacted part amounted to about 1%. A colorless, insoluble and fibrous form of the substance indicates presumably that the polymer molecules were awakened to further polymerization in linear structure by the action of the discharge. For a comparison other samples were kept for 10 minutes at 60°C. and 200°C. in a vacuum, but no change was observed and the samples were dissolved completely in hot water.

(2) **Styrene.** Styrene, distilled in a nitrogen stream, was distilled into a glass ampule in vacuum, sealed, placed in water of 11°C., and exposed to the discharge for 30 minutes. As soon as the discharge began a white cloud was produced in the whole space of the gas phase and settled down slowly. The liquid phase became light yellow. The average molecular weight of 15,000 was obtained from the viscosity measurement of a benzene solution of purified colorless polymer, the value of K_m being taken as 1.1. The amount of reaction was about 1%. The light yellow substance, which was produced under the action of the discharge at dry ice temperature for 1 hour, can not be dissolved in benzene.

(3) **Glycine.** The discharge was showered on the crystalline glycine at 13°C., and on the sublimated stream of glycine at 160°C., and on the cold 10% aqueous solution of glycine at 0°C., inan evacuated ampule in all cases Only in the last case a dust-like colorless substance appeared. In all cases, however, the small amounts of the insoluble colorless substances were obtained, when the samples were dissolved in water. Glycine was detected by paper chromatography of the insoluble product in the first case, after a washing by hot water and hydrolysis by hydrochloric acid. This would suggest that the product was some sort of polymer of glycine.[1]

These effects would be caused by radicals, or ions, or radicalions, produced by the discharge.

We should like to express our sincere thanks to Dr. H. Okuyama, Dr. G. Meshizuka, and Dr. K. Narita for their* guidance about carbowax, styrene, and glycine, respectively.

Department of Chemistry, Faculty of Science, Osaka University, Osaka

1) S. Kume, T. Yamamoto, K. Otozai, and S. Fukushima, This Bulletin **26**, 93 (1953).

A New Route to DL-*threo*-1-*p*-Nitrophenyl-2-amino-1,3-propanediol

By Sumio Umezawa and Tetsuo Suami

(Received June 25, 1954)

During the course of synthetic investigations of E. Erlenmeyer's *threo* phenylserine[1], we have reduced the latter with a modified Raney nickel catalyst, and obtained a new oxazolidine derivative which appears to be 2-phenyl-4-(α-hydroxybenzyl) oxazolidine (I). Starting from this oxazolidine derivative, we have

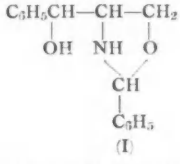

(I)

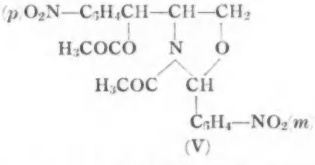

(V)

now synthesized DL-chlorampphenicol, an important antibiotic found by scientists of Parke, Davis and Company.

The *threo*-phenylserine ethyl ester was reduced in ethanol at about 50°C. with a modified Raney-nickel which was prepared by the ordinary digestion-procedure at 30°C. for one hour. After working up by evaporation and recrystallization, the above described oxazolidine (41%), m.p. 138–139°C. was obtained. *Anal.* Calcd. for $C_{18}H_{17}O_2N$: C, 75.4; H, 6.67; N, 5.50. Found: C, 75.1; H, 6.58; N, 5.53%. Acetylation of the oxazolidine derivative (I) with acetic anhydride at room temperature

1) E. Erlenmeyer, *Ber.*, **25**, 3445 (1892).

yielded an N-acetyl derivative (II) (82%), m.p. 145–146°C. *Anal.* Calcd. for $C_{18}H_{19}O_3N$: N, 4.72. Found: N, 4.64%. The failure of II to hydrolyze under Kunz's conditions[2] demonstrated that II is an N-acetyl derivative. Further acetylation of II with acetic anhydride in pyridine gave a viscous product (III), which on nitration with mixed acid (conc. H_2SO_4: conc. HNO_3=1:1) under ice-cooling for 30 minutes, finally at 15°C. for one hour, led to a viscous product (IV) containing a small quantity of crystals. The latter, after recrystallization, appeared to be 2-(*m*-nitrophenyl)-4-(*α*-hydroxy-*p*-nitrobenzyl)-oxazolidine (V) (12%), m.p. 192–193°C. *Anal.* Calcd. $C_{20}H_{19}O_8N_3$: N, 9.78. Found: N, 9.44%. V gave *m*-nitrobenzaldehyde on hydrolysis with dilute hydrochloric acid. The main part of IV usually remained viscous and oily. Hydrolysis with dilute hydrochloric acid, followed by neutralization with dilute sodium hydroxide, led to DL-*threo*-1-*p*-nitrophenyl-2-amino-1,3-propanediol, pale yellow crystals (49%), m.p. 143.5–145°C., which did not depress the melting point of an authentic sample obtoined by the synthetic route through *p*-nitroacetophenone[3] and, acylation with methyl dichloroacetate converted the product to DL-chloramphenicol.

It was also shown that the oxazolidine derivative (I) could be directly hydrolysed with dilute hydrochloric acid to DL-*threo*-1-phenyl-2-amino-1,3-propanediol (84%), m.p. 85–86°C., which led to the DL-chloramphenicol by the synthetic route described by Controulis and his coworkers.[4]

Applied Chemistry Department, Faculty of Engineering, Keio University
Koganei, Tokyo, Japan

2) A. Kunz and C. S. Hudson, *J. Am. Chem. Soc.*, **48**, 1982 (1926); M. L. Wolfrom, M. Königsberg, and S. Soltzberg, ibid., **58**, 409 (1936).
3) L. M. Long and H. D. Troutman, ibid., **71**, 2473 (1949).
4) J. Controulis, M. C. Rebstock and H. M. Crooks, ibid., **71**, 2163 (1949).

A New Method for Ultra Micro Determination of Ammonia or Organic Nitrogen

By Yoshimi OKADA and Hidesaburo HANAFUSA

(Received July 7, 1954)

The micro-Kjeldahl method is useful for rapid nitrogen analysis of various organic substances of low nitrogen content. However, it would be convenient to determine much smaller amounts of nitrogen in cases where the nitrogen content of the sample is very low or the amount of sample available is limited. For this purpose we replaced titration in this method by colorimetry with ninhydrin[1] and could determine 30 μg. of nitrogen by this modification.

This modified method is the same as the usual micro-Kjeldahl method except that the sample for single determination should contain 20–100 μg. nitrogen and the time of distillation is shortened to 1.5 minutes and 5 cc. of 1/100 N-H_2SO_4 is placed in an adapting flask. After distillation, the solution in the flask (usually 15–20 cc.) is diluted to 25 cc. with a citrate buffer (*p*H 5.0) and 1 cc. aliquot is taken to determine ammonia colorimetrically[1]. A standard curve was prepared previously with the solution of NH_4Cl (1–10 μg./cc.).

This method is particularly useful for the determination of amide-N of proteins, as the trouble of titration caused by octylalcohol, an anti-foaming reagent, can be eliminated completely. Some results by this method are shown in Table I.

TABLE I
EXAMPLES OF NITROGEN DETERMINATION BY AUTHORS' METHOD

Total-N

Sample	Found %	Calculated %
Acetanilide (354 μg.)	10.39	10.37
,, (425 μg.)	10.43	

Amide-NH_3

Sample	Found %	Reported %
Lysozyme (2.03 mg.)	1.88	1.7–2.0[2]
		1.87[3]
		2.08[4]
Taka-amylase A (2.87 mg.)	1.43	1.47[5]

By further modification of our method, by combining the diffusion method according to Conway[6,7], it would be possible to determine extremely small amounts of nitrogen. Experiments on this possibility are now in progress.

The authors wish to express their thanks to Prof. S. Akabori for his kind advice.

Laboratory of Biochemistry, Faculty of Science, Osaka University

1) S. Moore, W. H. Stein, *J. Biol. Chem.*, **176**, 367 (1948).
2) R. Monier, Y. Gendron, M. Julisz, C. Fromageot, *Biochim. Biophys. Acta*, **8**, 588 (1952).
3) C. Fromageot, M. Privat de Garilhe, ibid., **4**, 509 (1950).
4) J. C. Lewis, N. S. Snell, D.J. Hirshmann, H. Fraenkel-Conrat, *J. Biol. Chem.*, **186**, 23 (1950).
5) S. Akabori, et al., To be published.
6) E. J. Conway, et al., *Biochem. J.*, **36**, 655 (1942).
7) M. Rovery, C. Fabre, P. Desnuelle, *Biochim. Biophys. Acta*, **12**, 547 (1953).

The Structure of the So-called α-Δ⁵-Cholestenone Oxide

By Susumu MORI and Fumikazu MUKAWA

(Received July 23, 1954)

The structure of the so-called α-Δ⁵-cholestenone oxide has not yet been precisely proved.[1,2] The study of it has shown that the compound is not an epoxide but a lactone. The reduction of the compound with lithium aluminium hydride in ether gave a diol (m.p. 129°C. Found: C, 80.09; H, 11.94, calcd. for $C_{27}H_{48}O_2$: C, 80.13; H, 11.96%), which was obtained pure in a good yield.

The diol showed a strong absorption peak in 3.0μ (Nujiol mull), indicating the presence of a hydrogen-bonded hydroxyl group, but no longer a peak in the 5.8μ region characteristic of carbonyl function. Oxidation of the diol with chromium trioxide-pyridine complex gave the known 3, 4-seco-Δ⁵-cholestene-3, 4-dioic acid (Diels' acid). Then it was converted into the dimethyl ester, which showed no depression of the melting point on admixture with an authentic specimen.

From a consideration of the results it seems most reasonable to conclude that the so-called α-Δ⁵-cholestenone oxide is an unsaturated lactone as illustrated by formula (I).

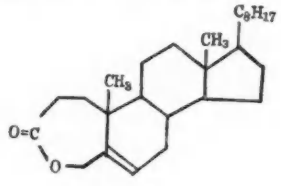

(I)

Department of Chemistry, Faculty of Science, Tokyo Metropolitan University, Setagaya, Tokyo

1) L. Ruzicka and W. Bosshard, *Helv. Chim. Acta*, **20**, 244 (1937).
2) Y. Urushibara and M. Chuman, This Bulletin, **22**, 273 (1949).

Action of p-Toluenesulfonyl Chloride as the Cold-setting Accelerator for Thermosetting Resins

By Shigehiko YAMADA

(Received March 16, 1954)

As the cold-setting accelerator for thermosetting resins, *p*-toluenesulfonyl chloride (PTSC) is widely used, but differing from free acids it does not readily develop its action. The fact is evident when we observe the viscosity and temperature changes with the setting time of cold setting resin solutions containing PTSC.

For this purpose the measurement of the electric resistivity change serves to a certain extent.

The platinum electrodes of 1 mm diameter were set in the resin solution at intervals of 10 mm and in the depth of 3 mm. The D.C. voltage of 3V was applied between these electrodes and the current was measured with setting time from which the resistivity was calculated.

PTSC used was colorless crystal with the exact m.p. of 69°C. Furfuryl alcohol used as the resin monomer, was distilled at 81°C under 20 mm Hg prior to use.

The results were summarized and indicated in Fig. 1.

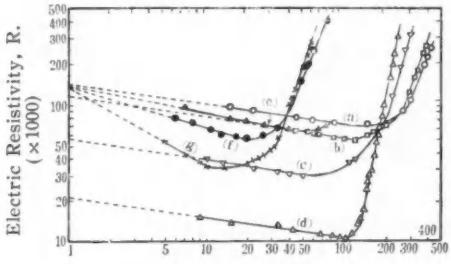

Setting time, t. (min.)

Fig. 1. The curves of electric resistivity versus setting time of the furfuryl alcohol containing PTSC.
Furfuryl alcohol 7.00 g, PTSC (a) 0.207 g, (b) 0.300 g, (c) 0.600 g, (d) 1.003 g, temp. 31.7±03°C.
Furfuryl alcohol 7.00 g, PTSC 0.207 g, (e) 37.3±0.3°C (f) 47.7±0.3°C (g) 57.7±0.3°C.

It can be seen in this figure that each curve consists of three parts. Of these, the initial part of resistivity decrease satisfying the approximate formula $R=kt^{-s}$, indicates the decomposition of the sulfonyl chloride, and the final increase following the relation $R=K'\cdot t^{z'}$, can be explained only by the resinification. The intermediate part is supposed to be transitional.

As for the initial stage, a similar change was also observed in the case of the measurement on the furfuryl alcohol in dioxane and the resole in dioxane using 500 V megger.

The constants of the above two formulas, K, Z, and Z' were calculated from Fig. 1, which were found to satisfy the following approximate formulas.

$$K=Ae^{-\alpha c}, \qquad Z=Be^{\beta\theta}, \qquad Z'=Sc^{b}$$

(A, B, S, α, β and b are constants, c the

catalyst concentration, and θ the setting temperature).

Further, the point of intersection made by the extension of initial and final linear portions can be regarded as the point of complete decomposition of PTSC. The time T corresponding to this point was approximately expressed by

$$T = pc^{-q}$$ (p, q are constants).

In addition, it was observed that the time T required for the complete decomposition, was remarkably affected by the setting temperature. (Change of temperature from 32°C to 58°C reduces T to ca. 1/10, while 5 times increase of concentration of the accelerator only reduces T to ca. 1/2 of the value at 32°C).

Thus it is suggested that to develop the accelerator action of PTSC, the temperature rise is more effective than the accelerator increase.

Technical Research Laboratory, Tokai Electrode Mfg. Co., Fujisawa

Procedure for the Preparation of the New Nickel Catalyst

By Yoshiyuki URUSHIBARA and Shigeo NISHIMURA

(Received August 19, 1954)

In a preliminary note[1] one of the authors (Y.U.) reported that metallic nickel and copper precipitated from the aqueous solutions of their soluble salts by means of zinc dust are active catalysts for hydrogenation in the presence of caustic alkali or when digested with aqueous caustic alkali before use. Since then, the activity of the new nickel catalyst has been much improved. The following is the procedure for obtaining the greatest activity that has been so far attained.

Ten grams of zinc dust, as fine as possible, and about 3 cc. of distilled water are put in a round flask of 100 cc. capacity and heated on a boiling waterbath. A stirrer reaching the bottom is installed. Ten cc. of an aqueous solution containing 4.04 g. of nickel chloride, $NiCl_2 \cdot 6H_2O$, is heated to ebullition, and added to the zinc dust by means of a pipet, with vigorous agitation in a few sec. The solids are at once collected on a glass filter by suction, washed with a small quantity of hot distilled water, transferred into 160 cc. of 10% aqueous caustic soda contained in an Erlenmeyer flask as quickly as possible, and digested at 50–60° for 15–20 minutes with occasional stirring. Then, the supernatant liquid is removed, and the solids are washed with 40 cc. of distilled water of 50–60° two times, and finally with the solvent of hydrogenation, e. g. ethanol. The rinsings are always removed by decantation.

In this way, a catalyst consisting of about 1 g. of nickel and 4.7 g. of zinc, and acting as good as 1 g. of Raney nickel catalyst (e. g. W 7) is obtained and can be used for hydrogenation or reduction of ketones, nitriles, oximes, a double bond conjugated with a carbonyl or a carboxyl group, etc., at the ordinary temperature and pressure.

Free carboxylic acids diminish the activity of the nickel catalyst. Hence, they are neutralized with caustic alkali before introducing the catalyst, or hydrogenated in solution in aqueous alkali. For instance, cinnamic acid is easily reduced to hydrocinnamic acid in solution in aqueous caustic soda.

In case the alkali remaining on the catalyst is undesirable, digestion in a saturated aqueous solution of sodium chloride followed by washing with hot distilled water will remove the majority of the adsorbed alkali. For instance, the reduction of nitrobenzene to aniline is better performed with a so-treated catalyst.

If 80 cc. instead of 160 cc. of 10% caustic soda is used in digestion, the activity is increased by about 10%, but the weight of the catalyst amounts to about 10 g. corresponding to the more quantity of matters remaining undissolved.

Department of Chemistry, Faculty of Science, Tokyo University

1) Y. Urushibara, This Bulletin, **25**, 230 (1952).

ADDITIONS AND CORRECTIONS

Additions and Corrections Volume 26, 1953

M. FUJIMOTO: Eine Neue Methode zur Darstellung von Eisenrhodanidenlösung mit dem Kationenaustauschenden Harze.

Page 353. Next figure is inserted as it was omitted.

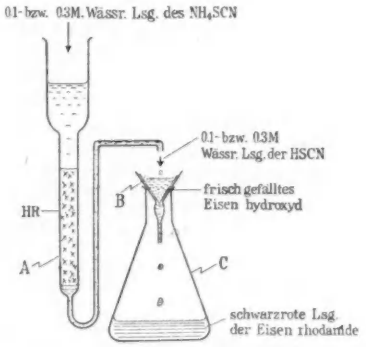

Abb. 1. Apparat zur Darstellung der Eisenrhodanidenlösung.

T. ISEMURA, H. HOTTA and T. MIWA: Surface Chemistry of High Polymers. I

Page 382. In col. 3 in Table II, for "pressure Surface" read "Surface pressure".

Page 383. In Figs. 6 and 7, the curves of them should be exchanged each other.

Page 384. In col. 1, ref. 9, for "Biochem." read "Biol. Chem.".

H. Hotta. Surface Chemistry of High Polymers. II.

Page 389. In the line of Amilan in Table IV, for "7.2" and "50" read "6.9" and "48", respectively; in col. 2, line 13, eliminate the words of "in organic solvent".

Page 390. In col. 1, ref. 14, for "Biochem." read "Biol. Chem.".

K. SONE: Electronic Remarks on the Origin of the Anomalous Color of Some Organic Iron. III.

Page 467. In the subject for "Iron. III. Complex" read "Iron (III) complex". In col. 1, line 1 and 2 from the bottom, for "show a similar intense absorption band" read "show similar intense absorption bands".

Page 469. In equation (1′)

"$\left[:\ddot{O}- \right.$ H $\left. \bigcirc \cdot \right]^{+}$" (B)

"$\left[:\ddot{O}- \right.$ H $\left. \bigcirc \cdot \right]^{+}$" (B)

Page 470. In col. 2. line 14, for "compound" read "compared". In equation (B), for "Fe^{++}" read "Fe^{+++}".

Additions and Corrections Volume 27, 1954

M. TANAKA: Emploi du péroxyde d'argent dans le dosage volumétrique et colorimétrique du vanadium.

Page 10. In reference (2), for "This Bulletin" read "Ce Bulletin".

Page 12. In col. 1, line 30, for "excés" read "excès".

K. SHINODA and K. KINOSHITA: Critical Concentration for Micelle Formation and its Aggregation Number in Aqueous Solutions of Paraffin Chain Salts.

Page 75. In col. 1, equation (4.2),

for "$\frac{\partial^2 E_n}{\partial n^2} = m\omega/\sqrt{2}\ n_0^{3/2} - 2\sqrt{2}\,\sigma^2 K^2 S_n^{3/2}/D\pi^{1/2} n_0^{1/2} = 0$"

read "$\frac{\partial^2 E_n}{\partial n^2} = m\omega/2\sqrt{2}\ n_0^{3/2} - \sqrt{2}\,\sigma^2 K^2 S_n^{3/2}/D\pi^{1/2} n_1^{1/2} = 0$"

In col. 1, equation (4.5),

for "$\log C = \log 1000/\nu - (x - x')/kT - 1$"

read "$\log C = \log 1000/N\nu - (x - x')kT - 1$"

S. WASHIZUKA: Quantitative Separation of Copper by Thiourea from Homogeneous Solution.

Page 77. In col. 1, line 10, for "H" read "pH".

Page 78. In col. 1, lines 6, 11 and 2, 10 from the bottom and In col. 2, line 11, for "H" read "pH". In Fig. I, for "(1/2)" read "(%)".

Page 79. In col. 1, line 30, for "metri-cally" read "metrically". In Table VI, insert "g." to the next line of "Copper taken," and "added," and insert "mg." to the next line of "Copper," and "metals.".

H. HOTTA: Surface Chemistry of High Polymers. III.

Page 81. In the lines of polyvinyl acetate and stearate in Table I, for "260" read "280".

Page 82. In the line of polyvinyl acetate in Table II, for "37" read "38".

M. TANAKA: État du fer dans les eaux des lacs.

Page 89. In col. 1, line 17 from the bottom, for "colloides" read "colloïdes". In reference (2), for "geochimie" read "géochimie". In reference (4), for "prés" read "près".

Page 90. In col. 1, line 14, for "invite" read "incite".

Page 93. In Fig. 2,

for "Couche supérieure Fe^{III} SO_4^{--}"
Couche anaérobie $\downarrow$ $\downarrow$
Vase Fe^{II} S^{--}
$\searrow$ $\swarrow$
FeS

read "Couche supérieure Fe^{III} SO^{4--}"
Couche anaérobie Fe^{II} S^{--}
Vase FeS

In Fig. 3,

for "Couche supérieure Fe^{III}"
Couche anaérobie Fe^{II}
Vase Fe^{II}

read "Conche supérieure Fe^{III}"
Couche anaérobie Fe^{II}
Vase Fe^{II}

In col. 1, line 6 from the bottom, for "centenu" read "contenu".

T. ISEMURA, H. HOTTA and S. OTSUKA: Surface Chemistry of High polymers. IV.

Page 94. In col. 1, line 15 from the bottom, for "curve" read "curve e".

Page 96. In col. 2, line 35, for "20 %[1])" read "20 %[11])".

Page 97. In col. 1, line 4, for "10 Å², in Fig. 5" read "10 Å², but curve c in Fig. 5".

M. TANAKA: Aluminium dans les eaux des lacs.

Page 99. In refence (7), col. 2, for "Aluminium mg l" read "Aluminium mg/l".

Page 100. In reference (8), for "D'aprés" read "D'après".

I. MIYAGAWA, Y. MORINO, and R. RIEMSCHNEIDER: The Dipole Moments of Some Polyhalocyclohexanes and Their Related Compounds. I.

Page 177. In reference (3), col. 2, for "Zeit. Naturforschung, 8b,000" read "Zeit. Naturforschung, 8b, 617", for "Comm. XXIII, ibid. 8b,000" read "Comm. XXIII, ibid. 8b, 701". In reference (4), for "Monat. Chem. 84,000" read "Monat. Chem. **84**, 1068".

Page 180. In Fig. 4, the white circle at the 3p-position in the isomer (3) should be the black one.

E. HIROTA: The Electrostatic Effect of the Solvents on the Frequency Shifts and the Intensity Changes of the Infrared Absorption Spectra.

Page 295. In col. 1, line 19, for "Eq. (1)'" read "Eq. (1),".

Page 296. In Table II, col. 5, for "2.6_7" read "3.6_7". In col. 1, line 4 from the bottom, for "Melecules." read "Molecules.".